APPLICATION OF ECOLOGICAL THEORIES TO THE GUT MICROBIOME AND BIFIDOBACTERIAL COMMUNITIES

尾島　望美
Miriam Nozomi Ojima

TABLE OF CONTENTS

ABSTRACT

This doctoral thesis presents two studies that utilize infant-gut associated bifidobacteria as a study system to test theories in community ecology. Bifidobacteria are the first colonizers of the human gut microbiome and a critical taxon that is said to significantly affect host health and physiology. The first study (Chapter II) examines the role of priority effects in the initial structuring of bifidobacterial communities. The second study (Chapter III) evaluates the role of bifidobacteria after the gut microbial community is established. This study tests the efficacy of bifidobacteria as a probiotic species and its role in the ecological recovery after antibiotic-induced disturbance.

The first study described in Chapter II uses four infant-gut associated bifidobacterial species (*Bifidobacterium bifidum* JCM 1254, *Bifidobacterium breve* UCC2003, *Bifidobacterium longum* subspecies *longum* MCC 10007, and *Bifidobacterium longum* subspecies *infantis* ATCC 15697^{T}) to examine the role of priority effects, or the effect of species arrival order on community composition. Human milk oligosaccharides (HMOs) were used as a carbon source. Consistent with the genomic analysis performed in this study, the four bifidobacterial species displayed a variety of species-specific HMO assimilation phenotypes and competitive abilities in HMO-supplemented environments. Results of culturing experiments showed that assembly history and priority effects significantly affected community structure, as the identity of the first colonizer and the second colonizer had a significant effect on the outcome of the community. Priority effects allowed *B. breve*, a species predicted to be a weak competitor in terms of HMO assimilation, to dominate. Further analysis with previously published *in vivo* gut microbial community composition data from a cohort of 41 infant-mother pairs also suggested that *B. breve* benefitted from priority effects. The results of this study found that infant gut-associated microbes are subject to assembly history and priority effects, and that colonization during the early stages of assembly is critical for the development of the community.

The second study described in Chapter III examines the efficacy of *B. bifidum* JCM 1254 as a probiotic strain. Using mouse models, repeated disturbance to the gut microbiome was introduced through three different antibiotics, and *B. bifidum* was administered after each disturbance event. The effect of antibiotic administration diminished with repetitive use, showing that the gut microbiome retains memory of past disturbances. Furthermore, the response of the gut microbiome varied by each antibiotic type, which consequently affected the efficacy of *B. bifidum* administration. Results show that although *B. bifidum* was not effective in recovering species diversity, it reduced gut inflammation when antibiotic administration caused an increase in proinflammatory species. The findings show that different types of

disturbances determine the identity of the taxa that survive in the community, which ultimately affects the response of the gut microbiome to subsequent recovery interventions.

In this doctoral thesis, the author presents interdisciplinary studies that combine concepts and experimental methods from molecular biology, community ecology, and bioinformatics. Using bifidobacteria as a study system, the two studies described above explore how theories in community ecology can be used to understand the dynamics within host-associated microbial communities and their role in host health and disease. Furthermore, the author hopes that the application of ecological theories could be utilized to improve currently available microbiome-based therapies that are aimed at restoring or maintaining the ecosystem services provided by healthy gut microbial communities.

LIST OF ABBREVIATIONS AND TERMS

Abbreviation	Term
2'-FL	2'-Fucosyllactose
3-FL	3-Fucosyllactose
AA	Anthranilic Acid
AAD	Antibiotic-Associated Diarrhea
ANOVA	Analysis of Variance
ATCC	American Type Culture Collection
BLAST	Basic Local Alignment Search Tool
bp	Base Pairs
CAGR	Compound Annual Growth Rate
DFAST	DDBJ Fast Annotation and Submission Tool
DNA	Deoxyribonucleic Acid
EFA	Exploratory Factor Analysis
ESBL	Extended-Spectrum β-Lactamase
FDH	Fucose Dehydrogenase
FMT	Fecal Microbiome Transplant
Fuc	Fucose
Gal	Galactose
GAM	Gifu Anaerobic Medium
GH	Glycoside Hydrolase
Glc	Glucose
GlcNAc	*N*-Acetylglucosamine
HMOs	Human Milk Oligosaccharides
HPLC	High-Performance Liquid Chromatography
IBD	Inflammatory Bowel Disease
IgA	Immunoglobulin A
ITS	Internal Transcribed Spacer
JCM	Japan Collection of Microorganisms
Lac	Lactose
LDFT	Lactodifucotetraose
LNB	Lacto-*N*-biose I
LNDFH	Lacto-*N*-difucohexaose
LNFP	Lacto-*N*-fucopentaose
LN*n*T	Lacto-*N*-*neo*tetraose

LNT	Lacto-*N*-tetraose
MCC	Morinaga Culture Collection
MRS	De Man, Rogosa, Sharpe (Medium)
NCBI	National Center for Biotechnology Information
NCIMB	National Collection of Industrial Food and Marine Bacteria
NEC	Necrotizing Enterocolitis
NGS	Next-Generation Sequencing
NMDS	Non-Metric Multidimensional Scaling
OD	Optical Density
ORF	Open Reading Frame
OTU	Operational Taxonomic Unit
PCA	Principal Components Analysis
PCR	Polymerase Chain Reaction
PERMANOVA	Permutational Multivariate Analysis of Variance
QIIME	Quantitative Insights Into Microbial Ecology
qPCR	Quantitative Polymerase Chain Reaction
rm-ANOVA	Repeated Measures Analysis of Variance
RNA	Ribonucleic Acid
rRNA	Ribosomal Ribonucleic Acid
RPKM	Reads Per Kilobase of exon per Million mapped reads
SCFA	Short-Chain Fatty Acids
SE	Standard Error
SRA	Sequence Read Archive
subsp.	Subspecies
UCC	University College Cork Culture Collection
YCFA	Yeast, Casitone, Fatty Acids (Medium)

Chapter I

GENERAL INTRODUCTION

The human gastrointestinal tract is host to an abundant and diverse community of microbes, collectively referred to as the gut microbiome. A study by Sender et al. (2016) estimates that the gut microbiome consists of around 4×10^{13} microbial cells, which is approximately as many as the number of human cells in the body. Given the abundance of microbes within the gut microbiome, it is no surprise that they have a significant potential to influence host physiology. The gut microbiome is known to aid in food digestion and nutrient absorption by breaking down carbohydrates that are otherwise inaccessible to the host, such as dietary fibers (Daïen et al., 2017) and host-produced complex glycans like human milk oligosaccharides (HMOs) and mucin (Sela et al., 2008). Other studies have shown associations between the composition of the gut microbiome and the development of the immune system (Round and Mazmanian, 2009; Kau et al., 2011). Any imbalances in a healthy microbiome (dysbiosis) on the other hand, have been linked to diseases such as obesity (Ley et al., 2005), inflammatory bowel disease (IBD) (Nishida et al., 2018), and type 2 diabetes (Qin et al., 2012).

With the advancement in next-generation sequencing (NGS) and metagenomic technologies, studies elucidating the relationship between the gut microbiome and host health have increased significantly over the last two decades. Furthermore, the use of gnotobiotic animal models has allowed studies to experimentally determine correlations between specific taxa and disease states. For example, a study by Jiang et al. (2002) found that the development of IBD was accelerated in mice mono-associated with *Helicobacter muridarum.* Another study by Fei and Zhao (2013) found that the inoculation of *Enterobacter cloacae* B29 isolated from a morbidly obese human individual induced obesity in gnotobiotic mice. Although gnotobiotic mice are a useful tool for examining the effect of specific taxa on host physiology, studies often present casual relationships and lack mechanistic explanations. Moreover, some studies indicate that certain disease states do not develop in the absence of other gut microbes (Bäckhed et al., 2007). This suggests that the mechanisms of pathology within the gut microbiome are rarely simple, but rather highly context-dependent and influenced by community interactions within microbiomes (Walter et al., 2020). However, studies have only recently begun to examine the gut microbiome within the context of community ecology.

The goal of community ecology is to explain and predict the mechanisms that determine temporal and spatial patterns of species diversity. However, most current ecological theories are developed based on experimentation with higher eukaryotic communities and have yet to be tested in host-associated microbial communities. Ecological communities both shape and are shaped by their environments, but unlike eukaryotic communities and free-living microbial communities, host-associated microbial communities are distinct in that they form mutualistic relationships with their host environments, thereby becoming a holobiont (Margulis, 1991). The human holobiont is an ecological system under selective pressure that minimizes conflict between host and microbe, creating a symbiotic relationship. In this

symbiosis, the human host provides a niche for the gut microbial community to occupy. The selective pressure exerted by the host can also affect microbe to microbe interactions, as selection can favor competitive outcomes that are beneficial to the host. In turn, the gut microbiome as a community provides ecosystem services that increase the fitness of their host. This mutualistic relationship accelerates host-microbe coevolution, making the gut microbiome a unique system in which theories in community ecology are currently underexplored.

To address the research gaps in both gut microbiome studies and community ecology, this doctoral thesis examines two concepts: assembly theory and disturbance ecology. In this thesis, I used host-associated gut microbial communities, with a focus on infant gut-associated bifidobacteria. Bifidobacteria are Gram-positive and anaerobic bacteria with high guanine and cytosine (G + C) content (> 50 %) (Shah, 2011), belonging to the Actinobacteria phylum. Bifidobacteria were first isolated by Henri Tissier in 1899 from breastfed infant feces (Tissier, 1900) and are one of the first colonizers and symbionts of the human gut. The guts of infants, especially breastfed infants, are rich in bifidobacteria due to selection by HMOs found in breastmilk (Roger et al., 2010). HMOs are a group of oligosaccharides with a degree of polymerization greater than 3 and are the third most abundant solid component in breastmilk after lactose and lipids (Urashima et al., 2012). Despite being an abundant component in breastmilk, it provides no nutritional value to the host as it is resistant to pancreatic digestion (Kunz et al., 2000; Urashima et al., 2012). HMOs pose a strong selective pressure in the gut microbiome as bifidobacteria and a limited subset of gut microbes possess the enzymatic genes to utilize them (Macrobal et al., 2010; Ruiz-Moyano et al., 2013; Katayama, 2016; Matsuki et al., 2016; Sakanaka et al., 2020). Furthermore, the composition of the initial gut microbiome that forms during infancy is said to have consequences for host health that last throughout adulthood. Although the available literature is mostly correlative data, studies suggest that the lack of a bifidobacterial community is linked to the development of allergy and atopic dermatitis, as well as an impairment in the immune system (Kalliomäki et al., 2001; Di Gioia et al., 2014). In addition to being a critical species in the initial formation of the human gut microbiome, bifidobacteria have gained attention as probiotics. Bifidobacteria are said to confer several health benefits to the host, such as the prevention and treatment of colorectal cancer (Sekine et al., 1985; Le Leu et al., 2010), anti-obesity effects (Kondo et al., 2010; Stenman et al., 2014; Moya-Pérez et al., 2015), and the suppression of inflammation (Riedel et al., 2006; Medina et al., 2008). Due to their unique role as both a pioneer species of the human gut and a commonly used probiotic taxon, bifidobacteria proved to be an ideal model system to test both assembly theory and disturbance ecology, as described below.

Assembly Theory

Chapter II of this dissertation examines the process by which infant gut-associated bifidobacterial communities are formed. Bifidobacteria are one of the first colonizers of the human gut microbiome and a focal species of initial community assembly. However, due to limited opportunities for experimentation with human subjects, elucidating the factors and mechanisms of gut microbiome assembly remains difficult. Chapter II addresses this issue by utilizing a reductionist approach and examining the mechanisms of community assembly with infant gut-associated bifidobacteria, with a focus on priority effects. According to a synthesized framework proposed by Vellend (2010), community assembly is driven by four basic processes: dispersal, diversification, drift, and selection (Table I-1). Dispersal allows for taxa to colonize local habitats from a regional species pool. Within the local habitat, diversification adds new genetic variation and taxa. Then, deterministic selection based on species traits and stochastic drift shapes the relative abundances of local taxa. The following sections will briefly review the available literature regarding the gut microbiome and mechanisms of community assembly.

Dispersal

Dispersal refers to the movement of individuals across space and it is a fundamental process by which diversity accumulates in local microbial communities. Through dispersal, the niches available in the infant gut microbiome is colonized. The infant gut is generally considered sterile at birth and microbial colonization is thought to begin postpartum. Several factors contribute to the initial community assembly, such as mode of delivery (Bokulich et al., 2016; Akagawa et al., 2019), use of antibiotics by mother and infant (Yassour et al., 2016), and feeding method (breastfeeding or formula) (Ho et al., 2018). After birth, microbes from a variety of species pools can colonize the gut, but maternal microbes are one of the most significant sources. A recent study has shown that the neonatal oral fluid that infiltrates the infant nasal cavity during vaginal delivery is a possible transmission route for bifidobacteria (Toda et al., 2019). This is further corroborated by studies that show that the gut microbiome of infants born vaginally is dominated by taxa found in the mother's vagina, while the gut microbiome of infants born through cesarian section is dominated by taxa found on the human skin (Palmer et al., 2007; Dominguez-Bello et al., 2010). These studies strongly suggest that the maternal microbial reservoir is an important source of microbe acquisition for the early infant microbiome.

Diversification

Diversification refers to the generation of new genetic variation within a local community. Compared to communities of higher eukaryotes, local diversification occurs rapidly in the gut microbiome due to large population sizes and high growth rates. A recent study by Zhao et al., (2019) examined the within-microbiome evolution of *Bacteroides fragilis* in a cohort of 12 healthy individuals and found that *B. fragilis* adapted through *de novo* mutations. Thus, diversification was observed within individuals. Bacteria can also inherit mutational changes through horizontal gene transfer, and data from the Human Microbiome Project suggests that horizontal gene transfer occurs frequently within the adult human gut microbiome. A study by Liu et al. (2012) identified 13,514 horizontal gene transfer genes, most encoding for catalytic functions and metabolic processes, in 308 prokaryotic species. However, diversification occurs as a result of persistent selective pressure, and the infant gut microbiome experiences frequently changing selective pressures (i.e., host immune system development, breastfeeding, and the introduction of solid foods). Consequently, the extent to which horizontal gene transfer and diversification affects community assembly in the infant gut remains poorly understood (Lerner et al., 2017; Sprockett et al., 2018).

Selection

Selection creates differences in community structure based on fitness and niche differences among taxa. As a host-associated microbial community, the infant gut microbiome faces frequently shifting sources of selective pressures, primarily from diet and the immune system. At birth, the infant's main source of food is breastmilk. HMOs found in breastmilk are a group of structurally diverse oligosaccharides with more than 200 distinct structures (Ninonuevo and Lebrilla, 2009) that are resistant to enzymatic digestion and low gastric pH (Engfer et al., 2000). As a result, HMOs reach the intestine intact and act as a substrate for gut microbes. However, only a subset of microbes (*Bifidobacterium* species, some *Bacteroides* species, and a limited group of *Clostridium* species) possess the genes to utilize HMOs (Macrobal et al., 2010). Consequently, HMOs provide a competitive advantage to HMO-utilizing taxa over other gut microbes, and the guts of breastfed infants are often dominated by *Bifidobacterium* species (Tannock et al., 2013; Matsuki et al., 2016). Furthermore, the most drastic change in community composition occurs at the cessation of breastfeeding, suggesting a sudden shift in selective pressure (Yatsunenko et al., 2012). In addition to diet, the oxygen concentration within the infant gut exerts selective pressure. The gut microbiome becomes increasingly anaerobic postpartum, which selects for facultative or strict anaerobes. A study by Ferretti et al. (2018) found that microbes that

originate from the maternal gut, the majority of which are anaerobic strains, are more persistent and ecologically better adapted to the infant gut than microbes from other maternal body sites. The immune system could also exert selective pressure on the microbiome, causing microbial communities to become more body-site specific. Furthermore, as the gut microbiome can affect host health, selection is expected to favor microbial traits that are beneficial to the host.

Drift

While selection is a deterministic force that alters community structure, ecological drift refers to the random changes in the relative abundance of species. However, distinguishing the effect of drift from other processes is challenging, and very few studies examine its effect within the gut microbiome. One study using synthetic bacterial communities found that the importance of ecological drift increases when selection is high and dispersal is low (Fodelianakis et al., 2020). Drift also becomes important when species abundance is low, as low-abundance species are more likely to be randomly pushed to extinction (Gilbert and Levine, 2017). A study examining the rate of evolution in a commensal *Escherichia coli* strain observed limited genomic diversity and found little evidence of selection, possibly due to small population sizes (Ghalayini et al., 2018). Although there are other possible explanations, the absence of diversification and selection for this *E. coli* population suggests that drift plays a larger role in bacterial adaptation for taxa with small population sizes. However, this study did not explicitly test for ecological drift. Consequently, ecological drift remains difficult to characterize in the gut microbiome, as multiple confounding factors could contribute to the low abundance of microbial populations, such as dispersal limitation, high susceptibility to disturbance, or low competitive ability.

Table I-1 | Summary of the ecological processes involved in community assembly.

Process	Definition	Examples in the Gut Microbiome
Dispersal	Movement of individuals across space	Possible vertical transmission of vaginal microbes to the infant's gut during vaginal delivery (Toda et al., 2019)
Diversification	Locally generated, new genetic variation	Adaptive evolution of *Bacteroides fragilis* in healthy individuals (Zhao et al., 2019)
Selection	Deterministic force that alters community structure based on fitness differences among taxa	Enrichment of taxa that can utilize HMOs (bifidobacteria) in breastfed infant guts (Fallani et al., 2010; Macrobal et al., 2010)
Drift	Stochastic change in relative abundance of taxa	Documented examples in the gut microbiome limited
Priority Effects	Effect of assembly history on final community composition	The relative abundance of *Bacteroides* at birth affects the three-year maturational trajectory of the gut microbiome (Yassour et al., 2016)
Niche Pre-emption	Early arriving species inhibit colonization by later colonizers by reducing resources available	Prior colonization by *Bacteroides thetaiotaomicron* in the colonic crypt physically prevents later-arriving isogenic strains from colonizing (Lee et al., 2013; Whitaker et al., 2017)
Niche Modification	Early arriving species change the nature of available niches, consequently changing the identities of later arriving species	Depletion of oxygen by Enterobacteriaceae in the infant's gut may be facilitating colonization by obligate anaerobes (Bokulich et al., 2016)

The processes described above often exert interactive effects, and the relative importance of each process is difficult to isolate in the gut microbiome. For example, feeding mode (formula or breastmilk) affects both dispersal and selection. Breastmilk contributes to dispersal as it harbors its own microbiome, with the majority of the taxa belonging to the Proteobacteria, Firmicutes, and Actinobacteria phyla (Moossavi et al., 2019). In addition to the selective pressures posed by HMOs, the antimicrobial factors in breastmilk, such as lactoferrin and immunoglobulin A (IgA), can further select the members of the gut microbiome. As a result, the gut microbiome of formula-fed infants experiences altered dispersal and selection compared to that of breastfed infants.

Another example of such interactive effects is priority effects, which will be discussed in detail in Chapter II. Priority effects, or the effect of dispersal history and species arrival order on community structure, operate through two mechanisms. The first mechanism, niche pre-emption, occurs when the early arriving species sequester and reduce the amount of resources available for later-arriving species. The second mechanism, niche modification, occurs when the early arriving species alters the types of available niches and consequently determines which later-arriving species can colonize the niche (Fukami, 2015). Priority effects can determine the nature of species interactions within the community, and consequently alter how selection, drift, and diversification operate. Several recent papers have highlighted the need to examine the role of priority effects in the initial assembly of the human gut microbiome (Martínez et al., 2018; Sprockett et al., 2018). However, because experimental opportunity with infant subjects is limited, the study described in Chapter II will examine the role of priority effects in a controlled laboratory setting using four infant gut-associated *Bifidobacterium* strains. With medium supplemented with HMOs as the carbon source, the colonization history was manipulated to examine the effect of assembly history on community composition.

Disturbance Ecology

Chapter III addresses the role of bifidobacteria in established gut microbial communities. Specifically, the chapter explores its role in the recovery after ecological disturbance. In addition to assembly history, the history of disturbances is another factor that shapes the gut microbiome. An ecological disturbance is defined as an abiotic or biotic event that causes sudden structural changes to the community composition. Disturbance events remove some portion of resident individuals and create an opportunity for the remaining community members to increase in abundance, or for new colonists to establish within the community (Sousa, 1984). The type of disturbance determines which individuals and traits are selected for over time, and communities are predicted to adapt over evolutionary time. Furthermore, the community's response to disturbance reveals features that are otherwise difficult to detect, such as stability and resilience, as well as interspecies interactions and dependencies. The stability of an ecological community can be described through engineering resilience and ecological resilience. The former refers to the rate at which a community returns to a single steady-state after disturbance, while the latter refers to the amount of disturbance a community can tolerate before its trajectory is altered to a different stable state (Peterson et al., 1998). While resilience is often described in terms of species diversity and community composition, assessing resilience in terms of ecosystem functioning and services may be especially important for gut microbiome studies (Costello et al., 2012), given the importance of the gut microbiome for human health.

Within the gut microbiome, antibiotics are a common source of disturbance. Approximately 30 % of patients in the United Kingdom are prescribed antibiotics at least once a year (Shallcross et al., 2017), and up to 3 % of the population in the European Union is exposed to pharmacologic doses of antibiotics daily (Goossens et al., 2005). In Japan, approximately 1.6 % of the population is prescribed antibiotics on a given day (Japan Ministry of Health Labour and Welfare, 2016). More than 20 classes of antibiotics have been produced since 1930 (Coates et al., 2002), and the spectrum and mode of activity vary by each antibiotic. Consequently, the effect of antibiotics on the gut microbial community varies significantly by the type, dosage, and frequency of administration. While many studies focus on the emergence of antibiotic-resistant strains, relatively few studies have addressed the long-term adverse effects of antibiotics on the structure and composition of the gut microbial community. A study by Jernberg et al. (2007) found that antibiotic administration can have lasting consequences on the gut microbiome. For example, the administration of clindamycin, a broad-spectrum antibiotic that targets anaerobes, caused a decline in *Bacteroides* that lasted for two years. A different study by Dethlefsen and Relman (2011) examined the effect of repeated antibiotic exposure using ciprofloxacin, a fluoroquinolone antibiotic with a broad spectrum of activity, in human subjects and found that while the gut microbiome recovered relatively quickly to its initial state, repeated antibiotic use caused the recovery to be incomplete. These examples show that antibiotic disturbance can have significant and often lasting effects on the community composition of the gut microbiome.

Recent studies suggest that the administration of probiotics, or microbial strains such as *Bifidobacterium* and *Lactobacillus* that are consumed for therapeutic purposes, can alleviate the negative effects of antibiotic-induced dysbiosis (Grazul et al., 2016; Ekmekciu et al., 2017). Probiotics are said to aid in correcting dysbiosis and prevent antibiotic-associated diarrhea (AAD) by filling in the niche cleared by antibiotics and preventing pathogen colonization (Guo et al., 2019). A study by Gueimonde et al., (2007) suggested that probiotics can physically inhibit pathogen colonization by attaching to the host's epithelial cells. Other studies have shown probiotic species to act through the production of short-chain fatty acids and other acidity-related mechanisms (Fukuda et al., 2011), production of bacteriocins (Corr et al., 2007), and disruption of quorum sensing (Medellin-Peña et al., 2007). However, the research regarding the efficacy of probiotics after antibiotic-induced dysbiosis remains inconclusive. For example, a study by Suez et al. (2018) also found that some probiotic strains produce anti-microbial peptides, which inhibited, rather than promoted, recovery after antibiotic disturbance. One of the issues with current probiotic research is that probiotics are often considered as a homogenous entity, even though the purported effects can vary significantly not only at the species level but also at the strain level. Many studies utilize a pre-mixed blend of probiotic species, and the specific role of bifidobacterial species in the recovery after antibiotic-induced disturbance warrants further research. Therefore, Chapter III examines

the efficacy of a probiotic strain, *Bifidobacterium bifidum* JCM 1254, against three antibiotics with differing spectrums and modes of action.

Despite recent advances in sequencing technologies, questions remain regarding how to best sample and test for factors that affect structural, functional, and temporal variations in the gut microbiome. There is a growing interest in examining the gut microbiome through the lens of community ecology, but the development of theory-based, microbiome-specific hypotheses are limited (Costello et al., 2012; Koskella et al., 2017). To address these research needs, the studies presented in this dissertation utilizes approaches from both microbiology and community ecology, as well as bioinformatics, to empirically test for ecological theories in host-associated microbial communities.

Chapter II

THE ROLE OF PRIORITY EFFECTS IN BIFIDOBACTERIAL COMMUNITIES

Summary

Bifidobacteria are one of the first colonizers of the human gut, and human milk oligosaccharides (HMOs) found in breastmilk are crucial for the formation of a bifidobacteria-rich gut microbial community in infants. While the presence of bifidobacteria during infancy has been linked to a variety of health-promoting effects, little is known about how bifidobacterial communities are initially formed in the infant gut. This study focused on four infant-gut associated bifidobacteria *(Bifidobacterium bifidum* JCM 1254*, Bifidobacterium breve* UCC2003*, Bifidobacterium longum* subspecies *longum* MCC 10007*, Bifidobacterium longum* subspecies *infantis* ATCC 15697^{T}) that employ a variety of species-specific strategies for HMO consumption. Through genomic analysis and monoculture experiments, phenotypes of each strain were first characterized. Co-culturing experiments in medium supplemented with HMOs were performed to test for priority effects, by manipulating colonization histories. Pairwise culturing experiments revealed differences in competitive outcomes between each species pair, which were significantly affected by inoculation order as well as species traits. Four-species assemblages also showed that the structure of bifidobacterial communities, as well as the behavior of growth curves, was significantly influenced by assembly history and subject to priority effects. Bifidobacterial communities extracted from publicly available metagenome data from a cohort of infant-mother pairs were examined for further analysis. Results show that the identity of colonizers during the early stages of community assembly affects community outcomes. Furthermore, the findings of this study suggest that *B. breve* can significantly benefit from priority effects, as it dominated in both *in vitro* and *in vivo* systems. In conclusion, the results of this study show that priority effects are prevalent in infant gut-associated microbes, highlighting the importance of initial community assembly and its implications for the maturation trajectory of the gut microbiome.

Introduction

The initial composition of the human gut microbiome during infancy has been linked to a variety of health conditions that can manifest themselves throughout adulthood. However, little is known about how the initial microbial community is acquired and structured. Past studies have shown that the postpartum microbial colonization period is critical for the development of the gut microbiome, and is affected by a variety of factors such as delivery mode (vaginal or cesarian section), food source (formula or breastmilk), and antibiotic use by both the mother and the infant (Bokulich et al., 2016; Akagawa et al., 2019). Several observational studies report that prior colonization by certain taxa affects the final

community structure of the gut microbiome. For example, in a cohort of 39 infants, variation in the initial abundance of *Bacteroides* species was associated with divergent microbial trajectories that lasted for at least 36 months postpartum (Yassour et al., 2016). Circumstantial evidence also suggests that the composition of the infant gut microbiome influences the risk of developing conditions such as metabolic disorders, obesity, and immune diseases later in life (reviewed by Turroni et al., 2020).

Given that the composition of the gut microbiome during infancy can have long-term consequences, there is a pressing need to understand the underlying mechanisms of initial community assembly. Studies in the past have elucidated the role of deterministic factors such as host genetics on the structure of the gut microbiome, which can select for specific taxa through niche-based mechanisms. However, host genetics only account for 20 % of the variation in community composition (Rothschild et al., 2018) and few studies have applied ecological theories, such as assembly history and priority effects, to examine host-associated microbial communities. Priority effects, or the effect of species arrival order on species interactions (Fukami, 2015), are predicted to significantly alter community development, especially during the early stages of community assembly. One study using plants demonstrated that the commensal microbiome in the plant phyllosphere was subject to priority effects (Carlström et al., 2019). In terms of gut-associated communities, a recent study using germ-free murine models showed that colonization history contributed more to inter-individual variation in the gut microbiome than the host immune system did (Martínez et al., 2018). Although few studies address the mechanisms of priority effects in host-associated bacterial communities, one study by Lee et al., (2013) identified a genetic locus in *Bacteroides* species (commensal colonization factor, *ccf*) that allowed early-arriving *Bacteroides* species to gain access to colonic crypts, thereby preemptively excluding later-arriving colonizers. While these studies highlight the importance of assembly history, experimental evidence and mechanistic explanations for priority effects with human gut-associated microbes remain limited. Furthermore, no studies, to our knowledge, have explicitly tested for priority effects using infant gut-associated bacteria.

Bifidobacteria are one of the first colonizers of the infant gut and can occupy more than 70 % of the total microbiome during breastfeeding (Tannock et al., 2013; Matsuki et al., 2016). The initial colonization by bifidobacteria is crucial for the breakdown of human milk oligosaccharides (HMOs) found within breastmilk. HMOs are a group of complex unconjugated glycans that, despite being the third most abundant solid component in breastmilk, provide no nutritional value to the host as they are resistant to digestion by pancreatic enzymes (Engfer et al., 2000). HMOs also act as a selective agent that promotes the growth of bifidobacteria and other species that possess enzymes capable of metabolizing HMOs (Macrobal et al., 2010; Macrobal and Sonnenburg, 2012; Katayama, 2016; Sakanaka et al., 2020). While breastfeeding has been associated with higher incidences of bifidobacteria, the dominant species varies by geographic region and individual (Gore et al., 2008; Turroni et al., 2009), and recent studies have shown

that the bifidobacteria are absent in some breastfed infants (Lewis and Mills, 2017). The absence of a bifidobacterial community (bifidus flora) has been linked to health conditions such as diarrhea, respiratory infection, obesity, etc. (Brown et al., 1989; López-Alarcón et al., 1997; von Kries et al., 1999). In such infants, bifidobacteria may have been absent during a critical colonization window and the early stages of community assembly (Tannock et al., 2016), as infants born via cesarian section have a lower abundance of bifidobacteria (Tannock et al., 2013; Reyman et al., 2019). As a countermeasure, bifidobacteria are used as probiotics and therapeutic interventions for preterm infants (Kitajima et al., 1997; Underwood et al., 2013; Plummer et al., 2018). However, the reported efficacy of exogenously administered bifidobacteria varies among studies, and persistent colonization remains an issue (Costeloe et al., 2016; Suez et al., 2019). The application of ecological theories, such as priority effects, could improve strategies for microbiome-based therapeutic interventions, as well as explain the differential establishment of bifidobacterial species within the infant gut.

This study tested for the role of assembly history in the structuring of infant gut-associated bifidobacterial communities in a controlled laboratory setting. The four bifidobacterial species used in this study, *Bifidobacterium bifidum* JCM 1254, *Bifidobacterium breve* UCC2003, *Bifidobacterium longum* subspecies *longum* MCC 10007 (*B. longum*), and *Bifidobacterium longum* subspecies *infantis* ATCC 15697^{T} (*B. infantis*), employ varied and species-specific strategies for HMO assimilation. For example, both *B. bifidum* and *B. infantis* can consume most types of HMOs, but the former extracellularly degrades while the latter imports HMOs whole (Sakanaka et al., 2020). These species-specific strategies are predicted to alter competitive outcomes. Therefore, in medium supplemented with HMOs as a selective agent, the colonization histories were experimentally manipulated to examine its effect on the community structure as well as HMO utilization. Culturing data were also compared to publicly available *in vivo* fecal metagenome data from a cohort of infant-mother pairs to further validate the findings. By doing so, we aimed to understand the role of priority effects in the bifidus flora and to unravel complex interactions within the microbiome through the context of community ecology.

Materials and Methods

Chemicals

Fuc, Glc, Gal, 2-AA (anthranilic acid), and sodium cyanoborohydride were purchased from Nacalai Tesque (Kyoto, Japan). GlcNAc and Lac were purchased from Wako Pure Chemical Industries (Osaka, Japan). The following sugars were purchased from Dextra Laboratory (Reading, UK): LN*n*T and LNFP I. 2'-FL, 3-FL, LDFT and LNT were obtained from IsoSep (Tullinge, Sweden), or provided as gifts

from Glycom A/S (Hørsholm, Denmark). LNFP II, LNFP III and LNDFH I were purchased from Carbosynth (Berkshire, UK) and isomaltoheptaose was purchased from Seikagaku Kogyo (Tokyo, Japan). LNB was synthesized as described previously (Nishimoto and Kitaoka, 2007), and provided by Dr. M. Kitaoka at Niigata University. All other reagents that we used were of analytical grade.

Preparation of Oligosaccharides from Human Milk

Milk samples were collected from healthy Japanese mothers who had not taken any antibiotics for at least 1 month before collection at Nagao Midwife Clinics (Kyoto, Japan), with the support of Dr. J. Hirose at the University of Shiga Prefecture. Informed consent was obtained from all mothers. The study was reviewed and approved by the Ethics Committee of Kyoto University (R0046) and was performed per the Declaration of Helsinki. HMOs were purified from the collected human milk samples as described previously (Asakuma et al., 2011). During the purification process, sialyl oligosaccharides were eluted near the void fractions as polymeric compounds, and therefore absent from the HMO mixture used in this study. A small amount of Lac, which are contaminants derived from the HMO purification process, was also detected. The composition of the HMO mixture used in this study was determined by analysis with HPLC and is summarized in Table II-1.

Table II-1 | Structures and initial concentrations of HMOs used in this study, at 1 % (*w/v*).

Oligosaccharide	Structure	Concentration (mM)
Lactose	Galβ1–4Glc	0.75 ± 0.12
2'-FL	Fucα1–2Galβ1–4Glc	3.58 ± 0.54
3-FL	Galβ1–4(Fucα1–3)Glc	4.06 ± 0.59
LDFT	Fucα1–2Galβ1–4(Fucα1–3)Glc	0.49 ± 0.07
LNT	Galβ1–3GlcNAcβ1–3Galβ1–4Glc	1.21 ± 0.24
LN*n*T	Galβ1–4GlcNAcβ1–3Galβ1–4Glc	0.54 ± 0.08
LNFP I	Fucα1–2Galβ1–3GlcNAcβ1–3Galβ1–4Glc	0.56 ± 0.08
LNFP II + III	Galβ1–3(Fucα1–4)GlcNAcβ1–3Galβ1–4Glc (LNFP II) Galβ1–4(Fucα1–3)GlcNAcβ1–3Galβ1–4Glc (LNFP III)	0.89 ± 0.12
LNDFH I	Fucα1–2Galβ1–3(Fucα1–4)GlcNAcβ1–3Galβ1–4Glc	0.68 ± 0.08
Total		12.76 ± 1.52

* Abbreviations: 2'-FL, 2'-Fucosyllactose; 3-FL, 3-Fucosyllactose; LDFT, Lactodifucotetraose; LNT, Lacto-*N*-tetraose; LN*n*T, Lacto-*N*-*neo*tetraose; LNFP, Lacto-*N*-fucopentaose; LNDFH, Lacto-*N*-difucohexaose; Fuc, fucose; Glc, glucose; GlcNAc, *N*-Acetylglucosamine; Gal, galactose

** Concentration values represent average ± standard error (n = 4)

Bacterial Strains and Culture Conditions in HMO-Supplemented Medium

Four species that are representative of the infant gut-associated bifidobacterial community were used in the study. *Bifidobacterium bifidum* JCM 1254 and *Bifidobacterium longum* subspecies *infantis* JCM 1222 (ATCC 15697^{T}) (*B. infantis*) were obtained from the Japan Collection of Microorganisms (JCM; RIKEN Bioresource Center, Japan). *Bifidobacterium breve* NCIMB 8807 (UCC2003) was obtained from the National Collection of Industrial Food and Marine Bacteria Ltd. (NCIMB; Aberdeen, UK). *Bifidobacterium longum* subspecies *longum* MCC 10007 (*B. longum*) was provided by Morinaga Milk Industries, Co. Ltd. All strains used in this study were stored in glycerol stocks and kept frozen at −80 °C until use. All strains were routinely grown in and pre-cultured in Gifu Anaerobic Medium (GAM) broth (Nissui Pharmaceutical, Tokyo, Japan) under anaerobic conditions using the AnaeroPack system (Mitsubishi Gas Chemical Co., Tokyo, Japan) at 37 °C. Culturing experiments were performed in YCFA medium, a medium with yeast, casitone, and fatty acids (Duncan et al., 2002), which is known for supporting the growth of the majority of gut commensal species (Browne et al., 2016). As a carbon source, the medium was supplemented with 1 % HMOs or Lac as a positive control (*w/v*). All cultures were incubated under anaerobic conditions at 37 °C and growth was monitored by measuring OD_{600} at each time point.

Whole Genome Sequencing

Genomic sequencing for *B. bifidum* JCM 1254 was done with the support of Morinaga Milk Industries, Co. Ltd. Genomic DNA was extracted from *B. bifidum* JCM 1254 sub-cultured in de Mann, Rogosa, Sharpe (MRS) medium. The libraries were prepared using a Nextera XT DNA Library Prep Kit (Illumina Inc.) per manufacturer instructions. Paired-end sequencing (29-fold coverage) and quality trimming and *de novo* assembly of the raw read were conducted with an Illumina MiSeq platform with a MiSeq v3 Reagent Kit and the CLC Genomics Workbench (version 8.0) software packages (Qiagen, Valencia, CA, USA) with default settings. Contigs with less than 100 reads were removed. The open reading frame (ORF) predictions and annotations were performed with the DDBJ Fast Annotation and Submission Tool (DFAST) with the default settings (Tanizawa et al., 2016). Genomes for *B. breve* UCC2003 (Accession Number: NC_020517), *B. longum* MCC 10007 (Accession Number: SAMN06368573), and *B. infantis* ATCC 15697^{T} (Accession Number: NC_011593) were retrieved from the NCBI GenBank public database (https://www.ncbi.nlm.nih.gov/genbank/).

Bacterial genome annotation, in silico reconstructions, and phenotype predictions

In-depth genomic analysis was performed by A. Arzamasov at the Sanford Burnham Prebys Medical Discovery Institute. Subsystems-based, context-driven functional assignments of genes, curation, and reconstruction of HMO metabolism in *B. longum* subsp. *longum* MCC 10007, *B. longum* subsp. *infantis* ATCC 15697^{T}, *B. breve* UCC2003, and *B. bifidum* JCM 1254 were performed in the web-based mcSEED (microbial communities SEED) environment, a private clone of the publicly available SEED platform (Overbeek et al., 2014). Each strain was assigned with a predicted phenotype reflecting the ability (U) or inability (P: catabolic pathway present; 0: catabolic pathway absent) to utilize a specific carbohydrate (see Supplementary Table II-1). Furthermore, data on functional elements (transporters, glycoside hydrolases, downstream catabolic enzymes) involved in bifidobacterial HMO metabolism (Supplementary Table II-2) was collected by the following: (1) extensive literature search using PaperBLAST (Price and Arkin, 2017); (2) exporting information from the Carbohydrate Active enZyme (CAZy) (Lombard et al., 2014) and Transporter Classification (TCDB) (Saier et al., 2016) databases.

Experimental Design

To test for priority effects in infant-gut associated bifidobacterial communities, culturing was performed in three different phases: monocultures, pairwise cultures, and four-species assemblages. For pairwise cultures and four-species assemblages, colonization order was manipulated to examine its effect on community structure. For all culturing experiments, each strain was inoculated with an initial OD_{600} = 0.02 into YCFA medium containing 1 % HMOs as a carbon source, and sampling was performed every 4 hours for 24 hours. At each sampling time point, OD_{600} was measured to monitor growth. An aliquot of the culture medium was also collected and centrifuged. The supernatant was collected for sugar concentration analysis. The bacterial pellet was used for DNA extraction, which was performed using the phenol-chloroform method (Martínez et al., 2009).

All culturing experiments were performed in quadruplicate. Monoculture experiments for each strain were performed to characterize its growth in HMO-supplemented medium, as well as its sugar utilization profiles. Then, pairwise cultures were performed by allowing one species to colonize first and introducing the second species 12 hours later. As a control, both species were inoculated simultaneously (Figure II-1 A). All possible pairwise combinations were tested (Table II-2; Pairwise). A series of four-species assemblages were also performed, in which 8 assembly history sequences were randomly selected so that each species colonized the community first, twice. As a control, all four species were inoculated in

the community simultaneously (Table II-2; Four-Species Assembly). For four-species assemblages, each colonizer was introduced at 4-hour intervals (Figure II-1 B).

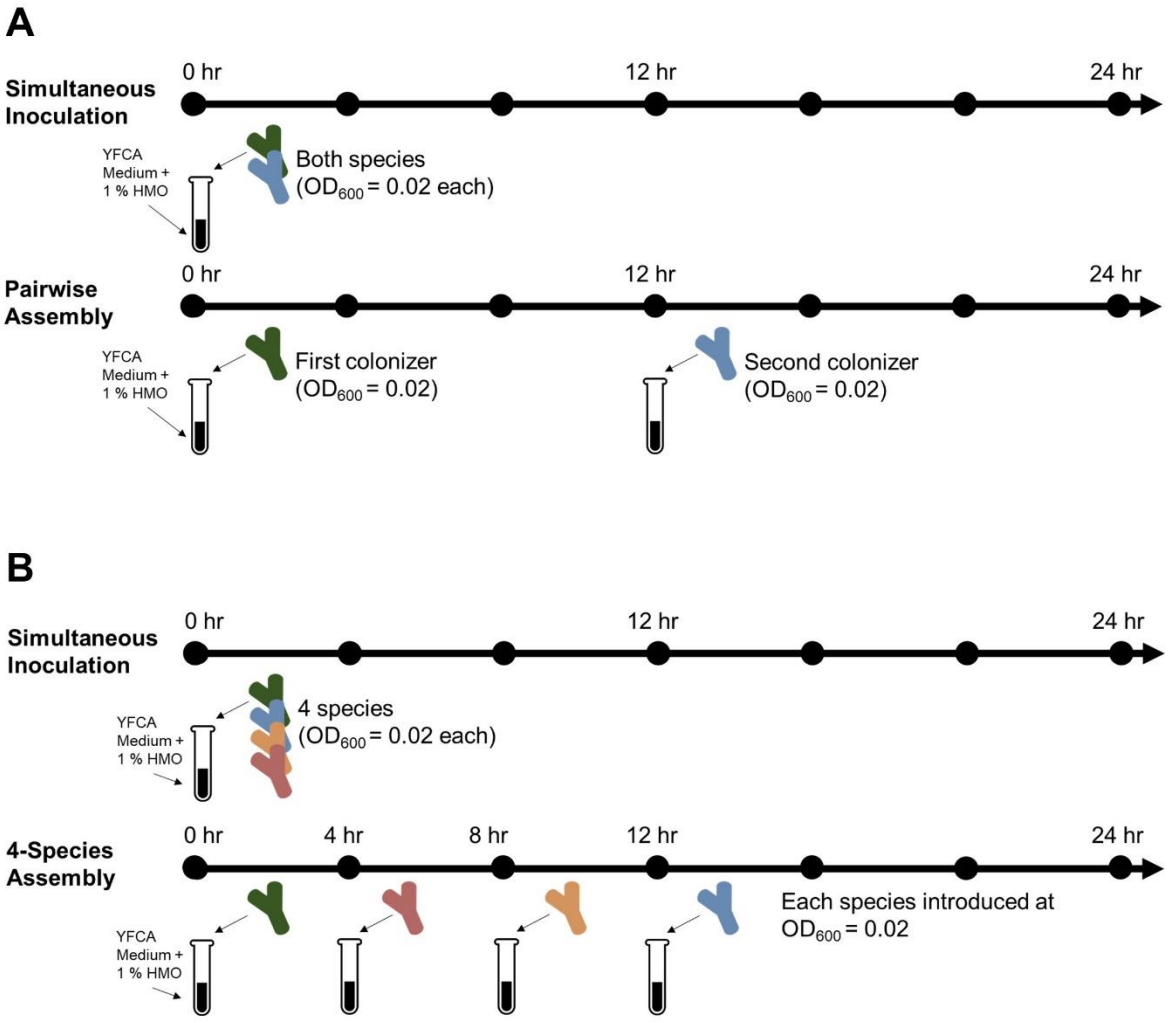

Figure II-1 | **Experimental Design.** All culturing experiments were performed in YCFA medium supplemented with 1 % HMOs (*w/v*) (n = 4). Sampling was performed every 4 hours for 24 hours, indicated by the black dots. All species were introduced at an initial OD_{600} = 0.02 at the time of inoculation. The assembly sequences examined in this study are listed in Table II-2. (A) For pairwise assembly, both members of each pair were inoculated simultaneously as a control. To test for the effect of colonization order, one species was inoculated first, and the second species was inoculated 12 hours later. (B) For four-species assembly, all four species were inoculated simultaneously as a control. The effect of colonization order was tested by introducing each species at 4-hour intervals until all species were inoculated.

Table II-2 | Community assembly sequences used in this experiment.

No.	Culture Type	Arrival Order 1	2	3	4
1	Monoculture	*B. bifidum*	-	-	-
2		*B. breve*	-	-	-
3		*B. infantis*	-	-	-
4		*B. longum*	-	-	-
5	Pairwise (12-hour interval)	*B. bifidum*	*B. breve*	-	-
6		*B. bifidum*	*B. infantis*	-	-
7		*B. bifidum*	*B. longum*	-	-
8		*B. breve*	*B. bifidum*	-	-
9		*B. breve*	*B. infantis*	-	-
10		*B. breve*	*B. longum*	-	-
11		*B. infantis*	*B. bifidum*	-	-
12		*B. infantis*	*B. breve*	-	-
13		*B. infantis*	*B. longum*	-	-
14		*B. longum*	*B. bifidum*	-	-
15		*B. longum*	*B. breve*	-	-
16		*B. longum*	*B. infantis*	-	-
17	Pairwise (Simultaneous)	*B. bifidum* +	*B. breve*	-	-
18		*B. bifidum* +	*B. infantis*	-	-
19		*B. bifidum* +	*B. longum*	-	-
20		*B. breve* +	*B. infantis*	-	-
21		*B. breve* +	*B. longum*	-	-
22		*B. infantis* +	*B. longum*	-	-
23	BIF -1	*B. bifidum*	*B. longum*	*B. infantis*	*B. breve*
24	BIF-2	*B. bifidum*	*B. infantis*	*B. breve*	*B. longum*
25	BRE-1	*B. breve*	*B. bifidum*	*B. longum*	*B. infantis*
26	BRE-2	*B. breve*	*B. longum*	*B. infantis*	*B. bifidum*
27	INF-1	*B. infantis*	*B. breve*	*B. longum*	*B. bifidum*
28	INF-2	*B. infantis*	*B. longum*	*B. bifidum*	*B. breve*
29	LON-1	*B. longum*	*B. bifidum*	*B. infantis*	*B. breve*
30	LON-2	*B. longum*	*B. breve*	*B. infantis*	*B. bifidum*
31	Four-Species (Simultaneous)	*B. bifidum + B. breve + B. infantis + B. longum*			

Sugar Concentration Analysis

Culture supernatant was collected at each time point, clarified by centrifugation, and stored at −30 °C until use. For analysis with HPLC, the samples were thawed and mixed with isomaltoheptaose (internal standard). The sugars were fluorescence-labeled with 2-AA, and the reaction mixtures were desalted by solid-phase extraction as described previously (Anumula, 2006; Asakuma et al., 2011). HPLC was performed using a Thermo U3000 HPLC system (Thermo Fisher Scientific, Waltham, MA). This was equipped with a TSKgel Amide-80 HR column (4.6 × 250 mm, φ = 5 μm) (Tosoh, Tokyo, Japan) at 65 °C, which was equilibrated with 85 % solvent A (acetonitrile) / 15 % solvent B (100 mM ammonium formate buffer, pH 4.3). The elution was performed using a linear increase of solvent B (from 15 % to 85 %) over 90 min at a flow rate of 1 mL/min. Using a Waters 2475 Fluorescence Detector (Waters Corp., Milford, MA), the labeled sugars were detected at an excitation wavelength of 350 nm and an emission wavelength of 420 nm. The concentrations of mono- and oligosaccharides remaining in the spent medium were calculated based on the standard curves generated using similarly labeled standard sugars, and the data were normalized using the internal standard. The concentration of Fuc was measured separately with a colorimetric assay using fucose dehydrogenase (FDH) as described previously (Cohenford et al., 1989).

Species Abundances

From the DNA extracted with bead-beating and the phenol-chloroform method (Martínez et al., 2009), the relative abundance of each species within each sample was quantified using real-time quantitative PCR (qPCR). The obtained relative abundance was then multiplied by the OD_{600} to show its relative proportion within the community at each time point. Real-time qPCR was performed with a Thermal Cycler Dice Real-Time System (TaKaRa Bio., Kyoto, Japan) as described previously (Kato et al., 2017). The primer sets used in this study are listed in Table II-3. Primer specificity was confirmed before the start of the experiment. Known concentrations of genomic DNA extracted from each species were used as reference curves for species-specific quantification.

Table II-3 | List of primers used in this study

Species		Primer Sequence	Reference
Bifidobacterium bifidum	F	5′-CCACATGATCGCATGTGATTG -3′	(Matsuki et al. 1998)
	R	5′-CCGAAGGCTTGCTCCCAAA -3′	
Bifidobacterium breve	F	5′-CCGGATGCTCCATCACAC -3′	(Matsuki et al. 1998)
	R	5′-ACAAAGTGCCTTGCTCCCT -3′	
Bifidobacterium longum subspecies *infantis*	F	5′- ACATCCAGGACCGTAACCTG -3′	(Toda et al. 2019)
	R	5′- GCTTGTGCAGCTCCGTCT -3′	
Bifidobacterium longum subspecies *longum*	F	5′- TTCCAGTTGATCGCATGGTC -3′	(Matsuki et al. 1998)
	R	5′- GGGAAGCCGTATCTCTACGA -3′	

Metagenome Data Mining and Taxonomic Profiling

Infant gut metagenomic data were obtained from SRA (Sequence Read Archive; Accession Number: PRJEB6456) (Bäckhed et al., 2015), and analyzed with the support of K. Yoshida at the Morinaga Milk Industries, Co. Ltd. Raw reads containing the letter 'N' (base pair not identified) were discarded. Reads containing the bacteriophage phiX DNA sequence were identified by mapping them against the reads using Bowtie2 (version 2.3.4.1) (Langmead and Salzberg, 2012) with preset options and discarded. Reads were trimmed for adapter sequences using cutadapt (version 2.9) (Martin, 2011), and reads containing quality values of 17 or less were consecutively tailed-cut at the 3' termini within the cutadapt program. Reads with lengths 50 or less were discarded. Next, reads were mapped against the human genome (GRCh 38) using Bowtie2. Those reads mapped on the human genome were discarded.

The high-quality reads were aligned to a pre-calculated operational taxonomic unit (OTU) dataset stored in VITCOMIC2 (Mori et al., 2018) using BLAST+ (version 2.6.0) (Camacho et al., 2009) (e-value $< 1 \times 10^{-8}$) so that reads were filtered for bacterial and archaeal 16S rRNA sequences, whereas tRNA, 23S rRNA, and the internal transcribed spacer (ITS) sequences were excluded. As a result, there were 51,607 ± 33,408 reads per sample (means ± standard deviation). The filtered reads were aligned to the LTP of the SILVA database (version 132) (Yarza et al., 2010, 2014) using BLASTn (e-value $< 1 \times 10^{-8}$, sequence identity > 97 %, alignment coverage > 80 %), and only top hits were selected. We then calculated the relative abundance of each bifidobacterial species. Note that analysis was performed at the species level and did not differentiate between subspecies. Therefore, *B. longum* and *B. infantis* populations are both categorized within the *B. longum* group. If a read was aligned to more than one

taxonomic sequence in the database with equal alignment scores, those taxonomies or genes were given a value of 1 divided by the number of taxonomies. Taxonomic ratios and RPKM were then calculated.

Microbiome data for the 98 infant-mother pairs were available for four different time points: the mother at the time of infant birth, and the infant at 0, 4, and 12 months of age. For analysis, we selected 41 pairs from the 98 available infant-mother pairs. We selected pairs in which the infant was vaginally delivered, exclusively breastfed until 4 months of age, and had no history of antibiotic use (Figure II-6 A).

Statistical Analysis

Statistical analysis was performed using R ver. 4.0.2 (www.r-project.org). The effect of colonization history on community composition was analyzed with several multivariate techniques. To determine the effect size and significance of each covariate with permutational multivariate analysis of variance (PERMANOVA), the 'envfit' function in the package 'vegan' (Oksanen et al., 2019) was used, and ordination was performed using nonmetric multidimensional scaling (NMDS). We also performed principal components analysis (PCA) with the 'princomp' function. The strength of priority effects was assessed using regression analysis by relating the final population abundance of each species to its arrival order. Negative relationships between population abundance and arrival order were considered to be indicative of inhibitive priority effects (Pu and Jiang, 2015). The metagenomic data extracted from public databases were also analyzed with the 'envfit' function and visualized with NMDS as described above.

Growth Experiments in 2'-FL Supplemented Medium

Further pairwise culturing experiments with *B. breve* and *B. infantis* were performed with 2'-FL and its constituent sugars (n = 3). YCFA medium was supplemented 1 % (*w/v*) with one of the following carbohydrate sources: 2'-FL, Lac, Glc, Gal, Fuc, Fuc + Lac (1:1 molar ratio), Fuc + Glc + Gal (1:1:1 molar ratio). The strains were inoculated into the medium with three different assembly sequences (Table II-2; Sequences 9, 12, 20) with an initial OD_{600} = 0.02, and the final community composition at 24 h was analyzed. The relative abundance of each strain was determined with real-time qPCR.

Additionally, the amount of Fuc expelled from *B. infantis* and *B. longum* cells was also examined (n = 3). *B. infantis* and *B. longum* were each inoculated at an initial OD_{600} = 0.02 in YCFA medium supplemented with 1 % (*w/v*) of 2'-FL. Culture supernatant was collected at each time point, clarified by centrifugation, and stored at −30 °C until use. The concentration of fucose was measured with a colorimetric assay using FDH (Cohenford et al., 1989).

Results

Characterization of Infant Gut-Associated Bifidobacterial Strains

Four infant gut-associated *Bifidobacterium* strains were used in this study: *B. breve* UCC2003, *B. bifidum* JCM 1254, *B. longum* MCC 10007, and *B. infantis* ATCC 15697^T. Predicted HMO-utilization phenotypes of each strain are summarized in Table II-4. Using the subsystem approach implemented in mcSEED, we first analyzed the representation of genes encoding transporters and catabolic pathways for HMO constituents/degradation products, namely glucose (Glc), galactose (Gal), *N*-acetylglucosamine (GlcNAc), fucose (Fuc), lacto-*N*-biose (LNB), and lactose (Lac). Second, we analyzed repertoires of glycoside hydrolases (GHs) and HMO transporters in each of the four *Bifidobacterium* strains, summarized in Figure II-2. Monocultures of each strain were also performed with 1 % (*w/v*) of Lac or HMOs (Figure II-3 A) and the concentration of the carbohydrates remaining in the culture supernatant was quantified (Figure II-3 B).

Overall, genes of intracellular Glc, Gal, GlcNAc, and LNB metabolic pathways were conserved in all four strains, suggesting a similar potential to catabolize these carbohydrates (Supplementary Table II-1, 2). The notable exception was the apparent absence of the Fuc catabolic pathway in *B. bifidum* JCM 1254, suggesting the inability of this strain to catabolize Fuc. In contrast, there were significant differences in gene representation of monosaccharide transporters, which were predicted to reflect differences in utilization of respective monosaccharides from the medium (Supplementary Table II-1). While all four strains possessed at least one Glc transporter, only *B. longum* MCC 10007 and *B. infantis* ATCC 15697^T had Gal transporters, GalP (GlcP) (Parche et al., 2006; Suzuki et al., 2008) and Blon_1383, respectively, and only *B. infantis* ATCC 15697^T and *B. breve* UCC2003 had the predicted Fuc transporter FucP (Supplementary Table II-2). All four strains were predicted to utilize lactose based on the presence of Lac permease LacS (O'Connell Motherway et al., 2013) and β-1,4-galactosidase Bga2A (GH2) (Yoshida et al., 2012) orthologs in all four genomes (Supplementary Table II-2).

With regards to the HMO utilization genes, the strains used in this study possessed varying sets of GHs and HMO transporters, reflecting different HMO utilization strategies within the *Bifidobacterium* genus. Overall, *B. infantis* ATCC 15697^T had the richest set of intracellular GHs and HMO transporters, whereas *B. bifidum* JCM 1254 had the richest set of extracellular GHs (Katoh et al., 2020).

All four strains were predicted to utilize LNT. *B. infantis* ATCC 15697^T and *B. breve* UCC2003 are predicted to transport LNT into the cell via GltABC (Garrido et al., 2011) and degrade it through a coordinated action of β-galactosidases Bga42A (GH42) and Bga2A (GH2) (Yoshida et al., 2012) and β-1,3/4/6-*N*-acetylglucosaminidase Hex1 (GH20) (Garrido et al., 2012). *B. longum* MCC 10007 and *B.*

bifidum JCM 1254 are both predicted to use extracellular lacto-*N*-biosidases LnbX (GH136) (Sakurama et al., 2013; Yamada et al., 2017) and LnbB (Wada et al., 2008), respectively, to cleave LNT into LNB and Lac, and then transport these disaccharides inside the cell. *B. longum* MCC 10007, unlike the other strains, was predicted to be unable to utilize LN*n*T based on the absence of any known orthologs of LN*n*T transporter genes (Blon_2345-2347 and NahS) (Garrido et al., 2011; James et al., 2016) in the genome of this strain. However, *B. longum* MCC 10007, together with *B. infantis* ATCC 15697^{T}, was predicted to utilize specific fucosylated HMOs (2'-FL, 3-FL, LDFT, LNFP I) based on the presence of orthologs of the FL transporter-2 (Sakanaka et al., 2019) and α-1,2-L-fucosidase BiAfcA (GH95) (Sela et al., 2012) genes. *B. infantis* also possesses BiAfcB, an α-1,3/4-L-fucosidase (GH29) (Sela et al., 2012). In contrast, *B. bifidum* uses extracellular fucosidase AfcA (GH95) and AfcB (GH29) (Katayama et al., 2004; Ashida et al., 2009) to release fucose from 2'-FL and 3-FL, and assimilate liberated lactose via LacS.

To examine HMO-consumption behaviors of the strains *in vitro*, each strain was cultured with either Lac (as the positive control) or HMOs, and sugar consumption was monitored using HPLC. Consistent with the genomic predictions, all strains grew well on Lac. Furthermore, the strains with the richest set GHs and HMO transporters, *B. bifidum* and *B. infantis* (Supplementary Table II-2), showed substantial growth (final OD_{600} > 0.7) with HMOs. *B. longum* showed moderate growth (final OD_{600} > 0.5), while *B. breve* showed limited growth (final OD_{600} < 0.3) (Figures II-2, II-3 A). Overall, the carbohydrate utilization profiles were consistent with the phenotypes predicted from genomic data, as *B. bifidum* and *B. infantis* consumed all types of HMOs. *B. longum* consumed fucosylated HMOs (2'-FL, 3-FL, LDFT, and LNFP I) as well as LNT, while *B. breve* only utilized LNT and LN*n*T (Figures II-2, II-3 B, Supplementary Table II-2). We note that although *B. longum* can neither consume LN*n*T nor grow in LN*n*T supplemented medium, we observed a slight decline in the amount of LN*n*T towards the end of *B longum* monoculture (Figure II-3 B).

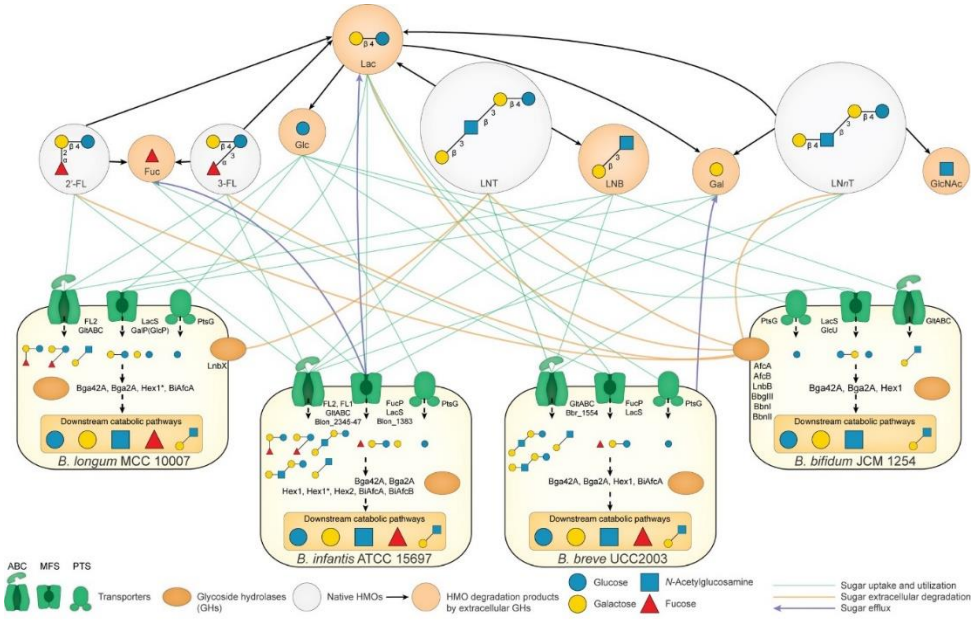

Figure II-2 | **Schematic summary of predicted HMO-utilization phenotypes of each bifidobacterial strain.** The HMO-utilization phenotypes of each bifidobacterial strain (*B. bifidum* JCM 1254, *B. breve* UCC2003, *B. infantis* ATCC 15697^{T}, and *B. longum* MCC 10007) were characterized based on genomic predictions and monocultures. Each strain is shown with its respective transporters and GHs (see Supplementary Table II-2). The utilization pathways for four representative HMO molecules (2'-FL, 3-FL, LNT, and LN*n*T) and their mono- and di-saccharide degradants (Lac, LNB, Fuc, Glc, Gal, GlcNAc) are shown. The green lines indicate sugar uptake and utilization by each strain. The orange lines connect bacterial enzymes with the degraded substrates. The black arrows connect HMO molecules with their degradants after extracellular degradation. The purple arrows indicate sugars that are expelled from the strains.

Table II-4 | Summary of predicted HMO-consumption phenotypes of the strains used in this study.

Strain	Characteristics
Bifidobacterium bifidum JCM 1254	Utilizes all types of HMOs through extracellular degradation, but leaves mono- and di-saccharides degradants unconsumed (Gotoh et al., 2018). Cannot utilize Fuc but expected to be a strong competitor.
Bifidobacterium breve UCC2003	Cannot utilize fucosylated HMOs and is limited to the use of LNT, LN*n*T, and other HMO degradants, such as Lac, LNB, Glc, and Fuc. Expected to be the weakest competitor.
Bifidobacterium longum subsp. *infantis* ATCC 15697^{T}	Utilizes all types of HMOs by importing them whole for intracellular degradation, and therefore expected to be a strong competitor.
Bifidobacterium longum subsp. *longum* MCC 10007	Capable of utilizing fucosylated HMOs (2′-FL, 3-FL, LDFT, LNFP I), but cannot utilize LN*n*T. Expected to be a moderate competitor.

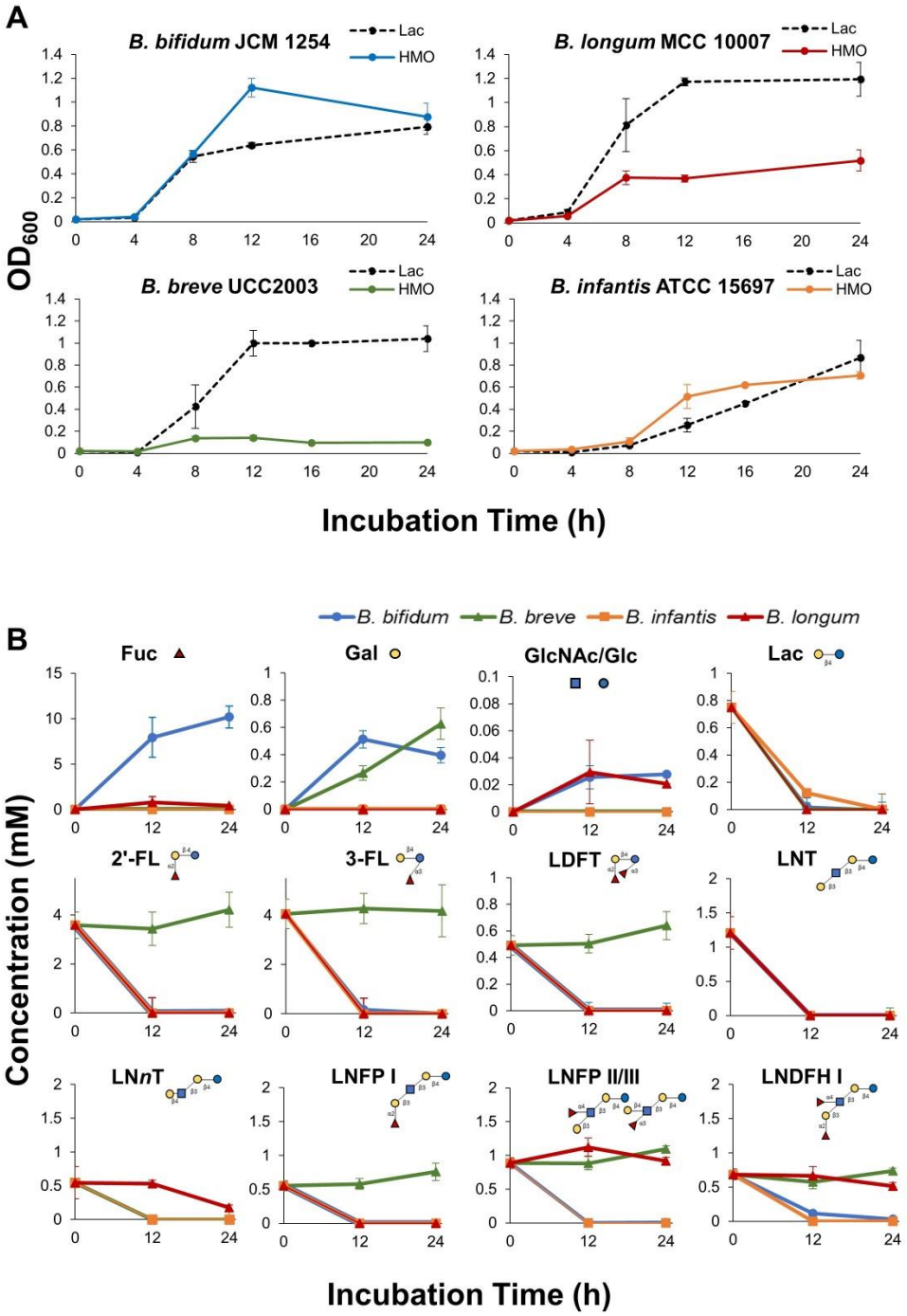

Figure II-3 | Monoculture growth and HMO-utilization profiles of strains used in this study. Each strain was grown in HMO-supplemented YCFA medium as monocultures (n = 4). A) Growth of each strain was monitored by measuring OD_{600} at each time point. All strains were also grown in Lac as a positive control, shown as black dotted lines. Error bars represent ± standard error. B) Culture supernatant was collected at each time point. The remaining sugars in the medium were labeled with 2-AA and analyzed by HPLC (as described in the Materials and Methods section). The consumption of each sugar by each strain is indicated by different colors (blue: *B. bifidum*, green: *B. breve*, orange: *B. infantis*, red: *B. longum*). Error bars represent ± standard error. It should be noted that LNB was not detected at the indicated time points.

Pairwise Culturing in HMO-Supplemented Medium

To determine whether priority effects influenced the outcome of competition in bifidobacterial species, we performed a series of pairwise cultures. For each pair, one species was inoculated into the culture medium first, and the second species was inoculated 12 hours later. As a control, both species were inoculated into the medium simultaneously. The growth curves of all pair and colonization history combinations are summarized in Figure II-4. A competitor was considered dominant if its relative abundance was > 50 % of the community.

When *B. bifidum* JCM 1254 was cultured with *B. infantis* ATCC 15697^{T}, the first colonizer dominated. Notably, *B. bifidum* was a stronger competitor overall as it dominated in simultaneous culture and maintained a stable population even when *B. infantis* was inoculated first. For *B. bifidum* and *B. longum*, *B. bifidum* dominated in all scenarios. Although *B. longum* did not go extinct when inoculated first, *B. bifidum* was the dominant competitor by 24 h (relative abundance: 54.7 %).

When *B. bifidum* was cultured with *B. breve*, *B. bifidum* dominated in simultaneous culture and when it was the first colonizer. Despite its limited HMO-consumption ability and low-growth in HMO-supplemented medium (Figure II-3), *B. breve* dominated and drove *B. bifidum* to near extinction when inoculated first. However, *B. breve* growth remained low until *B. bifidum* inoculation, with an average OD_{600} of 0.26 at 12 h. Twelve hours after *B. bifidum* inoculation, *B. breve* growth reached a final OD_{600} of 0.82, which is a 3-fold higher biomass compared to that of monoculture. A similar pattern was observed for the *B. breve* and *B. infantis* pair, in which *B. breve* growth remained low until the inoculation of *B. infantis*. After *B. infantis* was introduced, *B. breve* reached a final OD_{600} of 0.82 by 24 h.

In the *B. infantis* and *B. longum* pair, *B. infantis* generally dominated regardless of colonization order. As for the *B. breve* and *B. longum* pair, the final total OD_{600} was low in all assembly sequences (Simultaneous: 0.30, *B. longum* first: 0.50, *B. breve* first: 0.37), but *B. breve* dominated in all scenarios. While HMOs were completely consumed in most pair combinations by the end of the culturing period, larger oligosaccharides (LNFP II/III and LNDFH I) remained in the spent medium of *B. breve* and *B. longum* cultures (Supplementary Figures II-1, 2, 3, 4).

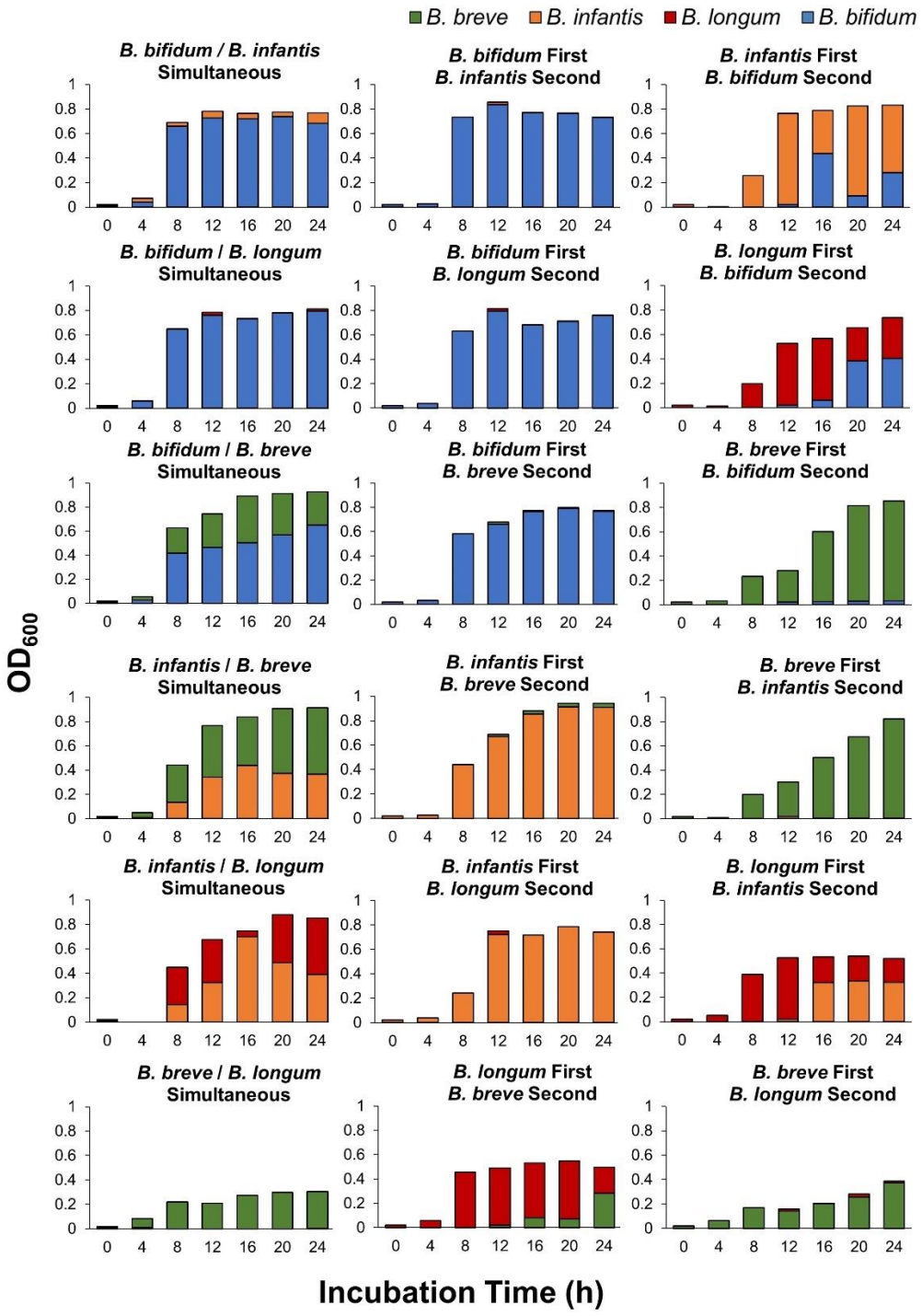

Figure II-4 | **Pairwise culturing results.** Pairwise culturing experiments were performed for all possible combinations, shown as the average of biological quadruplicates (n = 4). In simultaneous cultures, both species were introduced together into medium supplemented with HMOs at the beginning of the experiment. To test for the effect of assembly history, the first species was inoculated at the beginning of the experiment, and the second species was inoculated 12 hours later. OD_{600} was measured at each time point, and the relative abundance of each species was quantified using qPCR. The relative abundance of each strain is indicated by different colors (blue: *B. bifidum*, green: *B. breve*, orange: *B. infantis*, red: *B. longum*).

Four-Species Assemblages in HMO-Supplemented Medium

Next, assembly history was manipulated with all four bifidobacterial strains. As a control, all four species were inoculated simultaneously at the beginning of the experiment. Eight assembly sequences were randomly selected so that each species was the first colonizer twice (Table II-2).

As shown in Figure II-5 A, *B. breve* (relative abundance: 77.5 %) was the dominant competitor in simultaneous culture, followed by *B. bifidum* (relative abundance: 21.9 %) and *B. infantis* (relative abundance: 0.6 %) at 24 h, while *B. longum* was undetected and presumed to be extinct within 4 hours. For communities with *B. bifidum* as the first colonizer, *B. bifidum* was the dominant species in both BIF-1 and BIF-2 sequences with a final OD_{600} of 0.90 and 0.85, respectively. *B. breve* also dominated when it was the first colonizer. However, the overall growth of the community (final OD_{600}) was dependent on the identity of the second colonizer. While its final OD_{600} reached 0.90 when *B. bifidum* was the second colonizer (BRE-1), the final OD_{600} was 0.78 when *B. longum* was second (BRE-2). In assembly sequences in which *B. infantis* was first, *B. infantis* dominated when the second colonizer was *B. longum* (INF-2). However, *B. infantis* was outcompeted by *B. breve* when *B. breve* was the second colonizer (INF-1). With regards to *B. longum*, not only was it unable to become the dominant competitor in all assembly sequences, but it was also undetected by 24 h in all sequences, except for LON-1. In the LON-1 sequence, *B. longum* was inoculated first and followed by *B. bifidum*.

Principal components analysis based on the final community structure at 24 h revealed three different possible community outcomes: 1) *B. breve* dominant, 2) *B. bifidum* dominant, and 3) *B. infantis* dominant (Figure II-5 B; Supplementary Table II-3 A). Further analysis with PERMANOVA based on Bray-Curtis distances revealed that assembly history had a significant influence on final community structure ($F(8,27) = 64.28$, $p < 0.001$), and the identity of the first colonizer (Partial $R^2 = 0.91$, $p < 0.001$) and the second colonizer (Partial $R^2 = 0.04$, $p < 0.001$) determined final community outcome.

Regression analysis was performed to quantify the strength of priority effects. Calculations were performed to predict final population abundance of each species based on arrival order. A significant negative relationship was found for *B. breve* ($F(1,30) = 335.3$, $p < 0.001$, $\beta = -0.29$, $R^2 = 0.9179$), *B. bifidum* ($F(1,30) = 30.94$, $p < 0.001$, $\beta = -0.24$, $R^2 = 0.5077$), and *B. infantis* ($F(1,30) = 6.615$, $p < 0.05$, $\beta = -0.12$, $R^2 = 0.1807$), indicating that the earlier a species was introduced into the community, the higher its final abundance. However, no significant relationship was found for *B. longum* ($F(1,30) = 1.811$, $p > 0.05$, $\beta = -0.01$, $R^2 = 0.02854$).

We also examined the HMO utilization profiles of each assembly sequence (Supplementary Figure II-5). Principal components analysis based on the final HMO utilization profiles at 24 h showed that the first principal component, which was mainly driven by the amount of fucose remaining in the medium,

explained 98.77 % of the variation (Figure II-5 C, Supplementary Table II-3 B). One cluster contained communities dominated by *B. bifidum* with high amounts of fucose remaining in the spent medium. A second cluster contained communities dominated by *B. breve*, in which 3-FL and LNDFH I remained unconsumed.

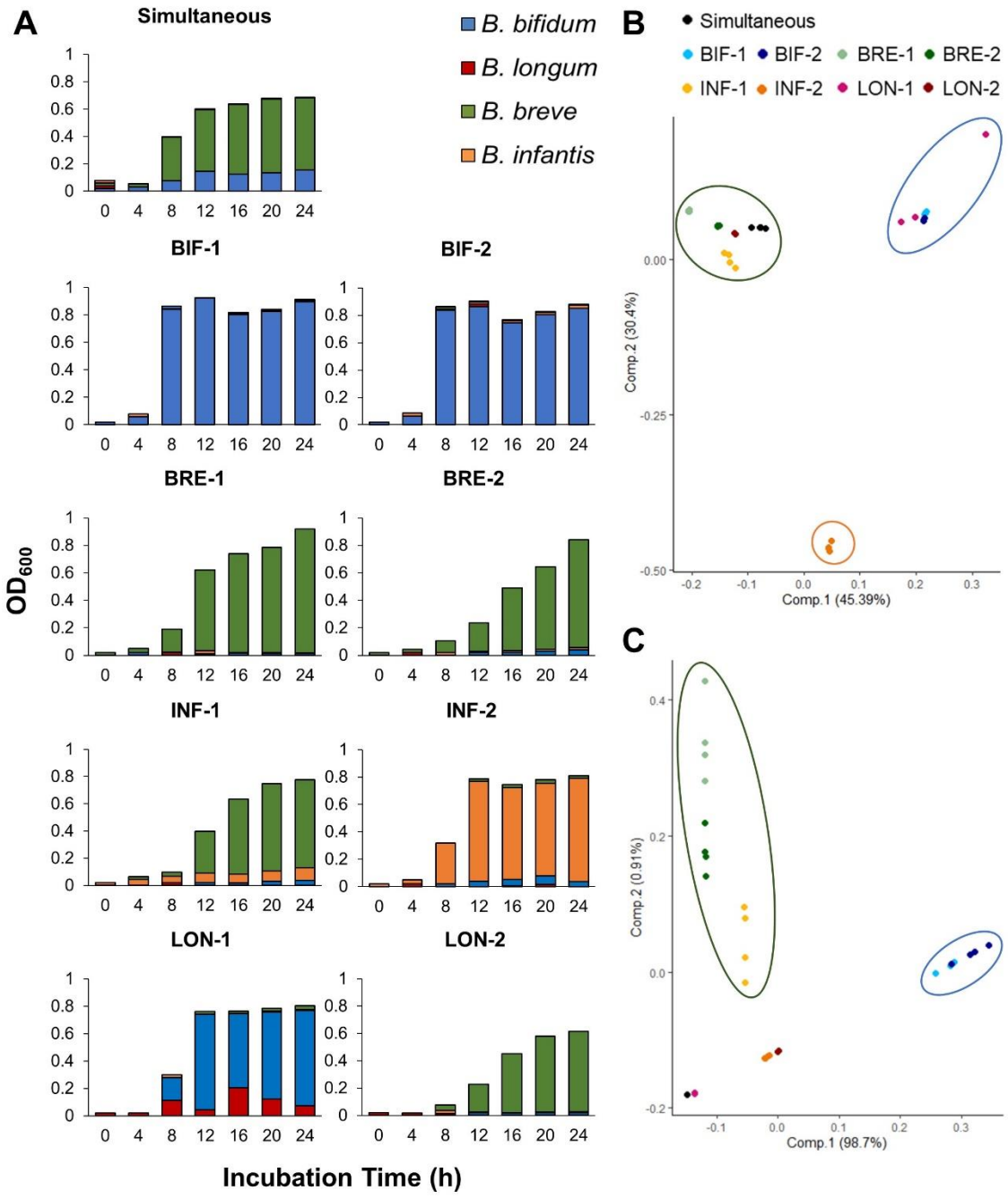

Figure II-5 | Results of four-species assemblages. Culturing experiments were performed with all four species, and assembly order was manipulated (n = 4). Assembly history sequences, summarized in Table II-2, were randomly selected so that each species was the first colonizer twice. As a control, all four species were introduced into medium supplemented with HMOs at the beginning of the experiment (Simultaneous). A) OD_{600} was measured at each time point, and the relative abundance of each species was quantified using qPCR. The relative abundance of each strain, shown as the average of biological quadruplicates, is indicated by different colors (blue: *B. bifidum*, green: *B. breve*, orange: *B. infantis*, red: *B. longum*). B) Principal components analysis was performed based on the final community composition at 24 h. Each color represents a different assembly sequence. Clusters are indicated by the blue (*B. bifidum* dominant communities), green (*B. breve* dominant communities), and orange circles (*B. infantis* dominant communities). C) Principal components analysis was performed based on the final HMO-utilization profiles at 24 h. Each color represents different assembly sequences, and clusters are indicated by the blue (communities with high amounts of fucose) and green (communities with 3-FL and LNDFH I unconsumed) circles.

Comparison with in vivo Data

Bifidobacterial communities in a cohort of 98 European infant-mother pairs from a study performed by Bäckhed et al. (2015) were analyzed. This metagenomic dataset followed the infant gut microbiome at 0, 4, and 12 months of age, as well as the mother's gut microbiome at the time of infant birth. From this cohort, 41 samples were selected based on the following criteria: infants who were vaginally delivered (to test for the effect of vertical transmission from the mother), exclusively breastfed infants (to test for priority effects in the presence of HMOs), and infants who had no history of antibiotic use (Figure II-6 A).

The microbiomes of infants at 4 months of age were analyzed. As factors, the abundance of each bifidobacterial species in the mother and in the infants at birth were tested. PERMANOVA revealed that the abundance of *B. breve* in the infant gut microbiome at birth contributed to the final community structure at 4 months (Partial $R^2 = 0.19$, $p = 0.0478$; Supplementary Table II-4). Furthermore, individuals with higher *B. breve* abundance at birth had a persistent *B. breve* population at 4-months old (Figure II-6 B; Supplementary Figure II-6), and there was a significant positive correlation between the *B. breve* abundance at birth and at 4 months (Pearson's $r = 0.58$, $p < 0.01$), suggesting that *B. breve* can benefit from priority effects. However, no significant correlation was observed for other species.

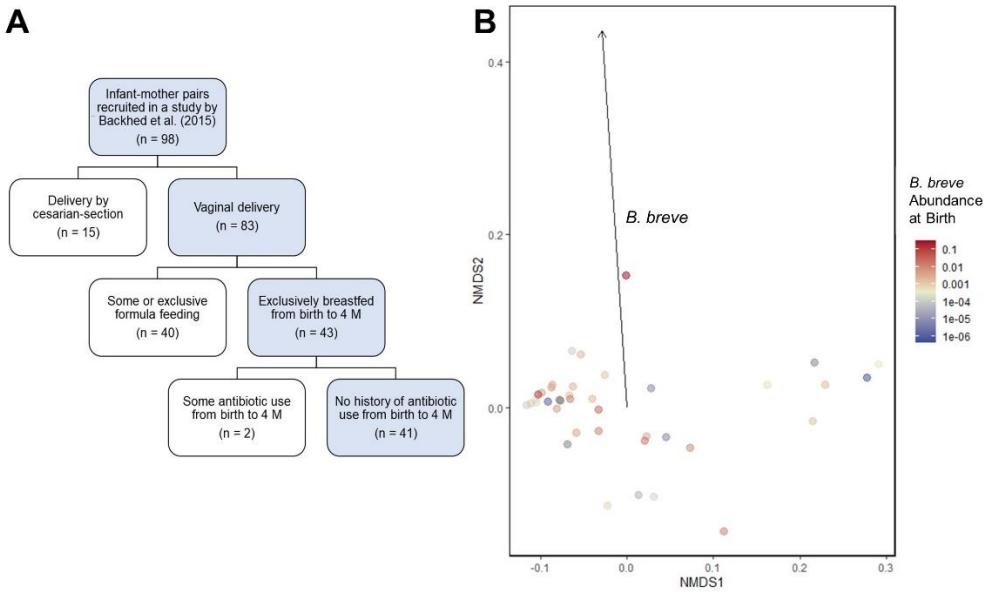

Figure II-6 | **Analysis of *in vivo* microbiome data.** A) Sample selection flow chart. Of the 98 infant-mother pair microbiome data, we selected 41 samples (shaded in blue) in which the infant was delivered vaginally, exclusively breastfed, and had no history of antibiotic use from birth. B) Nonmetric multidimensional scaling (NMDS) ordination plots of gut microbial community data from infants at 4 months of age. Each point corresponds to one individual. The color gradient indicates the initial *B. breve* abundance at birth. Statistically significant loadings are indicated as black arrows. (4M: 4-month-old infants)

Competition and Growth in 2'-FL Supplemented Medium

To further examine the competitive differences between *B. breve* and *B. infantis*, additional pairwise growth experiments were performed. *B. breve* and *B. infantis* were cultured in medium supplemented with 2'-FL and its constituent sugars (Lac, Fuc, Glc, Gal). Either *B. breve* or *B. infantis* was introduced first, and the other species was introduced 12 hours later. As a control, both species were introduced simultaneously. Apart from 2'-FL, the first colonizer dominated in the community, and *B. breve* dominated in simultaneous cultures (Supplementary Figure II-7).

We also performed monocultures with *B. infantis* and *B. longum* in medium supplemented with 1 % 2'-FL. For *B. infantis*, Fuc begins to accumulate in the spent medium between 8 and 12 h of culture and gradually decreases over the following 12 h. The accumulation of Fuc was significantly lower in *B. longum* cultures (Supplementary Figure II-8).

Discussion

Assembly history and priority effects dictate community outcome

This study utilized a reductionist approach that focused on infant gut-associated bifidobacterial communities in environments where HMOs are the primary carbon source. In this study, we were able to experimentally control the timing of species arrival, allowing us to evaluate the effect of assembly history and priority effects. Four strains that display a variety of species-specific mechanisms for HMO-assimilation were used. Based on the predicted phenotypes and monoculture data, we hypothesized that in HMO-supplemented medium, (1) *B. bifidum* JCM 1254 and *B. infantis* ATCC 15697^{T} would be strong competitors due to their ability to assimilate a variety of HMOs through extracellular and intracellular GHs, respectively, (2) *B. longum* MCC 10007 would be a moderate competitor, as it cannot consume LN*n*T, but can consume specific fucosylated sugars such as 2'-FL, 3-FL, LDFT, and LNFP I, and (3) *B. breve* UCC2003 would be a weak competitor due to its limited HMO consumption abilities (Figure II-2; Table II-4; Supplementary Table II-2).

Both inhibitory priority effects and facilitative priority effects were observed in this study. The former prevents the colonization of later-arriving species, while the latter promotes the growth of later-arriving species. In pairwise assembly, inhibitory priority effects were observed when the relative fitness difference, based on HMO-consumption abilities, between the two species was small and resource overlap was high. For example, when *B. bifidum* and *B. infantis*, two species that can consume all types of HMOs, were cultured together, the first colonizer became the dominant species (Figure II-4). Monoculture data showed that both *B. bifidum* and *B. infantis* consume the available HMOs within 12 hours (Figure II-3 B), consequently making the outcome of competition sensitive to assembly history and dependent on which species acquired the resources first (Fukami, 2015). On the other hand, priority effects were not observed when the predicted relative fitness difference was high. As predicted, *B. longum* did not gain dominance in any assembly sequence when cultured with stronger competitors such as *B. bifidum* and *B. infantis* (Figure II-4), as both species can assimilate the carbohydrates that are left unconsumed by *B. longum* (Figure II-3 B, Supplementary Table II-2). Unexpectedly, *B. longum* was also outcompeted by *B. breve*, despite *B. breve*'s limited HMO consumption-ability (Figure II-4). Furthermore, when cultured first, *B. breve* was able to dominate against stronger competitors (*B. bifidum* and *B. infantis*) despite considerable fitness differences, contradicting both theoretical and genomic predictions (Figure II-4). The possible reasons for *B. breve* dominance will be discussed in detail later.

The results of the four-species assemblages also showed that assembly history had a significant effect on the final community structure. Different assembly sequences gave rise to three different

community states (Figure II-5 B), which is a predicted consequence of priority effects (Chase, 2003; Schröder et al., 2005; Fukami, 2015). Furthermore, PERMANOVA results revealed that the identity of the first and second colonizer determined the community outcome, highlighting the importance of colonization during the early stages of assembly. For instance, in communities with *B. infantis* as the first colonizer (INF-1, INF-2), *B. infantis* dominated in INF-2, in which *B. longum* is the second colonizer, but it was outcompeted in INF-1 when *B. breve* was the second colonizer (Figure II-5 A). It is interesting to note that assembly history not only affected final community composition but also the behavior of growth curves. Both sequences in which *B. breve* was the first colonizer (BRE-1, BRE-2) gave rise to *B. breve*-dominant communities. Exponential growth was observed when *B. bifidum* was second, with the total OD_{600} reaching 0.59 in 12 h, while total OD_{600} was at 0.20 when *B. longum* was second (Figure II-5 A; BRE-1, BRE-2). The exponential growth is most likely due to the fact that *B. bifidum* extracellularly degrades HMOs, leaving the degradants available for competitors to consume (Gotoh et al., 2018). The importance of early colonizers is also seen in a longitudinal study by Yassour et al. (2016). The infants sampled in their study exhibited three different microbial community signatures at birth, which were mostly determined by delivery mode. The guts of infants born vaginally were dominated by Bacteroidetes and Actinobacteria, while the guts of infants born via cesarian section were dominated by Firmicutes and Proteobacteria. However, they also found that a small proportion of vaginally delivered infants exhibited a different microbial community signature, in which Proteobacteria, Actinobacteria, and Firmicutes were present. Differences between these three microbial signatures at birth persisted for at least the first three years of life. These results show that delivery mode and the environmental exposure at birth are significant factors in early life microbial colonization, as they determine the microbial species pool that the infant first contacts postpartum. This suggests that the pioneer colonizers in the gut microbiome are likely to exert a strong influence on community structure long term.

Competitive dominance of B. breve

The behavior of *B. breve* was contrary to our initial predictions based on genomic data. In monoculture, *B. breve* growth was limited in HMO supplemented medium (Figure II-3 A), and sugar concentration analysis revealed that it was only able to consume LNT and LN*n*T (Figure II-3 B, Supplementary Table II-2). Despite this, when *B. breve* was one of the earlier colonizers during community assembly, it outcompeted the other strains. While *B. breve* was not a dominant species in the *in vivo* infant gut microbiome data we analyzed (Bäckhed et al. 2015; Supplementary Figure II-6), PERMANOVA revealed that if *B. breve* was present in the infant gut microbiome at birth, it was more likely to persist in the community at 4 months of age (Figure II-6 B, Supplementary Figure II-6).

Regression analysis of the four-species assembly experiments further corroborated the fact that *B. breve* benefitted from priority effects.

Strong negative relationships between arrival order and relative abundance of each species at 24 h revealed by regression analysis are indicative of inhibitory priority effects (Pu and Jiang, 2015), which was seen for *B. bifidum, B. infantis,* and *B. breve*. For *B. bifidum*-dominant communities, most of the carbohydrates available in the environment were consumed within 8 hours of *B. bifidum* inoculation (Supplementary Figure II-1, II-5 A), suggesting that *B. bifidum* dominated through inhibitory priority effects and niche preemption. While inhibitory priority effects explain *B. bifidum* dominance, it is unlikely for *B. breve*-dominant communities, as sugars such as 3-FL and LNDFH I were unconsumed (Supplementary Figure II-5 B), and later-arriving strains that can utilize those sugars were unable to outcompete *B. breve.* This suggests that *B. breve* dominance is not necessarily due to niche preemption.

One possible explanation could be attributed to facilitative priority effects and the differential fucose-utilization phenotypes. In four-species assemblages, *B. breve* did not dominate when inoculated last (INF-2, LON-1; Figure II-5 A), but a small population persisted at 24 h. Examination of the HMO-utilization profiles of INF-2 and LON-1 showed that both communities had a high amount of fucose remaining in the medium at 12 h, which may have contributed to the persistence of *B. breve* (Supplementary Figure II-5 C, D). During pairwise culture, *B. breve* growth was significantly enhanced when co-cultured with *B. bifidum* or *B. infantis* (Figure II-4). However, while *B. breve* dominates when co-cultured with *B. longum,* the total biomass remained low (Figure II-4). Both *B. bifidum* and *B. infantis* liberated high amounts of fucose during HMO metabolization, while *B. longum* released a relatively small amount (Figure II-2, Supplementary Figure II-8, Supplementary Table II-2). In the *B. longum* and *B. breve* pairwise culture, *B. longum* released a small amount of fucose, which was consumed when *B. breve* was introduced (Supplementary Figure II-4). Among the four strains used in this study, genomic analysis shows that *B. breve* possesses the FucP transporter, which allows for the assimilation of fucose. As *B. bifidum* does not possess this transporter (Supplementary Table II-1, Supplementary Table II-2), niche differentiation may be allowing *B. breve* to maintain a competitive presence when cultured with *B. bifidum.*

However, *B. infantis* also possesses the FucP transporter (Supplementary Table II-1, Supplementary Table II-2). Therefore, to further examine possible causes that give *B. breve* competitive advantage, we performed pairwise competition assays in which *B. breve* and *B. infantis* were cultured in medium supplemented with 2'-FL and its constituent sugars (Lac, Fuc, Glc, Gal), and inoculation order was manipulated. Apart from 2'-FL, which *B. breve* cannot utilize, the first colonizer dominated in the community (Supplementary Figure II-7). However, *B. breve* dominated in simultaneous culture, suggesting that *B. breve* is a stronger competitor if it can utilize the available substrate. It is worth noting

that while *B. breve* cannot utilize 2'-FL, it maintained a population in simultaneous culture, possibly because of the monosaccharides, such as fucose, expelled from *B. infantis* cells (Supplementary Figure II-8; Asakuma et al., 2011). These results suggest that *B. breve* exhibits fast growth in the presence of sugars it can assimilate. Ecological theory predicts that for priority effects to occur, early colonizers need to quickly increase their population size to preempt or modify the niche (Fukami, 2015). While the fast growth rate of *B. breve* could explain strong priority effects for this species, its dominance is observed only after the arrival of competitors, and it is more likely that *B. breve* is benefitting from facilitative priority effects when grown with *B. infantis* and *B. bifidum.* It is possible that when *B. breve* is the prior colonizer, it is able to utilize the HMO-degradants provided by either *B. infantis* or *B. bifidum* and gain dominance within the community. However, when *B. breve* is the latter colonizer, the HMO-degradants are consumed by the other species and no longer available by the time *B. breve* arrives. The predicted mechanisms of facilitative priority effects for *B. breve* when cultured with *B. bifidum* and *B. infantis* are summarized in Figure II-7.

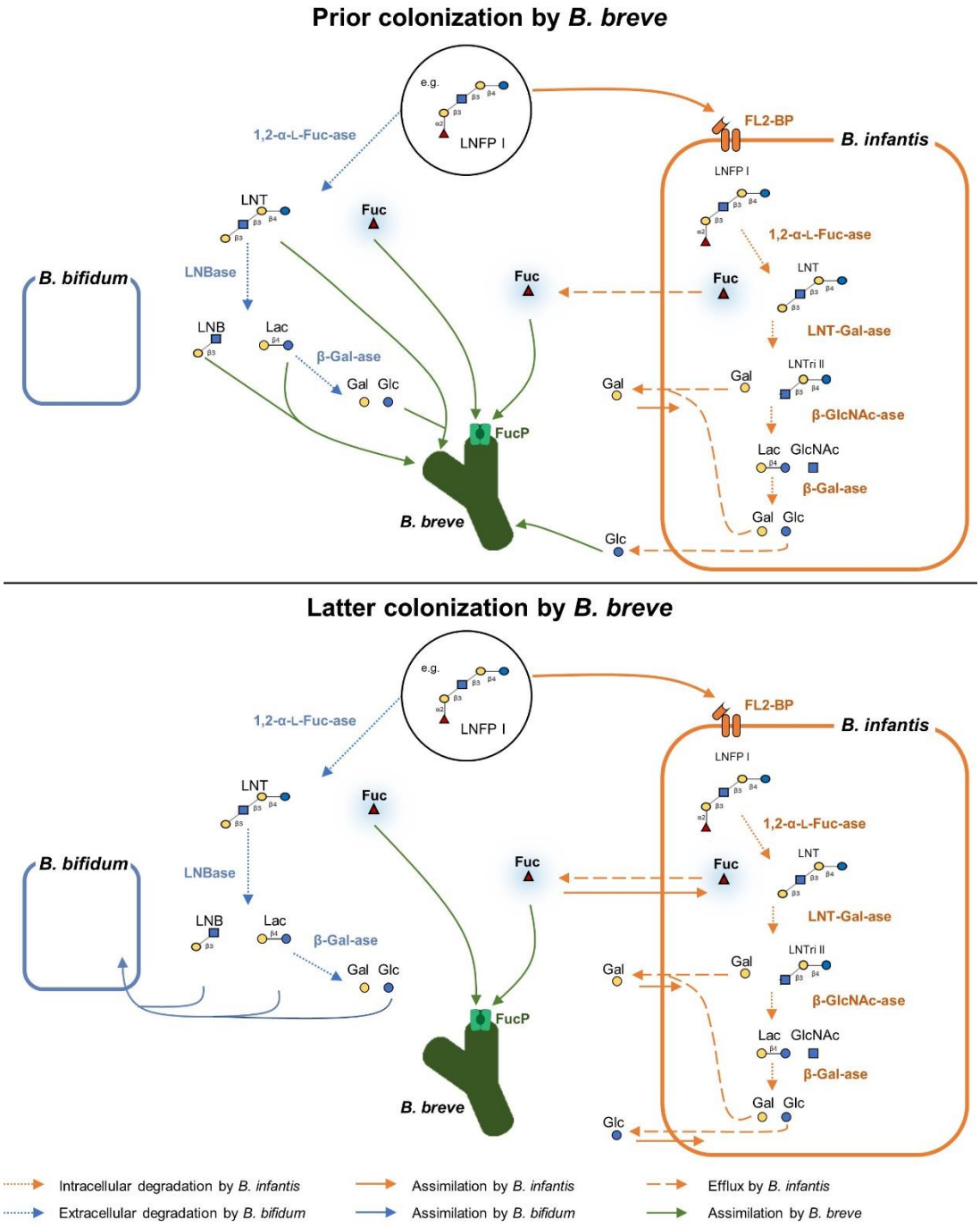

Figure II-7 | Predicted HMO-utilization pathways that enable *B. breve* to benefit from facilitative priority effects. The HMO-utilization pathways, with LNFP I as a representative example, are shown for *B. bifidum*, *B. infantis*, and *B. breve*. Similar mechanisms are expected for other fucosylated HMOs. Activity, enzymes, and transporters attributable to *B. bifidum* are shown in blue, *B. infantis* in orange, and *B. breve* in green. Solid lines indicate assimilation by each species, round-dot lines indicate enzymatic degradation, and dashed lines indicate efflux. If more than one species can utilize the sugar, the pathway predicted to be prioritized is shown. *B. breve* alone cannot assimilate LNFP I, but when *B. breve* is the prior colonizer (top panel), it is present and ready to utilize degradants as soon as they are made available by either *B. bifidum* or *B. infantis*. When *B. breve* is the latter colonizer (bottom panel), most of the degradants are consumed before *B. breve* is introduced. Abbreviations: LNT, Lacto-*N*-tetraose; LNFP, Lacto-*N*-fucopentaose; LNTri, Lacto-*N*-triose, Fuc, fucose; Glc, glucose; GlcNAc, *N*-Acetylglucosamine; Gal, galactose

We cannot exclude the possibility that these results are specific to the strain and medium we used. However, previous work with *B. breve* supports the notion that it is a strong competitor, as data shows that depending on the strain, this species grows well in HMO-supplemented medium (Ruiz-Moyano et al., 2013; Matsuki et al., 2016). Further analysis is needed to determine the mechanisms of *B. breve* dominance. *B. breve* may possess a genomic factor, similar to *ccf*, to gain priority access to the niches available in the intestinal environment (Lee et al., 2013). In our analysis of *in vivo* infant metagenome data, we found patterns suggesting that earlier colonization by *B. breve* at birth promote its persistence later in life. In future studies, we hope to perform further genomic analysis of the same *in vivo* dataset to identify specific genes that are co-occurring in communities with high *B. breve* abundance. Further competition experiments using knock-out strains of those identified genes could help elucidate the mechanism for *B. breve* dominance.

Application of priority effects for probiotics

The presence of priority effects in the bifidobacterial community used in our study, as well as theoretical and circumstantial evidence from previous work, suggests a potential for clinical applications in probiotic therapies. However, direct evidence is still lacking, as experimental manipulation of bacterial colonization in human subjects poses logistic difficulties as well as potential health risks. For instance, a clinical comparison of breastfeeding infant-mother pairs found that supplementation with probiotic species had a limited effect on the gut microbial composition, and in certain cases was associated with a higher risk of infections later in life (Quin et al., 2018). With regards to the use of *Bifidobacterium* species as a probiotic intervention, one study found that *B. breve* BBG-001 successfully colonized the guts of infants, if administered early (Kitajima et al., 1997). However, a randomized clinical trial using the same *B. breve* strain found that it was ineffective in preventing infant necrotizing enterocolitis (NEC), and colonization was only successful in infants at lower risk of adverse outcomes (Costeloe et al., 2016). Prematurely born infants pass through the birth canal rapidly and has aberrant access to maternal microbes (Walker, 2017). Consequently, bifidobacteria may not be one of the first colonizers of the gut for these infants. Although the etiology and pathogenic causes of NEC are still unknown, studies suggest that the onset of NEC is due to preemptive colonization of the preterm gut by undesirable taxa. One study found evidence to suggest that *Clostridium perfringens* colonizes the guts of infants who later develop NEC (De La Cochetière et al., 2004). Taken together, it is possible that prior colonization by pathogenic bacteria prevented colonization by *Bifidobacterium* species, and therefore limited the efficacy of probiotic interventions. These results suggest that the success of probiotic interventions is dependent on strain, timing, and presence of resident taxa, which might be, at least in part, affected by priority effects.

Conclusions

One of the weaknesses of this study is that it focused solely on bifidobacterial communities. Although bifidobacteria are dominant in the infant gut microbiome, their community dynamics are likely affected by other commensal microbes. For example, a study by Ferrario et al. (2015) found that *Bifidobacterium* species growth was dependent on the presence of cysteine produced by other commensals. Furthermore, as obligate anaerobes, bifidobacterial colonization in the infant gut may be dependent on prior colonization by oxygen-depleting taxa such as Enterobacteriaceae (Bokulich et al., 2016). Future work should address the effect of other taxa that are often present, such as *Bacteroides* and *Clostridium* species, as well as the effect of other metabolites.

Despite certain limitations, our results demonstrated the prevalence of priority effects in bifidobacterial communities. Moreover, the results of our study clearly show that *in vitro* community assembly experiments are critical for understanding the interspecies dynamics in infant gut-associated microbes and how those dynamics affect microbial community structuring. The results of our study also revealed the importance of early colonizers during the initial stages of community assembly. These findings draw several implications for the use of probiotic species and how they can be established in the gut more permanently in clinical settings, as colonization resistance is a continuing issue with probiotic therapies (Suez et al., 2019; Walter et al., 2020). In our study, we found that the identity of the first two colonizers in our four-species assembly determined the community outcome, and previous work suggests that once assembled, the community is resilient to both abiotic and biotic disturbances (Dethlefsen and Relman, 2011). Together, this implies that early introduction by just a few taxa can divert the trajectory of the gut microbial community. Therefore, the long-term persistence of bifidobacteria and other probiotic strains might be achieved if the infant gut microbiome is manipulated during the early stages of community assembly. However, the manipulation of bacterial colonization in human subjects should be approached with care, and the effects of specific strains and the timing of their administration on community assembly should be thoroughly evaluated before this practice is applied in clinical settings. With that in consideration, further experimental studies, combined with clinical data, could be used to selectively manipulate the gut microbiome in a way that is both predictable and advantageous to provide disease protection and health-promoting effects for the infant host.

Supplementary Figures and Tables

Supplementary Table II-1 | Summary of sugar utilization phenotypes based on genomic predictions.

Sugar	***B. longum* subsp. *longum* MCC 10007**	***B. longum* subsp. *infantis* ATCC 15697^T**	***B. breve* UCC2003**	***B. bifidum* JCM 1254**
Glucose	U	U	U	U
Galactose	U	U	P	P
N-Acetylglucosamine	P	P	P	P
Fucose	P	U	U	0
Lactose	U	U	U	U
LNB; GNB	U	U	U	U
LNT	U*	U	U	U*
LN*n*T	P	U	U	U*
2'-FL; 3-FL; LDFT; LNFP I	U	U	P	U*

Legend:

U = predicted utilizer (transporter, GH/catabolic enzyme genes are present)

P = predicted non-utilizer with a catabolic pathway
(GH/catabolic enzyme genes are present, but transporters are either absent or unidentified)

0 = predicted non-utilizer

*Extracellular degradation

Supplementary Table II-2 | Summary of genes related to HMO assimilation in the strains used in this study.

Name	Pathway	Annotation	Classification	*B. longum* subsp. *longum* MCC 10007	*B. longum* subsp. *infantis* ATCC 15697^T	*B. breve* UCC2003	*B. bifidum* JCM 1254	Reference
GalK	Galactose catabolism	Galactokinase	EC 2.7.1.6	MCC10007_0432	Blon_2062	Bbr_0492	LOCUS_16870	(Li et al. 2012)
GalE	Galactose catabolism	UDP-glucose 4-epimerase	EC 5.1.3.2	MCC10007_1574	Blon_0538	Bbr_0040	LOCUS_05330	(Nam et al. 2019)
GalT	Galactose catabolism	Galactose-1-phosphate uridylyltransferase	EC 2.7.7.10	MCC10007_0431	Blon_2063	Bbr_0491	LOCUS_16880	(Hidaka et al. 2009)
Pgm	Galactose catabolism	Phosphoglucomutase	EC 5.4.2.2	MCC10007_1664	Blon_1766;Blon_2184	Bbr_0742;Bbr_1595	LOCUS_12450	NA
NagK	GlcNAc catabolism	*N* -acetyl-glucosamine kinase, ROK family	EC 2.7.1.59	MCC10007_1232	Blon_0879	Bbr_1250	LOCUS_01520	(Egan et al. 2016)
NagA	GlcNAc catabolism	*N* -acetylglucosamine-6-phosphate deacetylase	EC 3.5.1.25	MCC10007_1229	Blon_0882	Bbr_1247	LOCUS_14260	(Egan et al. 2016)
NagB	GlcNAc catabolism	Glucosamine-6-phosphate deaminase	EC 3.5.99.6	MCC10007_1230	Blon_0881	Bbr_1248	LOCUS_14270	(Egan et al. 2016)
LnpA	LNB;GNB catabolism	1,3-β-galactosyl-*N* -acetylhexosamine phosphorylase	EC 2.4.1.211	MCC10007_1654	Blon_2174	Bbr_1587	LOCUS_01530	(Kitaoka et al. 2005)
LnpB	LNB;GNB catabolism	*N* -acetylhexosamine 1-kinase	EC 2.7.1.162	MCC10007_1653	Blon_2173	Bbr_1586	LOCUS_01500	(Nishimoto and Kitaoka 2007)
LnpC	LNB;GNB catabolism	UTP-hexose-1-phosphate uridylyltransferase	EC 2.7.7.10	MCC10007_1652	Blon_2172	Bbr_1884	LOCUS_01490	(Nishimoto and Kitaoka 2007)
LnpD	LNB;GNB catabolism	UDP-hexose 4-epimerase	EC 5.1.3.2	MCC10007_1651	Blon_2171	Bbr_1585	LOCUS_01480	(Nishimoto and Kitaoka 2007)
FumB	Fucose catabolism	L-fucose mutarotase	EC 5.1.3.29	NA	Blon_2305;Blon_2337	NA	NA	(James et al. 2019)
FumC	Fucose catabolism	L-fuco-β-pyranose dehydrogenase	EC 1.1.1.122	MCC10007_0307	Blon_2308;Blon_2339	Bbr_1291;Bbr_1743	NA	(James et al. 2019)
FumD	Fucose catabolism	L-fuconolactone hydrolase	EC 3.1.1.-	MCC10007_0306	Blon_2306	Bbr_1290;Bbr_1741	NA	(James et al. 2019)
FumE	Fucose catabolism	L-fuconate dehydratase	EC 4.2.1.68	MCC10007_0308	Blon_0344;Blon_2309;Blon_2340	Bbr_1292;Bbr_1744	NA	(James et al. 2019)
FumF	Fucose catabolism	2-keto-3-deoxy-L-fuconate aldolase	EC 4.1.2.18	MCC10007_0305	Blon_2338	Bbr_1289,Bbr_1740	NA	(James et al. 2019)
FumG	Fucose catabolism	Lactaldehyde reductase	EC 1.1.1.77	MCC10007_1571	Blon_0540	Bbr_1505	LOCUS_03860	(James et al. 2019)
Bga42A (BbgII)	GH	β-1,3/4/6-galactosidase	GH42	MCC10007_0485	Blon_2016	Bbr_0529	LOCUS_05840	(Goulas et al. 2009, Yoshida et al. 2012, Viborg et al. 2014, Amborgi et al. 2019)
Bga2A (BbgIV)	GH	β-1,4-galactosidase	GH2	MCC10007_0744	Blon_2334	Bbr_1552	LOCUS_05290	(Goulas et al. 2009, Yoshida et al. 2012, Ambrogi et al. 2019)
BbgIII	GH	Extracellular β-1,4-galactosidase	GH2	NA	NA	NA	LOCUS_06870	(Miwa et al. 2010)
Hex1	GH	β-1,3/4/6-*N* -acetylglucosaminidase	GH20	NA	Blon_0459	Bbr_1556	LOCUS_03400	(Garrido et al. 2012)
Hex1	GH	β-1,3/4/6-*N* -acetylglucosaminidase	GH20	MCC10007_1361	Blon_0732	NA	NA	(Garrido et al. 2012)
Hex2	GH	β-1,3/4-*N* -acetylglucosaminidase	GH20	NA	Blon_2355	NA	NA	(Garrido et al. 2012)
BbnI	GH	Extracellular β-1,3-*N* -acetylglucosaminidase	GH20	NA	NA	NA	LOCUS_09260	(Miwa et al. 2010)
BbnII	GH	Extracellular β-1,6-*N* -acetylglucosaminidase	GH20	NA	NA	NA	LOCUS_01150	(Miwa et al. 2010)
BiAfcA	GH	α-1,2-L-fucosidase	GH95	MCC10007_0304	Blon_2335	Bbr_1288	NA	(Sela et al. 2012)
BiAfcB	GH	α-1,3/4-L-fucosidase	GH29	NA	Blon_2336	NA	NA	(Sela et al. 2012)
AfcA	GH	Extracellular α-1,2-L-fucosidase	GH95	NA	NA	NA	LOCUS_17170	(Katayama et al. 2004)
AfcB	GH	Extracellular α-1,3/4-L-fucosidase	GH29	NA	NA	NA	LOCUS_05790	(Ashida et al. 2009)
LnbB	GH	Extracellular lacto-*N* -biosidase	GH20	NA	NA	NA	LOCUS_04020	(Wada et al. 2008)
LnbX	GH	Extracellular lacto-*N* -biosidase	GH136	MCC10007_1471	NA	NA	NA	(Sakurama et al. 2013)
GlcP(GalP)	Transport	Glucose; galactose; mannose transporter	MFS; SP Family	MCC10007_1663	NA	NA	NA	(Parche et al. 2006)
GlcU	Transport	Predicted glucose transporter	DMT; GRP Family	NA	NA	NA	LOCUS_04340	NA
PtsG	Transport	Glucose transporter	PTS; Glc Family	MCC10007_1662	Blon_2183	Bbr_1594	LOCUS_12500	(Parche et al. 2007)
Blon_1383	Transport	Predicted galactose transporter	MFS; SSS Family	NA	Blon_1383	NA	NA	NA
FucP	Transport	Predicted fucose transporter	MFS; FHS Family	NA	Blon_2307	Bbr_1742	NA	NA
LacS	Transport	Lactose transporter	MFS; GPH Family	MCC10007_0745	Blon_2331;Blon_2332	Bbr_1551	LOCUS_05300	(O'Connel-Motherway et al. 2013)
GltABC	Transport	LNT; LNB; GNB transporter	ABC; CUT1 Family	MCC10007_1655-MCC10007_1657^	Blon_2175-2177	Bbr_1588-1590	LOCUS_01540-01560^	(Garrido et al. 2011)
Blon_0883-0885	Transport	LNB; GNB transporter	ABC; CUT1 Family	NA	Blon_0883-0885	NA	NA	(Garrido et al. 2011)
Blon_2345-2347	Transport	LN*n* T transporter	ABC; CUT1 Family	NA	Blon_2345-2347	NA	NA	(Garrido et al. 2011)
Blon_2342-2344	Transport	LN*n* T (low affinity) transporter	ABC; CUT1 Family	NA	Blon_2342-2344	NA	NA	(Garrido et al. 2011)
NahS	Transport	LN*n* T transporter	ABC; CUT1 Family	NA	Blon_0462^^	Bbr_1554	NA	(Sakanaka et al. 2019)
FL1	Transport	2'-FL; 3-FL transporter	ABC; CUT1 Family	NA	Blon_0341-0343	NA	NA	(Sakanaka et al. 2019)
FL2	Transport	2'-FL; 3-FL; LDFT; LNFP I transporter	ABC; CUT1 Family	MCC10007_0309-MCC10007_0311	Blon_2202-2204	NA	NA	(Garrido et al. 2011)
Blon_2350	Transport	Predicted HMOs transporter	ABC; CUT1 Family	NA	Blon_2350	NA	NA	(Garrido et al. 2011)
Blon_2351	Transport	Predicted HMOs transporter	ABC; CUT1 Family	NA	Blon_2351	NA	NA	(Garrido et al. 2011)
Blon_2352	Transport	Predicted HMOs transporter	ABC; CUT1 Family	NA	Blon_2352	NA	NA	(Garrido et al. 2011)
Blon_2354	Transport	Predicted HMOs transporter	ABC; CUT1 Family	NA	Blon_2354	NA	NA	(Garrido et al. 2011)

^ ortholog predicted not to transport LNT
^^ ortholog is truncated

Supplementary Table II-3 | Factor loadings for principal components analysis based on A) the final community composition at 24 h and B) the concentration of HMOs remaining in the medium at 24 h for the four-species assemblages. Note that the absolute values for blank entries are less than 0.2, but not necessarily zero. The top two principal components are shown.

A)	Comp.1	Comp.2
B. bifidum	0.664	0.294
B. breve	-0.701	0.275
B. infantis	-0.896	-0.118
B. longum	0.252	0.185

B)	Comp.1	Comp.2
Fuc	0.999	
GlcNAc / Glc		
Gal		
LNB		
Lac		
2'-FL		
3-FL		0.830
LDFT		0.510
LNT		
LN*n*T		
LNFP I		
LNFP II/III		
LNDFH I		0.217

Supplementary Table II-4 | PERMANOVA of the covariant relationship between the abundances of each bifidobacterial species in the mother and in the infant at the time of birth, and the microbiome of the infant at 4 months of age. The effect sizes are represented in shades of green. (Significance levels: . p < 0.1, * p < 0.05)

Variables		Infant Microbiome (4 Months)		Variables		Infant Microbiome (4 Months)	
		R^2	p			R^2	p
	Total *Bifidobacterium* Abundance	0.083			Total *Bifidobacterium* Abundance	0.022	
	B. adolescentis	0.126			*B. adolescentis*	0.018	
	B. longum	0.044			*B. longum*	0.008	
	B. faecale	0.077			*B. faecale*	0.021	
	B. catenulatum	0.015			*B. catenulatum*	0.009	
	B. ruminantium	0.111			*B. ruminantium*	0.020	
	B. bifidum	0.021			*B. bifidum*	0.041	
	B. moukalabense	0.104			*B. moukalabense*	0.020	
	B. kashiwanohense	0.098			*B. kashiwanohense*	0.040	
	B. pseudocatenulatum	0.036			*B. pseudocatenulatum*	0.023	
	B. breve	0.059			*B. breve*	0.191	*
	B. dentium	0.098			*B. dentium*	0.018	
	B. animalis	0.154	.		*B. animalis*	0.029	
	B. pseudolongum	0.094			*B. pseudolongum*	0.047	
	B. tsurumiense	0.099			*B. tsurumiense*	0.020	
	B. saguini	0.004			*B. saguini*	0.007	
	B. actinocoloniiforme	0.017			*B. actinocoloniiforme*	0.048	
	B. stellenboschense	0.096			*B. stellenboschense*	0.136	
	B. asteroides	0.028			*B. asteroides*	0.016	
	B. choerinum	0.091			*B. choerinum*	0.045	
	B. ramosum	0.070			*B. ramosum*	0.008	
	B. eulemuris	0.058			*B. eulemuris*	0.048	
	B. lemurum	0.058			*B. lemurum*	0.046	
	B. gallicum	0.081			*B. gallicum*	0.034	
	B. merycicum	0.070			*B. merycicum*	0.009	
	B. angulatum	0.151			*B. angulatum*	0.011	
Mother	*B. tissierii*	0.016		At Birth	*B. tissierii*	0.050	
	B. hapali	0.087			*B. hapali*	0.021	
	B. callitrichos	0.066			*B. callitrichos*	0.024	
	B. scardovii	0.048			*B. scardovii*	0.017	
	B. reuteri	0.043			*B. reuteri*	0.013	
	B. thermacidophilum	0.062			*B. thermacidophilum*	0.018	
	B. aesculapii	0.101			*B. aesculapii*	0.004	
	B. pullorum	0.052			*B. pullorum*	0.119	
	B. biavatii	0.036			*B. biavatii*	0.015	
	B. indicum	0.030			*B. indicum*	0.008	
	B. thermophilum	0.060			*B. thermophilum*	0.017	
	B. myosotis	0.080			*B. myosotis*	0.093	
	B. mongoliense	0.052			*B. mongoliense*	0.008	
	B. subtile	0.041			*B. subtile*	0.014	
	B. aerophilum	0.028			*B. aerophilum*	0.016	
	B. saeculare	0.056			*B. saeculare*	0.039	
	B. bombi	0.033			*B. bombi*	0.031	
	B. boum	0.037			*B. boum*	0.017	
	B. cuniculi	0.076			*B. cuniculi*	0.033	
	B. bohemicum	0.075			*B. bohemicum*	0.041	
	B. magnum	0.021			*B. magnum*	0.036	
	B. gallinarum	0.046			*B. gallinarum*	0.042	
	B. crudilactis	0.044			*B. crudilactis*	0.011	
	B. psychraerophilum	0.039			*B. psychraerophilum*	0.010	
	B. coryneforme	0.032			*B. coryneforme*	0.000	
	B. aquikefiri	0.048			*B. aquikefiri*	0.022	
	B. minimum	0.115			*B. minimum*	0.003	

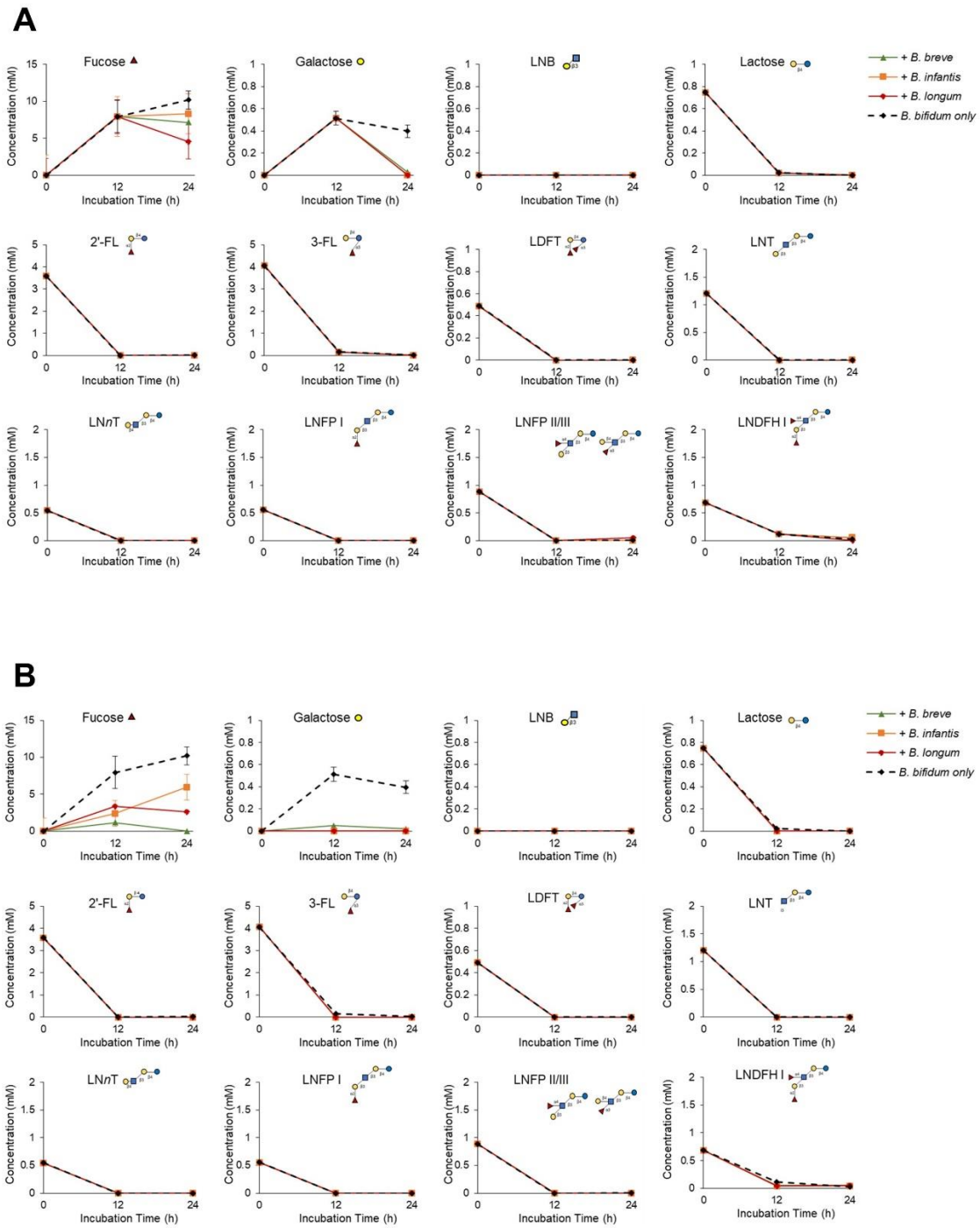

Supplementary Figure II-1 | HMO consumption profiles of pairwise cultures with *B. bifidum* as the focal species. Culture supernatant was collected at each time point (n = 4). The remaining sugars in the medium were labeled with 2-AA and analyzed by HPLC (as described in the Materials and Methods section). HMO consumption profiles are shown for pairwise cultures in which A) *B. bifidum* is inoculated first and the second species is inoculated 12 hours later, and B) *B. bifidum* is simultaneously cultured with other species. Black dotted lines indicate *B. bifidum* monoculture data (taken from Figure II-3 B), and competitors are indicated in different colors (green when cultured with *B. breve*, orange when cultured with *B. infantis*, and red when cultured with *B. longum*). Note that the presence of Glc/GlcNAc was not observed at the indicated time points. Error bars represent ± standard error.

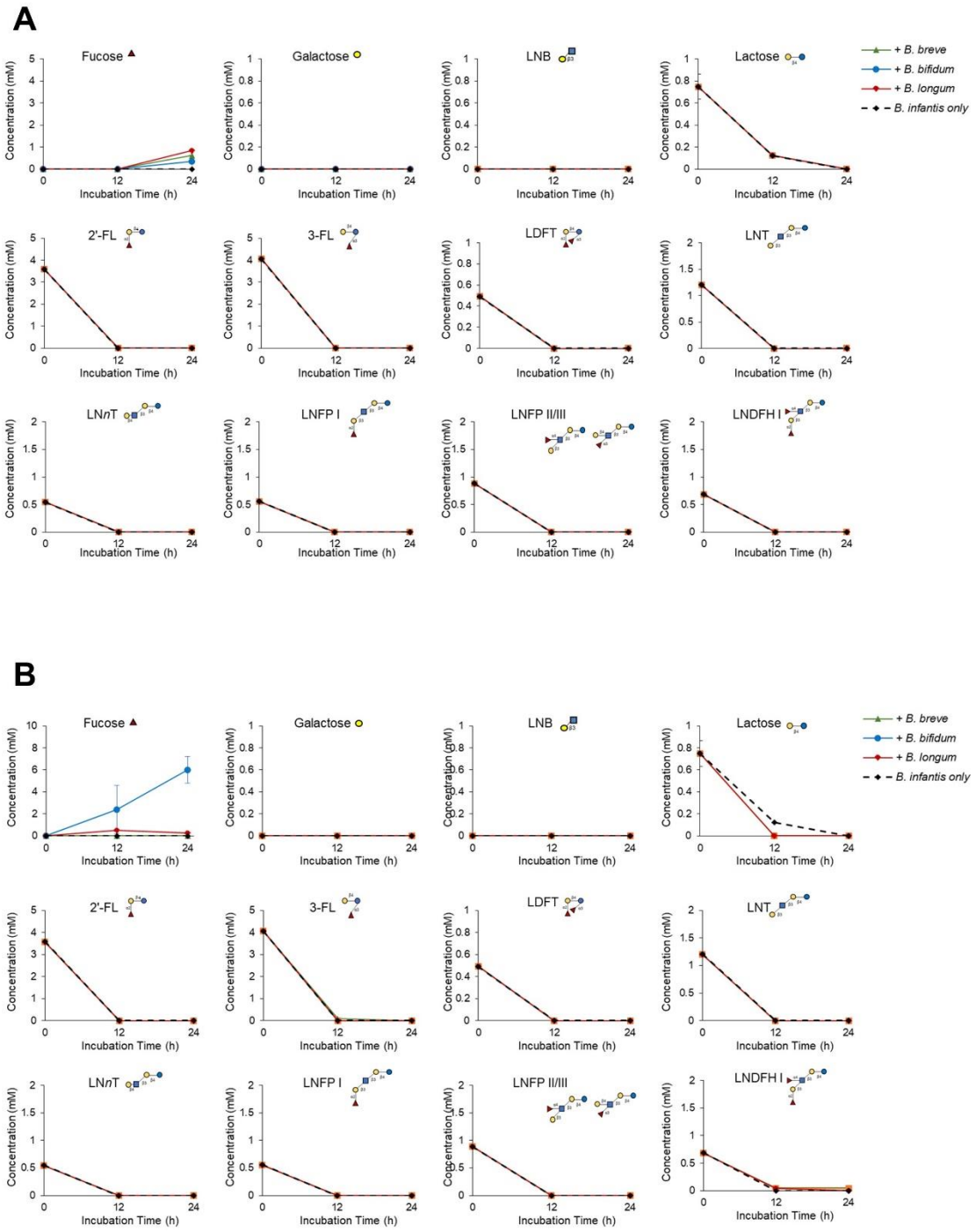

Supplementary Figure II-2 | HMO consumption profiles of pairwise cultures with *B. infantis* as the focal species. Culture supernatant was collected at each time point (n = 4). The remaining sugars in the medium were labeled with 2-AA and analyzed by HPLC (as described in the Materials and Methods section). HMO consumption profiles are shown for pairwise cultures in which A) *B. infantis* is inoculated first and the second species is inoculated 12 hours later, and B) *B. infantis* is simultaneously cultured with other species. Black dotted lines indicate *B. infantis* monoculture data (taken from Figure II-3 B), and competitors are indicated in different colors (green when cultured with *B. breve*, blue when cultured with *B. bifidum*, and red when cultured with *B. longum*). Note that the presence of Glc/GlcNAc was not observed at the indicated time points. Error bars represent ± standard error.

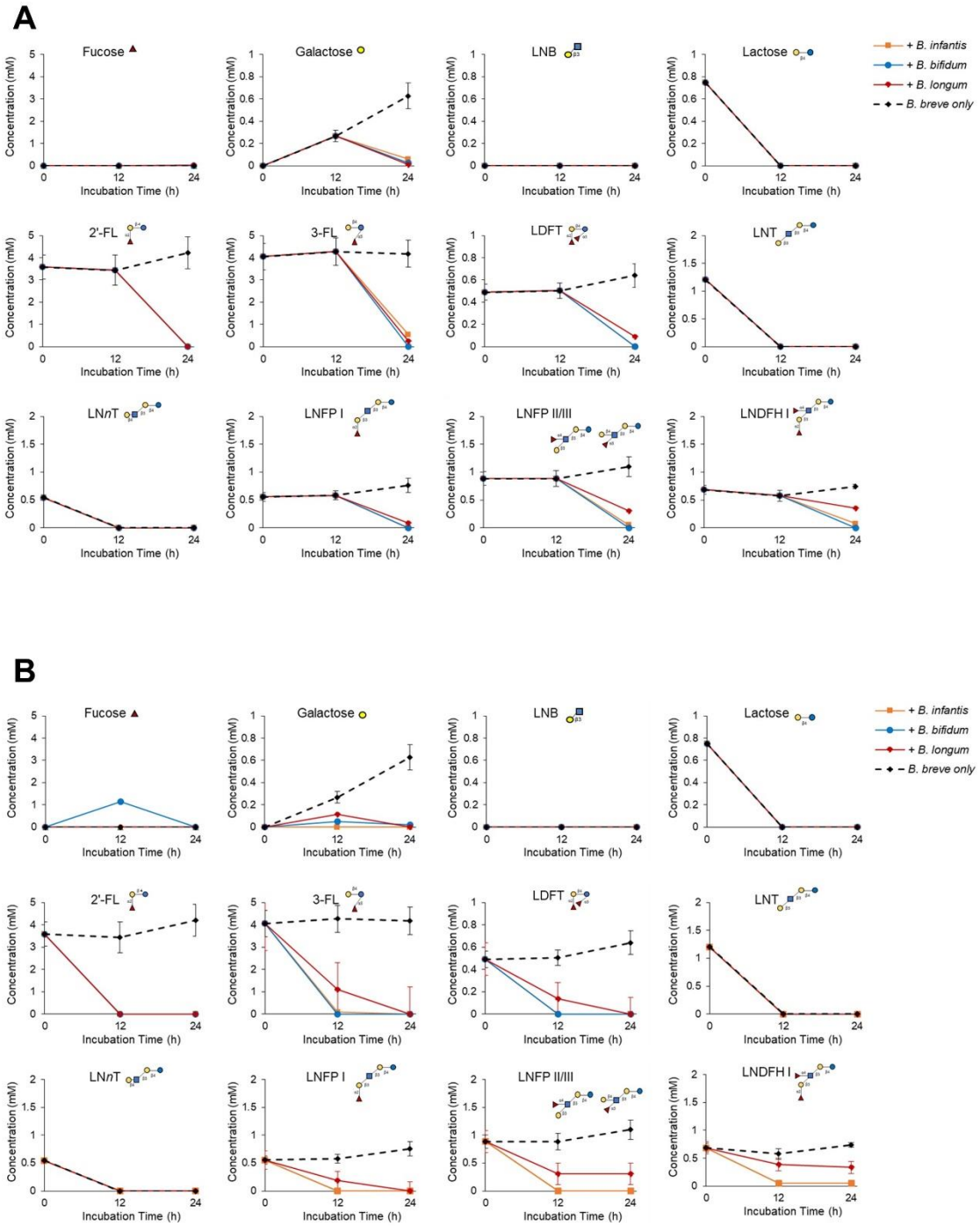

Supplementary Figure II-3 | HMO consumption profiles of pairwise cultures with *B. breve* as the focal species. Culture supernatant was collected at each time point (n = 4). The remaining sugars in the medium were labeled with 2-AA and analyzed by HPLC (as described in the Materials and Methods section). HMO consumption profiles are shown for pairwise cultures in which A) *B. breve* is inoculated first and the second species is inoculated 12 hours later, and B) *B. breve* is simultaneously cultured with other species. Black dotted lines indicate *B. breve* monoculture data (taken from Figure II-3 B), and competitors are indicated in different colors (orange when cultured with *B. infantis*, blue when cultured with *B. bifidum*, and red when cultured with *B. longum*). Note that the presence of Glc/GlcNAc was not observed at the indicated time points. Error bars represent ± standard error.

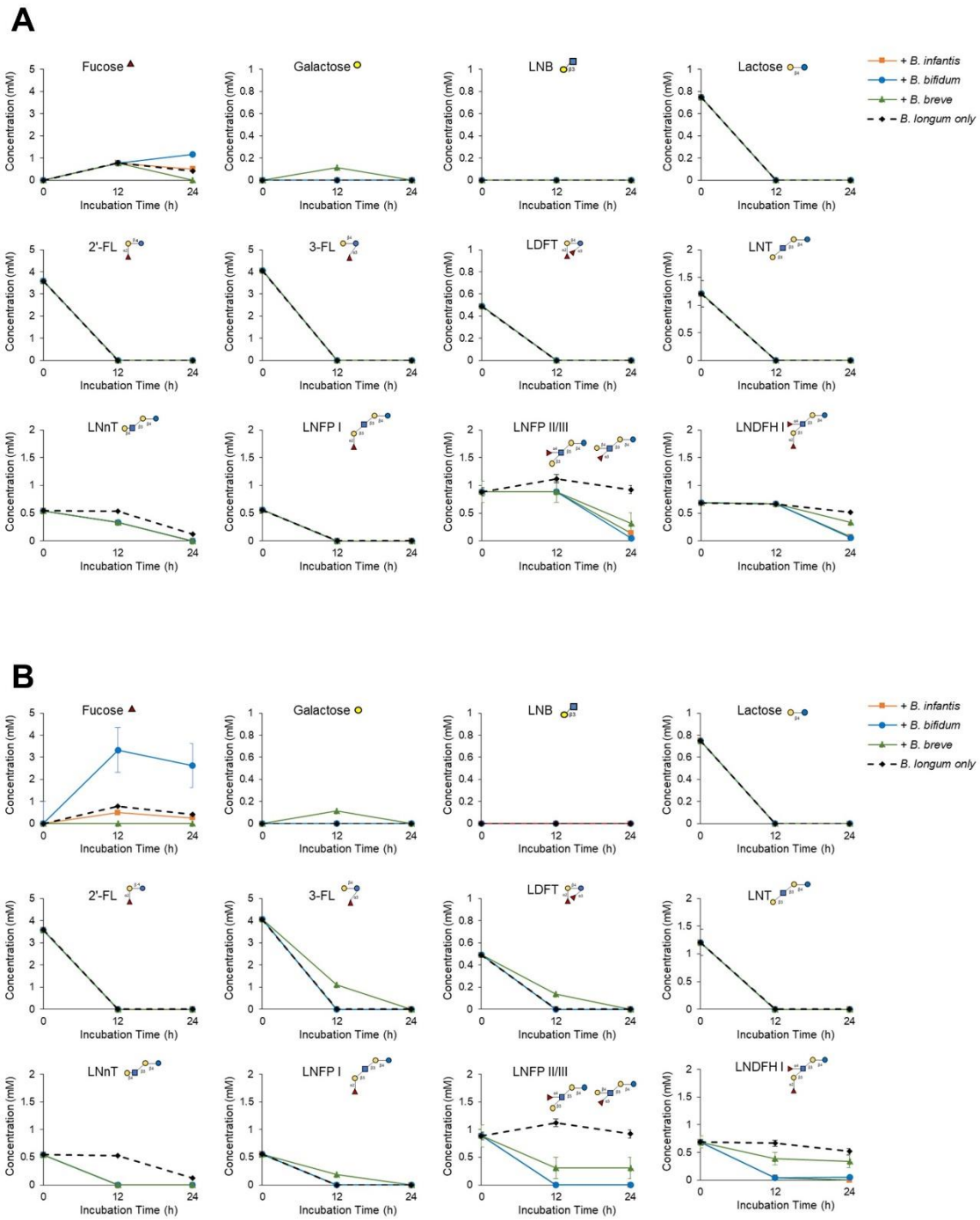

Supplementary Figure II-4 | HMO consumption profiles of pairwise cultures with *B. longum* as the focal species. Culture supernatant was collected at each time point (n = 4). The remaining sugars in the medium were labeled with 2-AA and analyzed by HPLC (as described in the Materials and Methods section). HMO consumption profiles are shown for pairwise cultures in which A) *B. longum* is inoculated first and the second species is inoculated 12 hours later, and B) *B. longum* is simultaneously cultured with other species. Black dotted lines indicate *B. breve* monoculture data (taken from Figure II-3 B), and competitors are indicated in different colors (orange when cultured with *B. infantis*, blue when cultured with *B. bifidum*, and green when cultured with *B. breve*). Note that the presence of Glc/GlcNAc was not observed at the indicated time points. Error bars represent ± standard error.

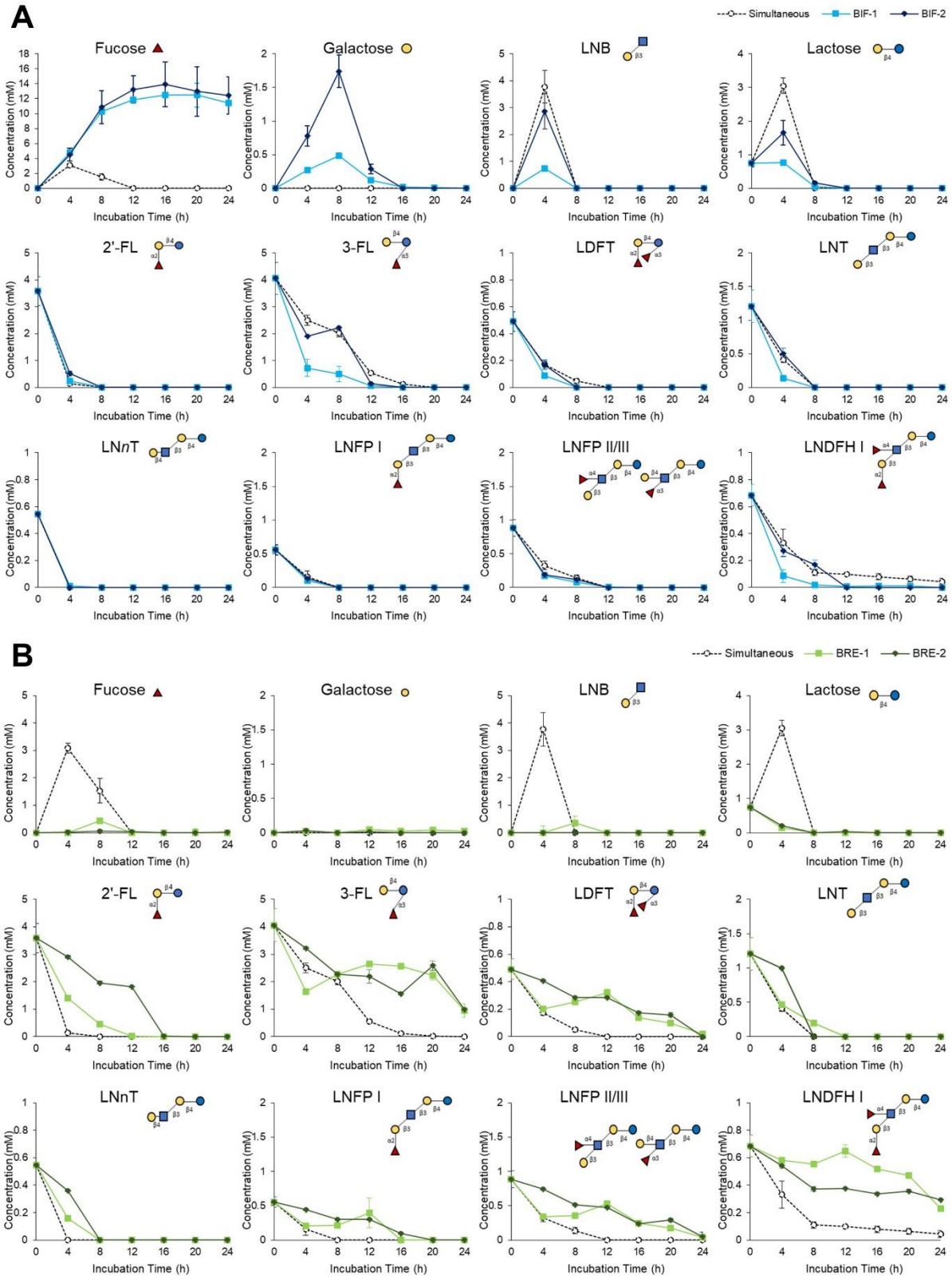
A
Simultaneous
BIF-1
BIF-2
Fucose
Galactose
LNB
Lactose
2'-FL
3-FL
LDFT
LNT
LNnT
LNFP I
LNFP II/III
LNDFH I
Concentration (mM)
Incubation Time (h)
B
Simultaneous
BRE-1
BRE-2
Fucose
Galactose
LNB
Lactose
2'-FL
3-FL
LDFT
LNT
LNnT
LNFP I
LNFP II/III
LNDFH I
Concentration (mM)
Incubation Time (h)

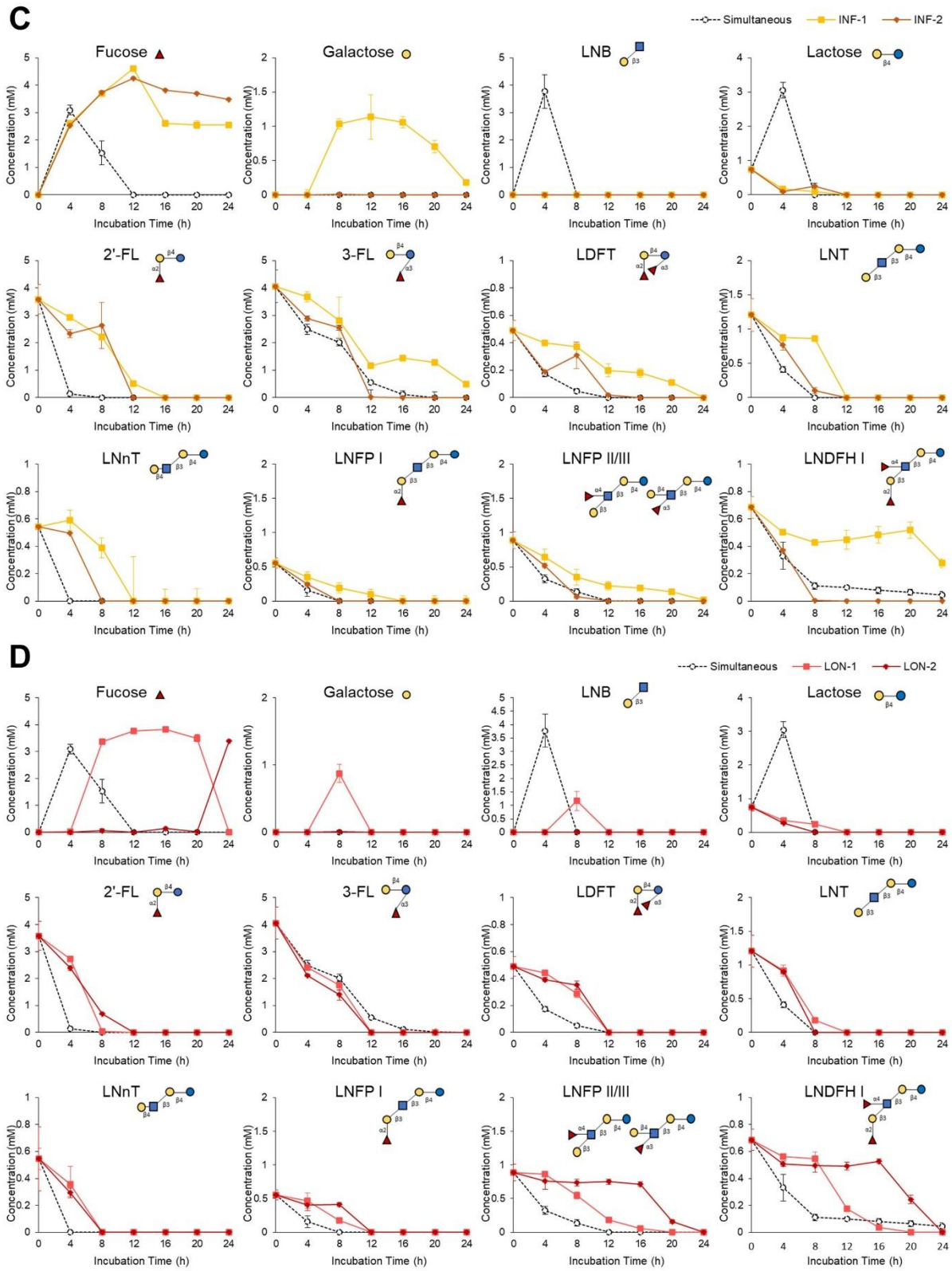
C
Simultaneous
INF-1
INF-2
Fucose
Galactose
LNB
Lactose
2'-FL
3-FL
LDFT
LNT
LNnT
LNFP I
LNFP II/III
LNDFH I
Concentration (mM)
Incubation Time (h)
D
Simultaneous
LON-1
LON-2
Fucose
Galactose
LNB
Lactose
2'-FL
3-FL
LDFT
LNT
LNnT
LNFP I
LNFP II/III
LNDFH I
Concentration (mM)
Incubation Time (h)

Supplementary Figure II-5 | HMO consumption profiles for four-species assemblages. Culture supernatant was collected at each time point (n = 4). The remaining sugars in the medium were labeled with 2-AA and analyzed by HPLC (as described in the Materials and Methods section). HMO consumption profiles are shown for four-species assemblages in which A) *B. bifidum* is inoculated first (light blue: BIF-1, dark blue: BIF-2), B) *B. breve* is inoculated first (light green: BRE-1, dark green: BRE-2), C) *B. infantis* is inoculated first (yellow: INF-1, orange: INF-2), D) *B. longum* is inoculated first (pink: LON-1, red: LON-2). The HMO consumption profile for the simultaneous culture is shown as the black dotted line (A-D). Note that the presence of Glc/GlcNAc was not observed at the indicated time points. Error bars represent ± standard error.

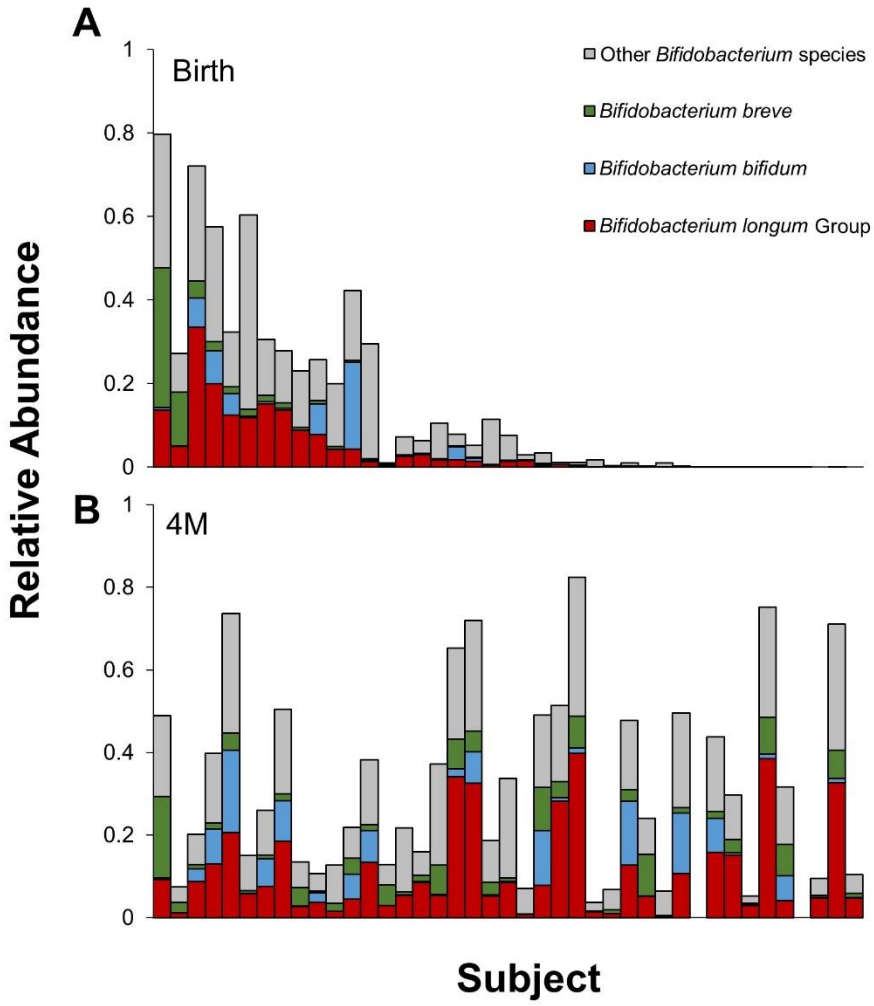

Supplementary Figure II-6 | Relative abundance of each bifidobacterial species in the infant gut at birth and at 4 months of age. The relative abundances of bifidobacterial species were extracted from the dataset published by Backhed et al. (2015) under the SRA Accession No. PRJEB6456. The samples selected based on the flowchart shown in Figure II-6 A at (A) birth and (B) 4 months of age (4M) are shown (n = 41). Each bar represents one individual, which is ordered by *B. breve* abundance at birth. *B. breve* is indicated in green, *B. bifidum* in blue, and *B. longum* in red. Note that the analysis did not differentiate between the *B. longum* subspecies.

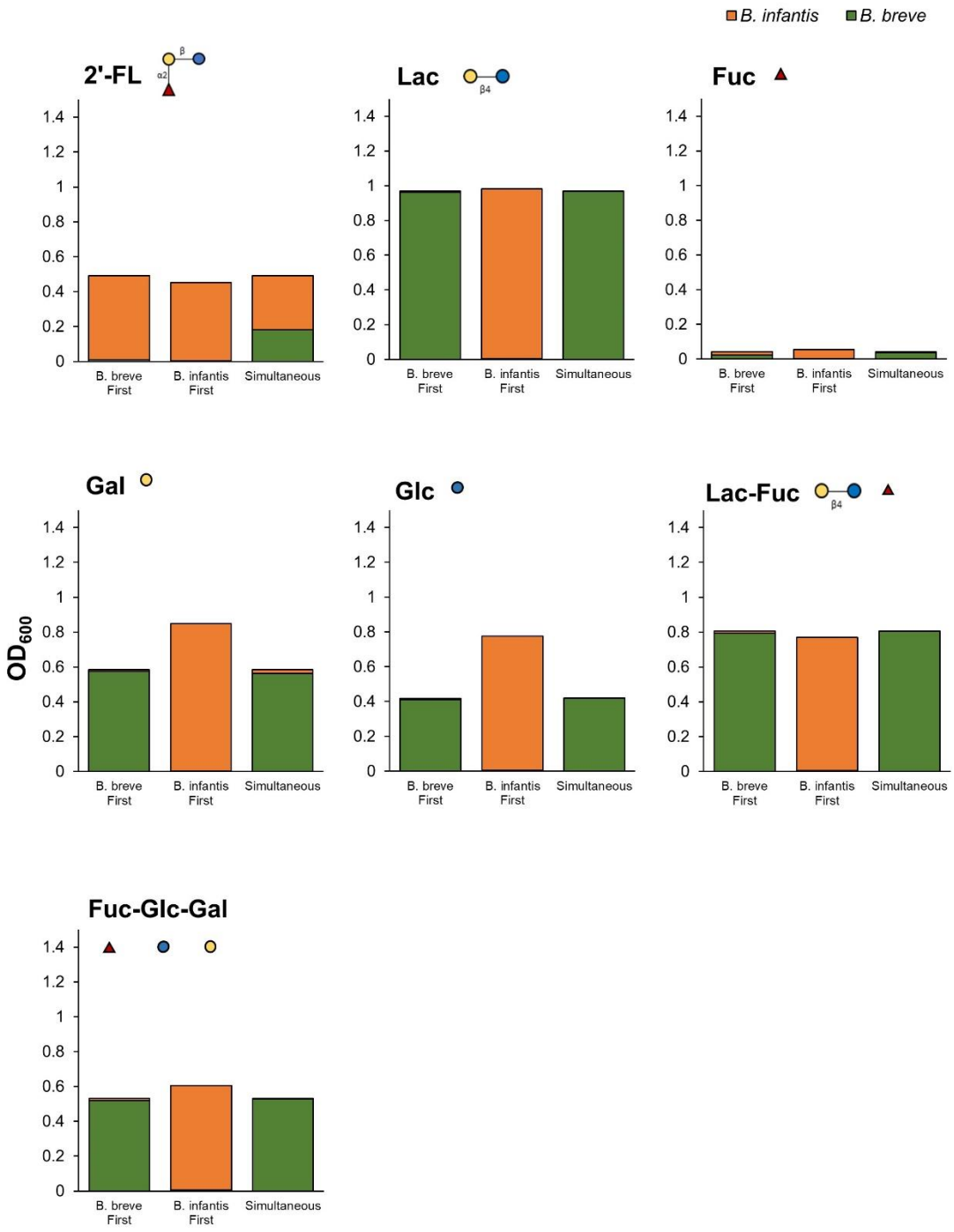

Supplementary Figure II-7 | Pairwise competition between *B. breve* and *B. infantis* in medium with 2'-FL and its component sugars. Pairwise culturing experiments were performed between *B. breve* and *B. infantis* in medium supplemented with 1 % (*w/v*) of the following sugars: 2'-FL, Lac, Fuc, Glc, Gal, a mixture of Lac and Fuc at 1:1 molar ratio, and a mixture of Fuc, Glc, and Gal at 1:1:1 molar ratio (n = 3). In simultaneous cultures, both species were introduced into medium supplemented together at the beginning of the experiment. The first species was inoculated at the beginning of the experiment, and the second species was inoculated 12 hours later. OD_{600} was measured at each time point, and the relative abundance of each species was quantified using qPCR. The relative abundance of each strain is indicated by different colors (Green: *B. breve*, orange: *B. infantis*).

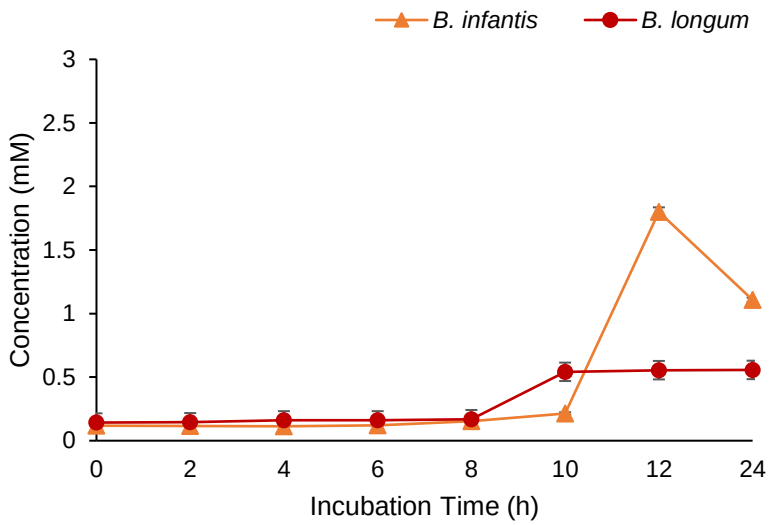

Supplementary Figure II-8 | Fucose efflux from *B. infantis* and *B. longum* when cultured with 1 % 2′-FL. *B. infantis* and *B. longum* were each cultured in medium supplemented with 1 % 2′-FL (*w/v*) (n = 3), and the amount of fucose in the culture supernatant was measured using a colorimetric assay at the indicated time points. *B. infantis* is indicated in orange, and *B. longum* is indicated in red.

Chapter III

THE ROLE OF BIFIDOBACTERIA IN THE RECOVERY AFTER REPEATED DISTURBANCES

Summary

Antibiotic administration can disturb the ecological balance of the gut microbiome and have long-term consequences. Probiotics have been proposed as a remedy for antibiotic-induced disturbance, but their efficacy remains uncertain. Thus, the effect of specific antibiotic-probiotic combinations on the gut microbiome and host health warrants further research. To test theories in disturbance ecology within the context of the gut microbiome, I used murine models and examined the effect of three antibiotics: vancomycin, a glycopeptide antibiotic that targets Gram-positive bacteria; amoxicillin, a moderate spectrum antibiotic; and ciprofloxacin, a broad-spectrum antibiotic that targets Gram-negative bacteria. Antibiotic administration was followed by one of the three following recovery treatments: *Bifidobacterium bifidum* JCM 1254 as a probiotic (PR); fecal transplant from healthy donor mice (FT); or natural recovery (NR). Antibiotic administration and recovery treatments were each repeated three times. The efficacy of each treatment was evaluated by measuring gut microbiome diversity, and recovery was assessed using the Bray-Curtis Index of Dissimilarity, which quantified the magnitude of microbial shift. Community composition was determined by sequencing the V3–V4 regions of the 16S ribosomal RNA gene. To assess host health, I measured body weight and cecum weight, as well as mRNA expression of inflammation-related genes by reverse-transcription quantitative PCR. Results show that community response varied by the type of antibiotic used, with vancomycin having the most detrimental consequences. As a result, the effect of probiotics and fecal transplants also varied by antibiotic type. For vancomycin, the first antibiotic disturbance substantially increased the relative abundance of taxa associated with gut inflammation, such as *Proteus* and other species in the phylum Proteobacteria. However, the effect of subsequent disturbances was less pronounced, suggesting that the response of the gut microbiome is affected by past disturbance events. Furthermore, although gut microbiome diversity did not recover, probiotic supplementation effectively limited cecum size enlargement and colonic inflammation caused by vancomycin. However, for amoxicillin and ciprofloxacin, the relative abundances of proinflammatory species were not greatly affected. As a result, the effect of probiotic supplementation on community structure, cecum weight, and expression of inflammation-related genes was comparatively negligible. The results of this study show that probiotic supplementation is effective, but only when antibiotics cause an increase in proinflammatory taxa, suggesting that the necessity of probiotic supplementation is strongly influenced by the type of disturbance introduced to the community.

Introduction

The ecological balance maintained by the gut microbial community has been shown to play an important role in host metabolism (reviewed by Rowland et al. 2018), nutrition (Yatsunenko et al., 2012), and immune function (Round and Mazmanian, 2009; Kau et al., 2011). However, dysbiosis, or a disturbance in the healthy microbiome, is suggested to cause a variety of health issues such as obesity (Ley et al., 2005), diabetes (Qin et al., 2012; Kostic et al., 2015), asthma (Stokholm et al., 2018), and inflammatory bowel disease (IBD) (Petersen and Round, 2014). While the gut microbiome is relatively stable over time and resilient to isolated disturbance events (Faith et al., 2013), the long-term effects of repeated disturbance remain poorly understood.

The gut microbiome can be disturbed through various events, such as the consumption of a high-fat diet (He et al., 2018), jet lag (Thaiss et al., 2014), and the use of medications, especially antibiotics (Theriot et al., 2014). While antibiotics are important in combating diseases caused by pathogenic bacteria, an unintended consequence is that they can also affect other beneficial and commensal species in the gut (Jernberg et al., 2007). Overuse of antibiotics can also lead to clinical issues such as the emergence of antibiotic-resistant strains (Levy and Marshall, 2004), weight gain (Cho et al., 2012; Gerber et al., 2016), and antibiotic-associated diarrhea (Hogenauer et al., 1998; Wiström et al., 2001; Elseviers et al., 2015). Furthermore, repeated antibiotic use can alter the composition of the gut microbiome long term (Dethlefsen and Relman, 2011).

Recently, probiotics, or live microbes exogenously administered for therapeutic purposes, have been suggested as a promising remedy for antibiotic-induced dysbiosis (Korpela et al., 2016; Ekmekciu et al., 2017). Probiotics have become increasingly popular — with a compound annual growth rate (CAGR) of 7.0 %, the global probiotics market is expected to reach 63 billion USD (approximately 6.6 trillion JPY) by 2023 (Global Market Insights, 2016). However, the efficacy of probiotic therapies is debated, as many probiotic strains do not remain in the gut long term (reviewed by Suez et al., 2019). Furthermore, a recent study showed that probiotics possibly inhibit, rather than promote, recovery, while autologous fecal microbiome transplants effectively restored gut microbiome diversity (Suez et al., 2018).

Fecal microbiome transplants (FMT) have been used as a treatment for severe antibiotic-induced dysbiosis (Shahinas et al., 2012) and provide relatively rapid recovery from dysbiosis (Suez et al., 2018). However, despite increasing reports of successful treatments, the methodology is unstandardized (Goldenberg et al., 2018), and challenges for clinical implementation remain. Furthermore, several side effects, such as weight gain and diarrhea, have been reported (Alang and Kelly, 2015). In 2019, a death from an infection caused by *Escherichia coli* strains that produce extended-spectrum β-lactamase (ESBL) after FMT was reported (U. S. Food and Drug Administration, 2019). While both probiotics and FMT are

promising therapeutic microbiome-based treatments, studies often report conflicting results, indicating a need for further research.

One of the difficulties with probiotics research is the variety of probiotic strains available, leading to variability in reported results. Species in the *Bacillus*, *Bifidobacterium*, *Enterococcus*, *Escherichia*, *Lactobacillus*, *Saccharomyces*, and *Streptococcus* genera are most often used in probiotic products. However, purported effects can vary not only at the species level but also at the strain level. When formula-fed infants were given either *Bifidobacterium longum* subspecies *infantis* (*B. infantis*) or *Bifidobacterium animalis* subspecies *lactis*, *B. infantis* was more effective in increasing fecal bifidobacteria and decreasing γ-Proteobacteria due to its superior ability to colonize the infant gut (Underwood et al., 2013). In a study by Gotoh et al., the addition of different *Bifidobacterium bifidum* strains to fecal cultures increased fecal bifidobacteria, but the ability of *B. bifidum* to increase the abundance of other bifidobacterial species varied by strain (Gotoh et al., 2018; Katoh et al., 2020).

Despite the diversity in both antibiotics and probiotic species, many studies utilize a single combination of broad-spectrum antibiotics and pre-made probiotic blends. Consequently, the effect of specific antibiotic-probiotic combinations remains relatively understudied. The type, intensity, and frequency of disturbance are important factors that shape ecological communities and their response to subsequent recovery treatments. Therefore, I introduced a repeated disturbance to the gut microbiome with three types of antibiotics that have different bacterial targets and modes of action: vancomycin, amoxicillin, and ciprofloxacin. As a probiotic, I used *Bifidobacterium bifidum* JCM 1254, an infant-gut associated species that extracellularly degrades complex sugars, such as human milk oligosaccharides (HMOs) and mucin *O*-glycans (Gotoh et al., 2018). Presented here is a comparative analysis of repeated antibiotic disturbance on the gut microbiome and the subsequent effect of probiotics on recovery in a lab-controlled experiment using mouse models.

Materials and Methods

Animals and Housing

A total of 40 female C57BL/6 mice were purchased from Japan SLC, Inc. (Shizuoka, Japan) at 8–10 weeks of age. Mice were housed individually in polycarbonate cages with bedding and given free access to drinking water and a basal diet, Oriental MF (Oriental Yeast Co., Ltd., Tokyo, Japan). The mice were kept under controlled conditions of humidity (70 %), lighting (12-h light/dark cycle), and temperature (22℃). The experiment began after a 2-week acclimation period. The protocols of the

experiment were approved by the Kyoto University Animal Experimentation Committee (Lif-K18009 and Lif-K19022). Animal experiments were performed from August 21, 2018, to June 17, 2019.

Antibiotics

Three different types of antibiotics were selected: vancomycin hydrochloride (Nacalai Tesque Inc., Kyoto, Japan), amoxicillin (LKT Laboratories, Inc., Minnesota, USA), and ciprofloxacin (LKT Laboratories, Inc., Minnesota, USA). The antibiotics were selected for their varied spectrum of activity and reported effects on the gut microbial community (Table III-1). Antibiotics were administered in drinking water for mice to ingest *ad libitum*. Concentrations of each antibiotic were calculated and adjusted for mice based on human dosages suggested by the US Food and Drug Administration (GlaxoSmithKline, 2006; Baxter Healthcare, 2007; Bayer HealthCare, 2017).

Table III-1 | The characteristics of the antibiotics used in this experiment.

Antibiotic	**Class**	**Bacterial Target**	**Dosage**
Amoxicillin	Penicillin	Moderate spectrum	0.22 mg / mL
Ciprofloxacin	Fluoroquinolone	Broad-spectrum, Gram-negatives	0.19 mg / mL
Vancomycin	Glycopeptide	Gram-positives	0.25 mg / mL

Experimental Design

Mice were divided into 10 groups (Table III-2), with one control group and 9 different antibiotic-recovery combinations, with four biological replicates per group. The sample size was calculated based on power analyses and the resource equation approach (Arifin and Zahiruddin, 2017). Each group received antibiotics (vancomycin, amoxicillin, or ciprofloxacin) in drinking water for one week (antibiotics week). After antibiotics were administered, mice were switched to normal water without antibiotics and were given one of the following recovery treatments for one week (treatment week): natural recovery (NR); *Bifidobacterium bifidum* JCM 1254 as a probiotic (PR); or fecal transplant from control mice (FT). The treatment week was followed by one week with no treatments to allow the mice to recover (recovery week). With the treatment week and recovery week combined, mice were given two weeks to recover from antibiotic administration, as past studies have reported that the gut microbiome

recovers within 1-2 weeks after disturbance (David et al., 2014; MacPherson et al., 2018). This was repeated three times for a total of three 3-week phases (Figure III-1). Mice in the control were provided with water without antibiotics throughout the 9-week experiment.

Table III-2 | List of treatment groups (antibiotic and recovery treatment combinations).

Treatment Group	Antibiotics	Recovery
Control		
A	Amoxicillin	Natural Recovery (NR)
AB	Amoxicillin	*B. bifidum* JCM1254 (PR)
AF	Amoxicillin	Fecal Transplant (FT; from Control)
P	Ciprofloxacin	Natural Recovery (NR)
PB	Ciprofloxacin	*B. bifidum* JCM1254 (PR)
PF	Ciprofloxacin	Fecal Transplant (FT; from Control)
V	Vancomycin	Natural Recovery (NR)
VB	Vancomycin	*B. bifidum* JCM1254 (PR)
VF	Vancomycin	Fecal Transplant (FT; from Control)

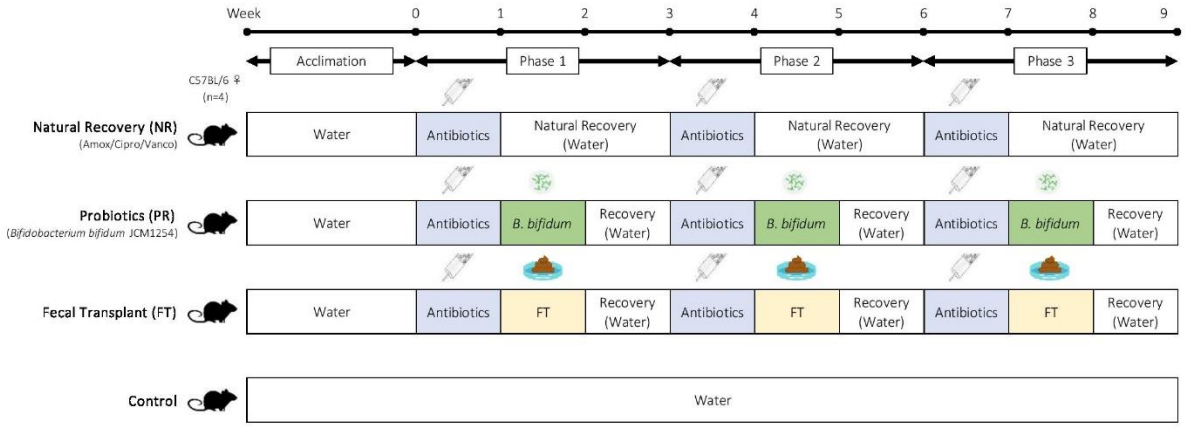

Figure III-1 | **Experimental design.** A total of 40 adult female C57BL/6 mice were used in this experiment. After a 2-week acclimation period, mice were given one of the following antibiotics for one week: amoxicillin, ciprofloxacin, or vancomycin. Antibiotic treatment was followed by one of the following recovery treatments: natural recovery (NR); *Bifidobacterium bifidum* JCM1254 as a probiotic (PR); and fecal transplant (FT). The recovery treatment was followed by 7 days of no treatments to allow the mice to recover. Each 3-week cycle was repeated three times during this 9-week experiment. Mice in the control were provided with water alone throughout the experiment. This figure is used with permission from the authors (Ojima et al., 2020).

To prepare for probiotic administration, Gifu Anaerobic Medium (GAM, Nissui Pharmaceutical, Tokyo, Japan) was inoculated with *B. bifidum* each day and incubated at 37 ℃ overnight. From the overnight cultures, bacterial suspensions were diluted in phosphate-buffered saline (PBS) at a concentration of 5 x 10^9 CFU per mL. 200 μL of the bacterial suspensions were administered to each mouse via oral gavage daily during the treatment weeks. For fecal transplants, a mixture of fresh feces collected from age-matched control mice was suspended in PBS at a concentration of 40 mg/mL and vortexed for 3 minutes. The mixture was then allowed to settle, and 200 μL of the supernatant was given to the mice via oral gavage daily during the treatment weeks. As a control, mice in the control and NR groups were given 200 μL of anaerobic PBS via oral gavage daily during the treatment weeks.

Body weight was measured as an indicator of feed intake and health. Fecal samples were collected from each mouse at the end of each week and stored at −30 ℃ and freeze-dried within a few days of collection. Freeze-dried fecal samples were stored at −30 ℃ until use for DNA extraction. At the end of the experiment, animals were humanely euthanized by cervical dislocation. Immediately after death, a midline incision was made to exteriorize the intestine and cecum. Cecum weight was measured, and intestinal tissue samples were stored in RNA*later* (Invitrogen, Taastrup, Denmark) at 4 ℃ until use for RNA extraction.

DNA Extraction

Freeze-dried fecal samples were placed in 2 mL plastic tubes with one 5.0 mm stainless steel bead and approximately 200 mg of 0.1 mm zirconia beads. The tubes were then vigorously shaken for 10 minutes at 1,500 rpm using the Shake Master NEO (Bio Medical Science, Tokyo, Japan) before extraction, as described previously (Sakanaka et al., 2019). Genomic DNA was extracted using a Qiagen QIAamp® DNA Fast Stool Mini Kit (Hilden, Germany) according to the manufacturer's instructions with a few modifications. Extracted DNA samples were stored at −30 ˚C until use.

Quantification of Total Bacterial Load Using Quantitative PCR

After genomic DNA extraction, the total bacterial load was quantified by measuring the number of copies of the 16S ribosomal RNA (16S rRNA) gene by quantitative PCR (qPCR). qPCR was performed with a Thermal Cycler Dice Real-Time System (TaKaRa Bio., Kyoto, Japan). Each reaction mixture (total volume: 15 μL) contained the following: 7.5 μL of TB Green® Premix Ex Taq™ II (TaKaRa Bio, Kyoto, Japan), 0.6 μL (10 pmol) of each forward (5'- ACTCCTACGGGAGGCAGCAGT -3') and reverse (5'- ATTACCGCGGCTGCTGGC -3') primers, 1 μL of extracted DNA (diluted to 5

ng/μL), and 5.3 μL of water. The cycling conditions included an initial denaturation of 10 min at 95 °C followed by 40 cycles of 95 °C for 30 s and 68 °C for 1 min. Known concentrations of genomic DNA extracted from *Bacteroides thetaiotaomicron* were used as reference curves for DNA quantification.

Microbiome Analysis

Microbiome analysis was performed with the support of Morinaga Milk Industry, Co. Ltd. Sequencing of the V3-V4 region of the 16S rRNA gene was performed with an Illumina MiSeq platform (Illumina, Inc., San Diego, CA, USA) as described previously (Odamaki et al., 2019). After removing sequences consistent with data from phiX reads from the raw Illumina paired-end reads, the sequences were analyzed using the QIIME2 software package version 2017.10 (https://qiime2.org/). After trimming of the forward and the reverse reads (30 bases from the 5' region and 90 bases from the 3' region, respectively), the paired-end reads were joined, and potential chimeric sequences were removed using DADA2 (Callahan et al., 2016). The taxonomical classification was performed using a Naive Bayes classifier trained on the Greengenes 13.8 16S rRNA reference set with a 99 % threshold of OTU full-length sequences. When possible, species were determined by Blastn analysis of the representative OTU sequences, for which the NCBI rRNA database was used.

Quantification of Inflammation-Related Gene Expression Using Reverse-Transcription qPCR

The expression of inflammation-related genes was quantified with the support of H. Takada from Kyoto University. Intestinal tissue samples were placed in 2 mL plastic tubes with one stainless steel bead (5.0 mm) and approximately 200 mg of 0.1 mm zirconia beads. Samples were homogenized by vigorous shaking for 20 minutes at 1500 rpm using the Shake Master NEO (Bio Medical Science, Tokyo, Japan). Following RNA extraction using NucleoSpin® RNA (TaKaRa Bio., Kyoto, Japan) according to the manufacturer's instructions, cDNA was synthesized from 500 ng of total RNA by reverse transcription (RT) using PrimeScript II 1st strand cDNA Synthesis Kit (TaKaRa Bio., Kyoto, Japan). To measure the expression of inflammation-related genes in the intestinal tissue, qPCR was carried out with a Thermal Cycler Dice Real-Time System (TaKaRa Bio Each RT-qPCR reaction contained the following: 7.5 μL of TB Green® Premix Ex Taq™ II (TaKaRa Bio., Kyoto, Japan), 0.6 μL (10 pmol) of each forward and reverse primers, 1 μL of the appropriately diluted cDNA solution, and 5.9 μL of water. The specificity of all primers was confirmed by analyzing the melting curves after the PCR was run. The cycling conditions were as follows: 95 °C for 30 s, followed by 40 cycles of 95 °C for 5 s, 60 °C for 30 s, and a dissociation phase with 95 °C for 15 s, 60 °C for 30 s, and 95 °C for 15 s. Standard curves were created for respective

genes using the PCR-amplified fragments as templates with oligo-dT primers. The primers were designed using Primer3 Plus software (http://www.bioinformatics.nl/cgi-bin/primer3plus/primer3plus.cgi), and the primer sets are listed in Table III-3.

Table III-3. Primer sets used for the quantification of inflammation-related gene expression with qPCR

Gene	Forward Primer (5'- 3')	Reverse Primer (5'- 3')
Actb	GCTCTTTTCCAGCCTTCCTT	AGGGAGACCAAAGCCTTCAT
Infg	CCTTTGGACCCTCTGACTTG	CGCAATCACAGTCTTGGCTA
Il1b	TGAAATGCCACCTTTTGACA	CTGCCTAATGTCCCCTTGAA
Il6	CACGGCCTTCCCTACTTCAC	TTCCAAGAAACCATCTGGCTA
Il10	CCAAGCCTTATCGGAAATGA	CATTCCCAGAGGAATTGCAT
Tnf	CCACATCTCCCTCCAGAAAA	CTCCCTTTGCAGAACTCAGG

Diversity/Similarity Metrics and Statistical Analysis

Statistical analyses were performed using R ver. 3.6.0 (www.r-project.org). Species richness (α diversity) of the samples was estimated by the number of OTUs in each microbial profile using the Shannon Index (Shannon and Weaver, 1949) and the Chao1 Index. Diversity indexes used in this study are summarized in Table III-4. Two-Way Repeated Measures ANOVA (rm-ANOVA) with Tukey's HSD post hoc test was used to determine the effect of each treatment over time. To determine the recovery of microbial communities, the magnitude of the microbial shift was quantified by comparing the microbiome profiles at baseline (Week 0) with profiles from other time points using the Bray-Curtis Dissimilarity Index. Community structure was further analyzed using principal components analysis (PCA) and exploratory factor analysis (EFA). One-Way ANOVA with post-hoc Dunnett's test was used to determine the statistical differences in cecum weight and expression of inflammation-related genes. Pearson's correlation analysis was used to identify specific taxa that were positively or negatively associated with cecum weight and expression of inflammation-related genes.

Table III-4. Summary of diversity indexes used in this study.

Index	Description
Shannon	An index that accounts for both the number of species and their respective relative abundances. Higher values indicate higher diversity and evenness within the community (Shannon and Weaver, 1949).
Chao1	An estimate for species richness based on the abundance of OTUs. Higher values indicate a higher diversity within a given community (Chao, 1984).
Bray-Curtis Dissimilarity	A measure of β-diversity that quantifies the dissimilarity between two different sites based on community composition. Values are bound between 0 and 1. If 0, the two sites similar and share all the same species. If 1, the sites are dissimilar and do not share any species (Bray and Curtis, 1957).

Results and Discussion

The goal of this study was to assess the efficacy of the probiotic strain, *Bifidobacterium bifidum* JCM 1254, in the recovery period after the repeated antibiotic disturbance. Using mouse models, the effect of three different antibiotics with varying bacterial targets and spectrum of activity were tested. A subsequent recovery treatment consisted of natural recovery, *B. bifidum* administration, or fecal transplants from healthy, age-matched donor mice from the control group. The key findings of this study are as follows: (1) the response of the gut microbiome varies significantly with the type of disturbance; (2) *B. bifidum* is most effective when antibiotic disturbance increases proinflammatory species; (3) probiotic supplementation does not restore the diversity of the gut microbiome to baseline levels but can contribute to the recovery of host health. These results provide insight into how disturbance ecology affects the gut microbial community and its response to recovery treatments.

Vancomycin significantly alters the gut microbiome and increases proinflammatory species

First, the effect of repeated exposure to vancomycin, ciprofloxacin, or amoxicillin on the structure of the gut microbiome was compared (see Table III-1 for spectrum and mode of action). To do so, each antibiotic was administered in drinking water for a week, and the mice were given two weeks of natural

recovery. This process was repeated three times (Natural Recovery; Figure III-1). Although statistically insignificant, the percent body weight increase tended to be greater for all antibiotics compared to control (Supplementary Figures III-1 A–C). The fecal microbiome was analyzed by meta-16S rRNA sequencing. For all antibiotic types, significant variation in bacterial load during the experiment was not observed (Supplementary Figures III-1 D–F). This may be because fecal samples were collected after 7 days of antibiotic administration, which could have allowed the taxa unaffected by the antibiotics to proliferate during that time. Similar trends with vancomycin (Cheng et al., 2017) and amoxicillin (Cabral et al., 2019) have also been previously reported.

However, the differences between antibiotics were clear when comparing α-diversity using the Shannon Index (evenness; Figure III-2 A) and the Chao1 Index (species richness; Figure III-2 B). The results of Two-Way rm-ANOVA show that the type of antibiotic had differential effects on α-diversity (Supplementary Table III-1). For ciprofloxacin, antibiotic administration had no significant effect on α-diversity over time. Ciprofloxacin has been shown to significantly alter the gut microbiome in human subjects (Dethlefsen and Relman, 2011), but has a limited effect on community structure in murine models (Schubert et al., 2015). Furthermore, ciprofloxacin is considered to have limited activity against anaerobic microbes (Goldstein and Citron, 1988). For amoxicillin, α-diversity was significantly reduced in terms of both evenness (> 34 % reduction; Figure III-2 A) and species richness (> 60 % reduction Figure III-2 B) after the first antibiotic disturbance event but recovered to control levels within two weeks. While this pattern continued after the second and third antibiotic disturbance events for species richness, evenness was not significantly affected after the first disturbance event, as amoxicillin is a β-lactam antibiotic that affects both Gram-positive and -negative bacteria. Of the three antibiotics, vancomycin had the strongest effect on α-diversity. The first antibiotic disturbance significantly reduced evenness (> 52 % reduction; Figure III-2 A) and richness (> 81 % reduction; Figure III-2 B), both of which did not recover throughout the experiment.

In addition to α-diversity, recovery was measured by quantifying the magnitude of the microbial shift from baseline (Week 0) using the Bray-Curtis Index of Dissimilarity (Figure III-2 C), and the results of Two-Way rm-ANOVA show that the differences in the antibiotic type significantly affected the microbial communities during recovery (Supplementary Table III-2). For this study, communities that returned to baseline community structures based on this index were considered as “recovered.” For both ciprofloxacin and amoxicillin, dissimilarity increased with each antibiotic disturbance event and gradually decreased over the following two weeks.

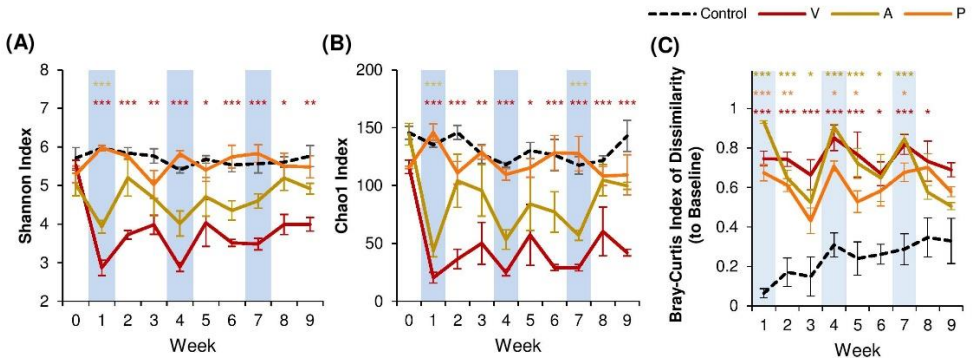

Figure III-2 | Comparison of the effects of vancomycin, ciprofloxacin, and amoxicillin on diversity metrices. Each antibiotic was administered for 7 days every 3 weeks, and changes to the fecal microbiome over time were observed by meta-16S rRNA sequencing. Alpha diversity measured by (A) Shannon Index and (B) Chao1 Index for each treatment over time ± standard error. (C) Bray-Curtis Index of Dissimilarity vs baseline for each treatment over time ± standard error. The Bray-Curtis Index was used to quantify the amount of microbial shift from the first day of the experiment (baseline) for each mouse. Colored asterisks indicate significance vs control for NR, PR, and FT groups based on Two-Way rm-ANOVA and Tukey's HSD post hoc test (*$p < 0.05$, **$p < 0.01$, ***$p < 0.001$). Data for the control samples are indicated as the black dotted line. Natural recovery data for vancomycin is in red, amoxicillin in yellow, and ciprofloxacin in orange. Figure modified with permission from Ojima et al., (2020).

Examination at the phylum level showed that each antibiotic disturbance event increased the relative abundance of Proteobacteria (12 %, ciprofloxacin; 20 %, amoxicillin), which then decreased over time (Figure III-3 A). Although some level of recovery was observed, the microbial communities did not return to baseline levels throughout the experiment, which is consistent with previous studies that report that repeated antibiotic use leads to incomplete recovery (Dethlefsen and Relman, 2011). With vancomycin, the microbial communities displayed patterns consistent with α-diversity, and community dissimilarity remained high throughout the experiment after the first antibiotic disturbance. At the phylum level, the relative abundance of Proteobacteria increased significantly after the first antibiotic disturbance event (70 %). Although this increase was diminished after the second (19 %) and third (8 %) antibiotic disturbance events, the presence of Proteobacteria was persistent throughout the experiment (Figure III-3 A). For all antibiotics, the increase in Proteobacteria was less pronounced with repeated disturbances. Further examination with principal components analysis (PCA) based on the microbial community composition corroborated these observations. For vancomycin- and amoxicillin-treated groups, PCA revealed that communities after the first antibiotic administration formed a separate cluster (Supplementary Figures III-2 A, B). The subsequent second and third antibiotic treatments for vancomycin and amoxicillin clustered closer to the control communities, lending further evidence to the fact that the gut microbiome retains the memory of past disturbance events (Dethlefsen and Relman, 2011). For ciprofloxacin-treated groups, however, the different treatments did not create clear clusters (Supplementary Figure III-2 C).

Further examination using exploratory factor analysis showed that the increase in Proteobacteria can be attributed to *Escherichia coli* for all antibiotics (Figure III-3 B, Supplementary Figure III-3, Supplementary Table III-3). However, for vancomycin, there were also increases in proinflammatory species associated with dysbiosis. For example, after the first antibiotic disturbance event, there was a notable increase in *Proteus* (34.7 %, relative abundance; Figure III-3 B, Supplementary Figure III-3), a genus associated with the onset of colitis (Shin et al., 2015). There was also an increase in the abundance of Desulfovibrionaceae (Figure III-3 B, Supplementary Figure III-3), a family of sulfate-reducing bacteria often associated with high-fat diets (Clarke et al., 2012) during Week 2 (a 350-fold increase compared to baseline). In disturbance ecology, the type of disturbance is a critical factor that determines which specific members of the community are selected for over time (Relman, 2012), and these results indicate that gut microbiome responses vary significantly by antibiotic type, with vancomycin having the most detrimental effects. Previous studies have shown that vancomycin is a particularly potent antibiotic that significantly reduces gut microbiome diversity (Vrieze et al., 2014) and causes intestinal dysbiosis (Cheng et al., 2017). Therefore, the following sections focus on vancomycin and how different treatments (fecal transplants or probiotic administration) could contribute to the recovery of the gut microbial community.

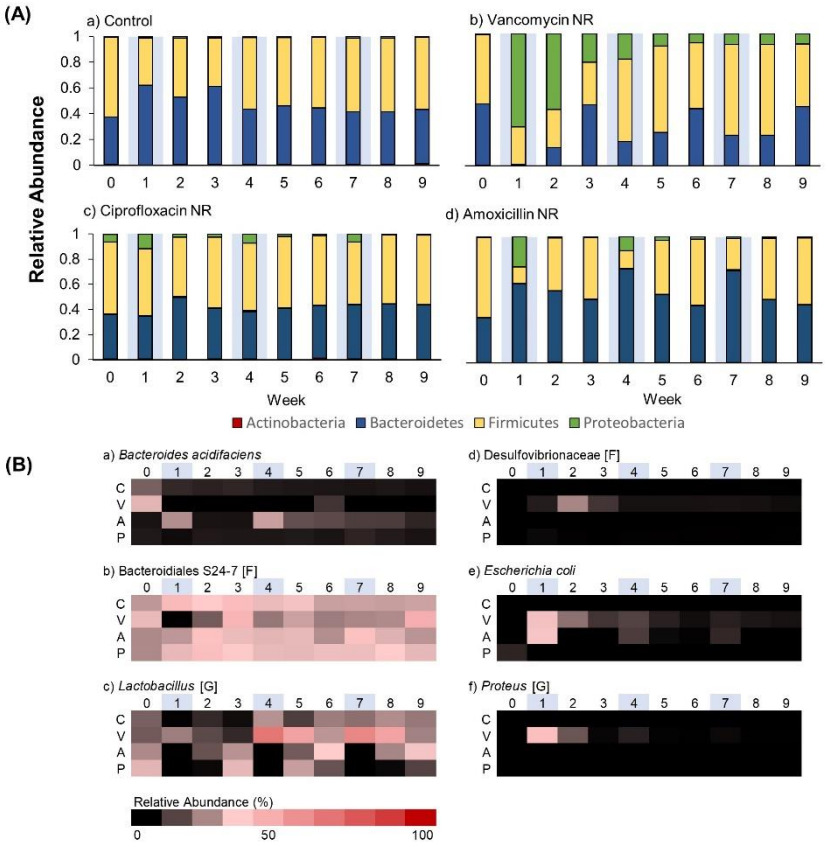

Figure III-3 | Comparison of the effects of vancomycin, ciprofloxacin, and amoxicillin on the gut microbiome. The community composition of the gut microbiome at each time point for each treatment was observed using meta-16S rRNA sequencing. (A) The microbial community at each time point at the phylum level for (a) control, (b) vancomycin, (c) ciprofloxacin, and (d) amoxicillin. (B) Heat map of taxa that significantly changed after antibiotic administration. Significant taxa were identified using factor analysis (factor loading > 0.2). The lowest taxonomic rank for which information was available is indicated in square brackets (F: family, G: genus). Weeks shaded in blue indicate weeks in which antibiotics were administered. Figure modified with permission from Ojima et al., (2020).

Fecal transplants restore gut microbiome diversity after vancomycin administration

Past studies have indicated that fecal transplants contribute to relatively rapid recovery after antibiotic-induced dysbiosis (Ekmekciu et al., 2017; Suez et al., 2018). After each vancomycin administration, I administered fecal transplants from healthy, age-matched control mice for a week. As expected, the fecal transplants produced a significant effect on both α-diversity metrics, as well as community dissimilarity (Supplementary Tables III-4, 5). α-Diversity was reduced after the first antibiotic disturbance event but completely recovered to control levels within two weeks of fecal transplants, and this pattern was observed for the subsequent disturbance events as well (Figures III-4 A, B). A similar pattern was observed for community dissimilarity, where each antibiotic administration increased dissimilarity, but fecal transplants restored community structures to baseline levels within two weeks

(Figure III-4 C). Examination of community membership revealed that, compared to the natural recovery groups (V), fecal transplants were effective in reducing the Proteobacteria populations that had increased with each vancomycin administration (Figure III-5 A). While Proteobacteria populations persisted in the natural recovery groups (relative abundance > 8 %), Proteobacteria were nearly undetectable within two weeks after fecal transplants (relative abundance < 1 %). The increase in inflammatory taxa such as *Proteus* was also suppressed (Figure III-5 B). These results are consistent with previous studies, which have shown that fecal transplants are effective in correcting dysbiosis and reducing inflammation. Furthermore, a recent study by Burrello et al. (2018) demonstrated that fecal transplants promote recovery by stimulating immune cells to produce IL-10 and that the beneficial effects of fecal transplants seem to be correlated with the persistence of protective taxa such as Lactobacillaceae, Bifidobacteriaceae, Erysipelotrichaceae, Ruminococcacceae, and Bacteroidales S24-7.

Bifidobacterium bifidum does not restore diversity but reduces intestinal inflammation

In addition to fecal transplants, probiotic supplementation has been linked to a variety of positive effects, such as reduced incidences of diarrhea in infants (Hotta et al., 1987), improvement in immune functions (Mohan et al., 2008), anti-obesity effects (Kondo et al., 2010; Stenman et al., 2014; Moya-Pérez et al., 2015), and recovery after antibiotic disturbance (Grazul et al., 2016; Ekmekciu et al., 2017). However, how effective probiotics are in restoring the disturbed gut microbial community after antibiotics remains a topic of debate (Suez et al., 2019). To assess the efficacy of probiotics in recovery after vancomycin administration, *Bifidobacterium bifidum* JCM 1254 was administered to mice via oral gavage for one week. Probiotic administration seemed to have little effect on recovery. Like the natural recovery groups, α-diversity did not return to baseline levels after the first antibiotic disturbance event (Figures III-4 A, B), and community dissimilarity remained high (Figure III-4 C). Similarly, Suez et al. (2018) also reported that a probiotic blend including *Lactobacillus*, *Bifidobacterium*, *Lactococcus*, and *Streptococcus* genera did not promote recovery after antibiotic-induced dysbiosis. These results suggest that species commonly called “probiotics” may be insufficient for community recovery.

The results of exploratory factor analysis showed that the relative abundance of *Lactobacillus* species, *Proteus* species, *E. coli*, and Bacteroidales S24–7 contributed significantly to community structure (Supplementary Table III-6). Although α-diversity did not recover, the first *B. bifidum* supplementation caused a two-fold increase in the relative abundance of Bacteroidales S24–7 (Figure III-5 B), a family of fermenters often associated with a healthy microbiome in mice that produce short-chain fatty acids (SCFA) and vitamin B (Evans et al., 2014; Rooks et al., 2014; Ormerod et al., 2016). While not as effective as fecal transplants, probiotics were also able to suppress the increase of Proteobacteria,

such as *E. coli* and *Proteus* populations (Figure III-5 B). Previous studies have also reported the reduction of Proteobacteria after *Bifidobacterium* supplementation. For instance, the administration of *Bifidobacterium longum* decreased the relative abundance of Proteobacteria and reduced the expression of the gene encoding TNF-α in mice (Lee et al., 2019), and *B. infantis* supplementation decreased γ-Proteobacteria in infants (Underwood et al., 2013). Furthermore, I observed that recovery treatments had a significant effect on cecum size (One-Way ANOVA: $F(3,12) = 5.513$, $p < 0.05$; Figure III-6 A). While mice in the natural recovery group (V) had a significantly larger cecum compared to the control (post hoc Dunnett's test: $p < 0.05$), the difference was insignificant for groups given *B. bifidum* (VB) and fecal transplants (VF), suggesting that cecal enlargement was corrected by *B. bifidum* administration and fecal transplants. A previous study has also reported an enlargement in the cecum of antibiotic-treated mice, possibly because of a decrease in intestinal motility (Puhl et al., 2012). Cecal enlargement may also have been caused by the increase of pro-inflammatory species. Further analysis with Pearson's correlation analysis revealed that there were strong positive correlations between cecum weight and the abundance of inflammatory taxa such as *Proteus* ($r = 0.91$, $p < 0.001$), and *E. coli* ($r = 0.84$, $p < 0.001$). Cecum weight and the expression of genes encoding IL-1β also showed a significant positive correlation ($r = 0.70$, $p < 0.05$).

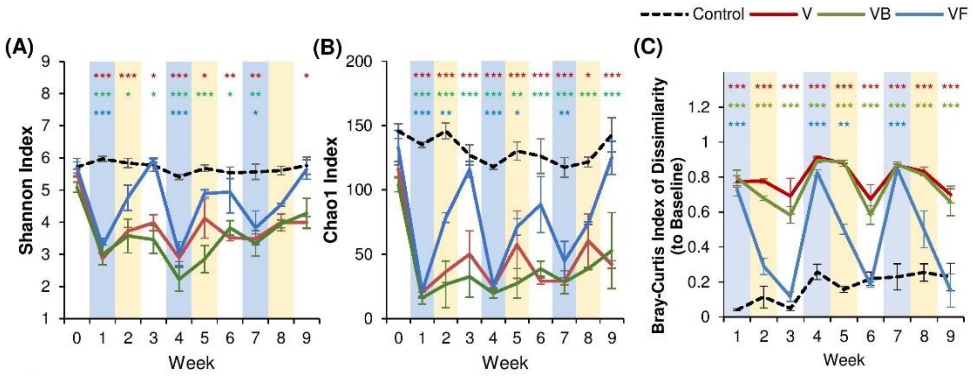

Figure III-4 | The effect of recovery treatments on the gut microbiome after vancomycin. Vancomycin administration was followed by either natural recovery (NR), *Bifidobacterium bifidum* (PR), or fecal transplants (FT), and changes to the gut microbiome were observed over time. Alpha diversity measured by (A) Shannon Index and (B) Chao1 Index for each treatment over time ± standard error. (C) Bray-Curtis Index of Dissimilarity vs baseline for each treatment over time ± standard error. The Bray-Curtis Index was used to quantify the amount of microbial shift from the first day of the experiment (baseline) for each individual. Colored asterisks indicate significance vs control for NR, PR, and FT groups based on Two-Way rm-ANOVA and Tukey's HSD post hoc test (*$p < 0.05$, **$p < 0.01$, ***$p < 0.001$). Data for the control samples are indicated as the black dotted line, with NR (V) groups in red, PR (VB) groups in green, and FT (VF) groups in blue. Figure modified with permission from Ojima et al., (2020).

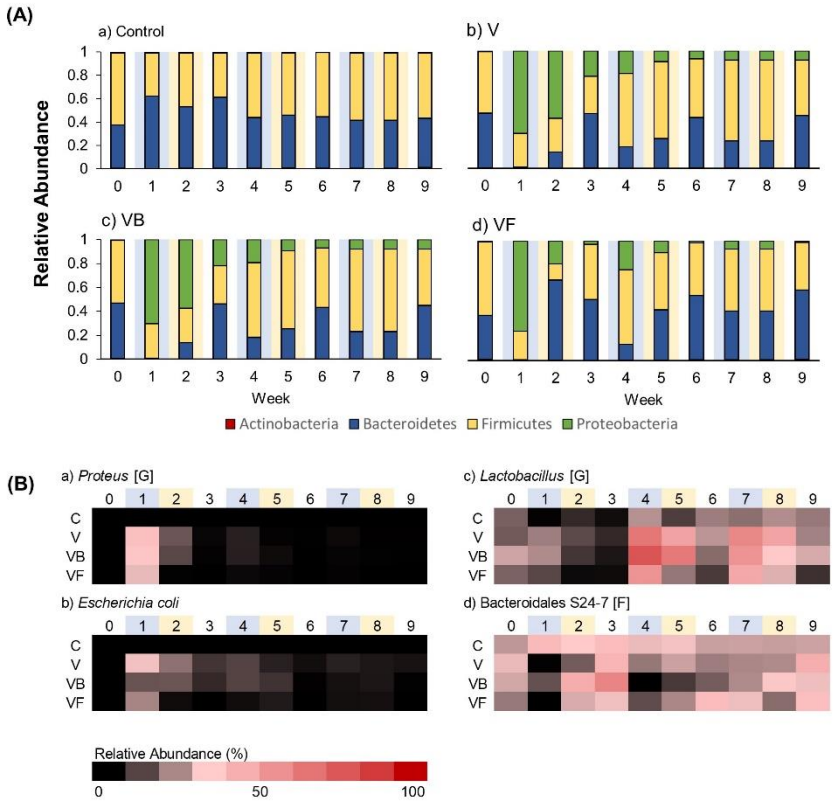

Figure III-5 | The effect of recovery treatments on the gut microbiome after vancomycin. The community composition of the gut microbiome at each time point for each treatment was observed using meta-16S rRNA sequencing. (A) The microbial community at each time point at the phylum level for (a) control, (b) V, (c) VB, and (d) VF. (B) Heat map of taxa that significantly changed after antibiotic administration. Significant taxa were identified using factor analysis (factor loading > 0.4). The lowest taxonomic rank for which information was available is indicated in square brackets (F: family, G: genus). Weeks shaded in blue indicate weeks in which antibiotics were administered, and weeks shaded in yellow indicate weeks in which a recovery treatment (natural recovery, probiotics, or fecal transplants) were administered. Figure modified with permission from Ojima et al., (2020).

Additionally, results of RT-qPCR indicate that the expression of genes encoding proinflammatory cytokines (IL-1β and INF- γ) in the colon was significantly increased in the natural recovery groups (Figures III-6 B, C), while expression was suppressed by probiotic administration and fecal transplants. Verma et al. (2019) recently identified *B. bifidum* cell surface polysaccharides as a factor that suppresses inflammation in the gut. Another possible anti-inflammatory mechanism may be modulated by indole-3-lactic acid (ILA) produced by *Bifidobacterium* species. ILA is an aromatic lactic acid and a metabolite of aromatic amino acids such as tryptophan and serves as a ligand for the aryl hydrocarbon receptor (AhR) that regulates intestinal homeostasis. Meng et al. (2019) found that ILA produced by *B. infantis* had anti-inflammatory effects on infant enterocytes *in vitro*. This metabolite is also reported to be produced by *B. bifidum* (Sakurai et al., 2019). A recent study by Laursen et al. (2020) has shown that *Bifidobacterium* species possess a specific enzyme that converts aromatic pyruvates, precursors of aromatic amino acids,

into aromatic lactic acids. Given these results, it is possible that *B. bifidum* supplementation suppresses the increase of proinflammatory species and ultimately reduces gut inflammation.

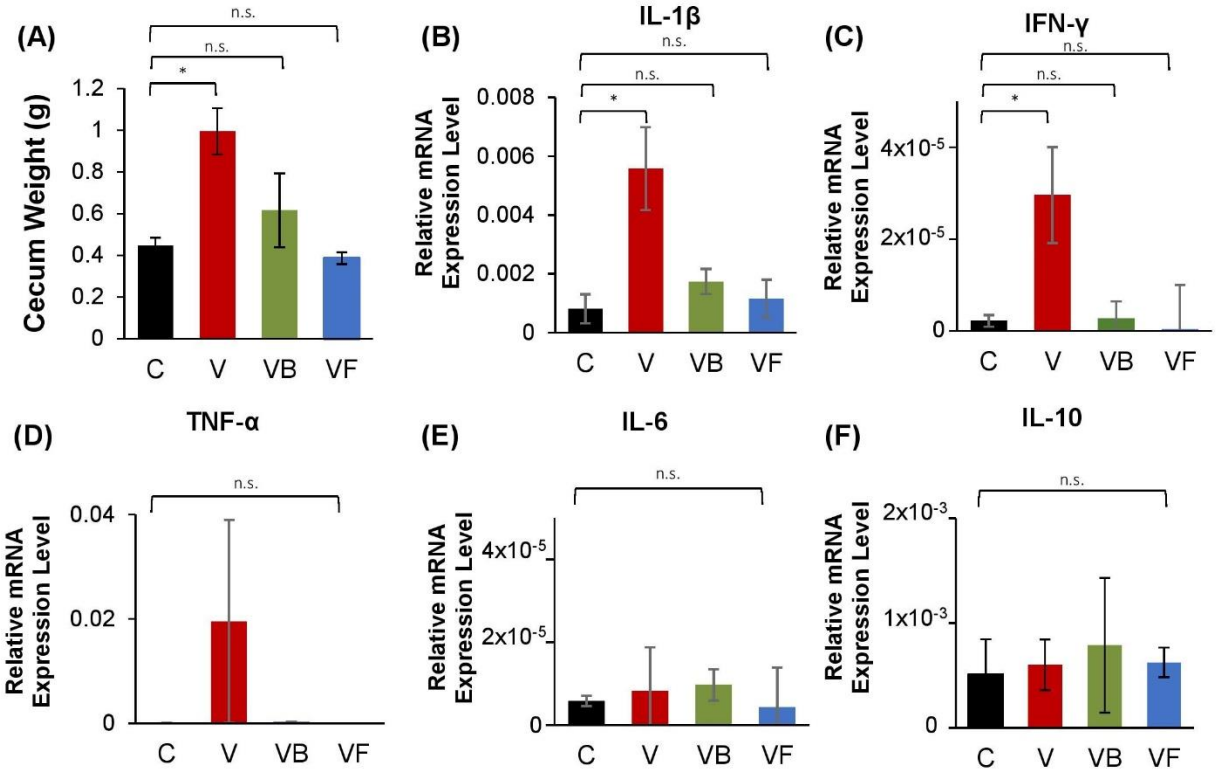

Figure III-6 | Changes in cecum size and expression of inflammation-related genes in vancomycin-treated mice. At the end of the experiment, cecum weight and the mRNA expression levels of inflammation-related genes in the large intestine for vancomycin-treated mice (C: control, V: vancomycin + natural recovery, VB: vancomycin + *B. bifidum*, VF: vancomycin + fecal transplant from control mice) were measured. (A) Cecum weight, relative mRNA expression of genes encoding (B) IL-β, (C) TNF-α, (D) INF-γ, (E) IL-6, and (F) IL-10 for vancomycin-treated mice, using Actb as a reference gene. Error bars indicate standard error, and significance was determined by One-Way ANOVA and Dunnett's test. (*$p < 0.05$, **$p < 0.01$, ***$p < 0.001$). This figure is used with permission from Ojima et al., (2020).

The expression of genes encoding TNF-α, IL-6, and IL-10 were also examined, but there were no significant differences between treatments (Figures III-6 D–F), suggesting that antibiotic-induced dysbiosis leads to the induction of specific inflammatory cytokines. This experiment was repeated for amoxicillin- and ciprofloxacin-treated mice. However, the effects of neither fecal transplants nor probiotics differed significantly from NR groups for α-diversity and community structure (Supplementary Figures III-6, 5), and no cecum enlargement was observed, even for antibiotic-treated groups (Supplementary Figures III-6 A, 7 A). As neither amoxicillin nor ciprofloxacin caused a bloom in pro-inflammatory species (Supplementary Figures III-4 B–F, 5 B–F), probiotics did not affect the expression

of inflammation-related genes after antibiotic administration. In the absence of inflammatory species, the effect of fecal transplants and probiotic supplementation was negligible.

Increase in Lactobacillus abundance potentially delays gut microbiome recovery

One common event observed for all antibiotics was the expansion of *Lactobacillus*, particularly for vancomycin- treated groups (Figure III-3 B). The increase in *Lactobacillus* abundance was especially noticeable after the second antibiotic administration, possibly because of its superior capability to tolerate disturbances. Past studies have shown *Lactobacillus* species to have a high level of vancomycin resistance (Gueimonde et al., 2013), as well as a relatively high tolerance to low pH (Corcoran et al., 2005; O'May et al., 2005). Furthermore, Suez et al. (2018) found that *Lactobacillus* was a microbiome-inhibitory species. Although unconfirmed in this study, the increased relative abundance of *Lactobacillus* may have contributed to the inhibited recovery from antibiotic administration.

Limitations

One limitation of this study is that it utilized a human-derived *Bifidobacterium* strain in murine models. Even in the human gut microbiome, the inability of probiotics to colonize the gut is a longstanding issue (Suez et al., 2019), but the lack of colonization was particularly evident in this study. Although samples were collected within 24 h of *B. bifidum* administration, its detection was limited in the 16S metagenomic analysis. Furthermore, prebiotics were not administered, possibly making colonization by *B. bifidum* in the gut even more difficult to achieve. A recent study by Cabral et al. (2019) has shown that the addition of fiber protected gut microbes from antibiotics, suggesting that the carbohydrates consumed in the diet alter the gut microbiome's response to disturbances. Therefore, to develop more efficient probiotic therapies, future studies should also consider the type of diet and prebiotics that are co-administered with antibiotics and probiotics.

Conclusions

Despite these limitations, this study provides insight into how the gut microbiome responds to repeated disturbances and subsequent recovery treatments. In clinical settings, antibiotics are prescribed both frequently and repeatedly. A study based in the United Kingdom found that approximately 30 % of patients are prescribed antibiotics at least once a year (Shallcross et al., 2017), although a different class of antibiotics is often re-prescribed with repeated use. Nonetheless, the results of our study elucidated

how the repeated use of different types of antibiotics affects the response of the gut microbiome to recovery treatments. The type of disturbance (i.e., affected species, frequency, magnitude, and duration) is a key factor in community structuring, and its effect should be considered when examining the gut microbial community. The disturbance type determines which specific taxa and functions within the gut microbiome are selected for (Relman, 2012); moreover, it also affects how the gut microbiome responds to the addition of probiotics. The results of this study showed that probiotics were effective in reducing gut inflammation without recovering gut microbiome diversity. Additionally, this study showed that probiotics were most effective when antibiotic disturbance caused an increase in proinflammatory species. The results of the study could be applied to clinical settings, where predicting the response of the gut microbiome to different recovery treatments after dysbiosis would offer potential benefit.

Supplementary Figures and Tables

Supplementary Table III-1 | Two-Way rm-ANOVA results for α-diversity metrics for natural recovery groups.

Shannon	Chi-Sq	Df	p value	Significance
Antibiotic-Type	142.7184	3	< 2e-16	***
Week	0.1738	1	0.6768	
Antibiotics × Week	3.1144	3	0.3743	

Chao 1	Chi-Sq	Df	p value	Significance
Antibiotic-Type	94.9894	3	< 2e-16	***
Week	6.0514	1	0.0139	*
Antibiotics × Week	0.3801	3	0.9443	

Significance codes: *p < 0.05, **p < 0.01, ***p < 0.001

Supplementary Table III-2 | Two-Way rm-ANOVA results for based on Bray-Curtis Index of Dissimilarity for natural recovery groups.

	Chi-Sq	Df	p value	Significance
Antibiotic-Type	65.9684	3	3.11E-14	***
Week	0.3231	1	0.5698	
Antibiotics × Week	25.8446	3	1.03E-05	***

Significance codes: *p < 0.05, **p < 0.01, ***p < 0.001

Supplementary Table III-3 | Factor loadings based on exploratory factor analysis for natural recovery groups. Note that the absolute values for blank entries are less than 0.2, but not zero.

	Factor 1	Factor 2	Factor 3
Lactobacillus [G]	0.926644	-0.27507	
Proteus [G]		0.392107	-0.32282
Escherichia coli		0.499274	-0.45402
Desulfovibrionaceae [F]			-0.21764
Bacteroides acidifaciens			0.457251
Bacteroidales S24-7 [F]	-0.24224	-0.64117	-0.50964

Supplementary Table III-4 | Two-Way rm-ANOVA results for α-diversity metrics for vancomycin-treated groups.

Shannon	Chi-Sq	Df	p value	Significance
Treatment	138.5642	3	< 2e-16	***
Week	0.3842	1	0.5354	
Treatment × Week	1.0472	3	0.7898	

Chao1	Chi-Sq	Df	p value	Significance
Treatment	177.8706	3	< 2e-16	***
Week	3.4694	1	0.06251	
Treatment × Week	3.2894	3	0.3743	

Significance codes: *p < 0.05, **p < 0.01, ***p < 0.001

Supplementary Table III-5 | Two-Way rm-ANOVA results for based on Bray-Curtis Index of Dissimilarity for vancomycin-treated groups.

	Chi-Sq	Df	p value	Significance
Treatment	65.9684	3	3.11E-14	***
Week	0.3231	1	0.5698	
Treatment × Week	25.8446	3	1.03E-05	***

Significance codes: *p < 0.05, **p < 0.01, ***p < 0.001

Supplementary Table III-6 | Factor loadings based on exploratory factor analysis for vancomycin treated groups. Note that the absolute values for blank entries are less than 0.2, but not zero.

	Factor 1	Factor 2	Factor 3
Lactobacillus [G]	0.867991	-0.39684	
Proteus [G]		0.655285	0.403186
Escherichia coli		0.356525	0.300518
Bacteroidales S24-7 [F]	-0.40856	-0.51367	0.650558

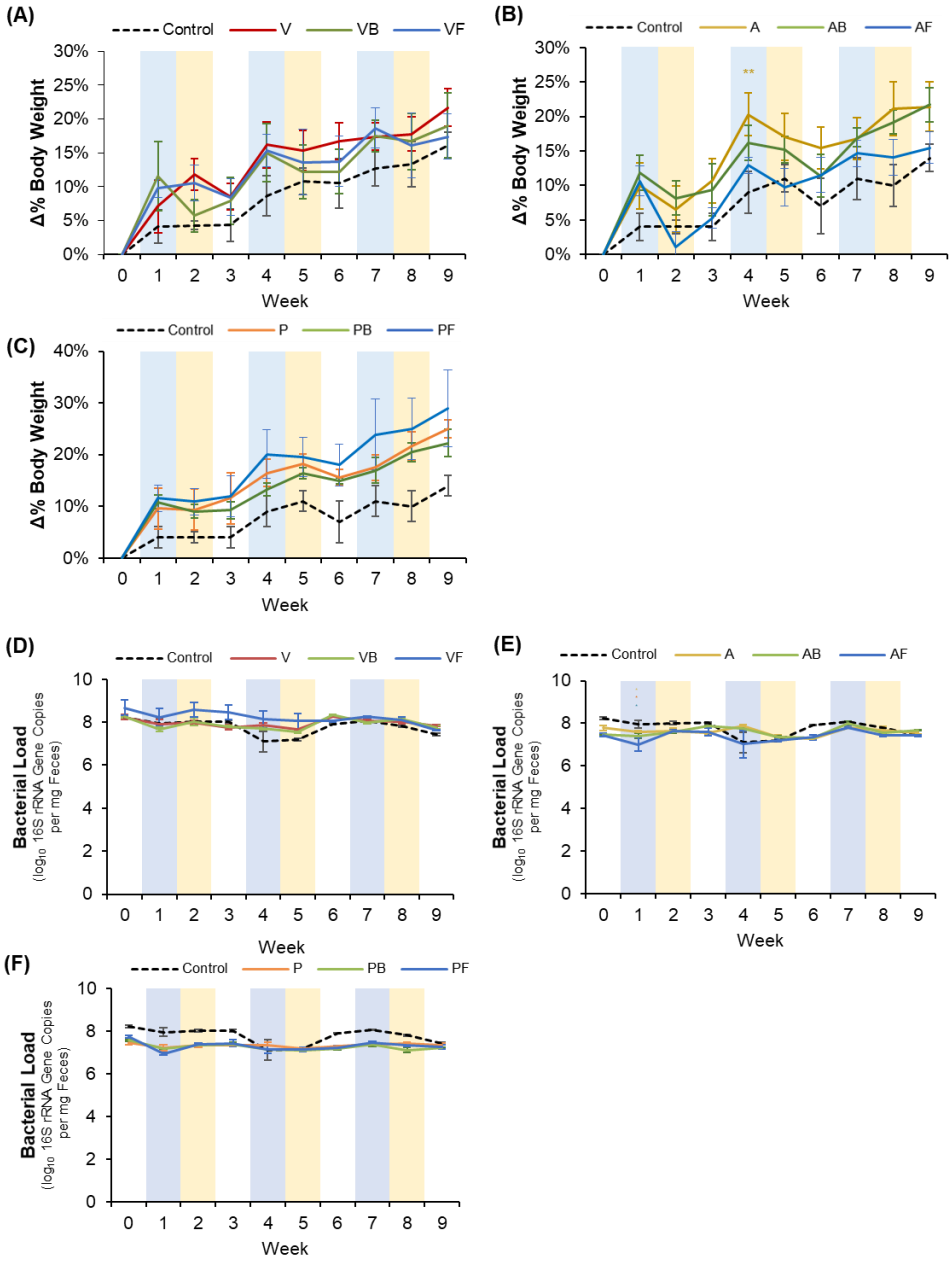

Supplementary Figure III-1 | Change in body weight and bacterial load over time. Percent change in body weight over time for A) vancomycin, B) amoxicillin, and C) ciprofloxacin. Total bacterial load measured by the number of 16S rRNA gene copies per mg of feces using qPCR D) vancomycin, E) amoxicillin, and F) ciprofloxacin. Weeks shaded in blue indicate weeks in which antibiotics were administered, and weeks shaded in yellow indicate weeks in which recovery treatments (natural recovery, probiotics, or fecal transplants) were administered. This figure is used with permission from Ojima et al., (2020).

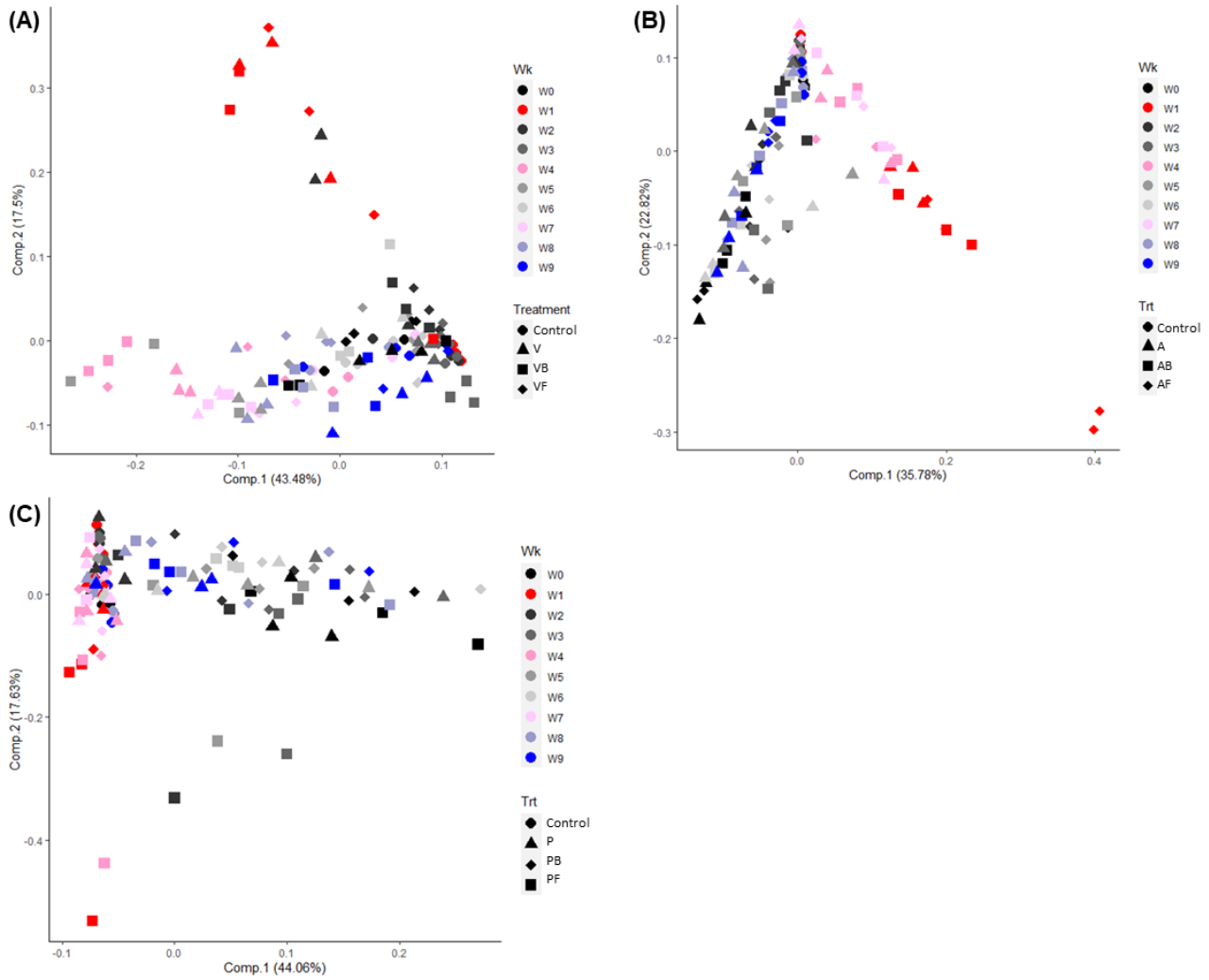

Supplementary Figure III-2 | Principal components analysis plot based on the microbial community composition. Principal components analysis was performed based on microbial community composition for A) vancomycin-treated groups, B) amoxicillin treated groups, and C) ciprofloxacin treated groups. Treatment is denoted by different shapes (circle: control, triangle: natural recovery, diamond: *B. bifidum*, square: fecal transplant) for each antibiotic group. Baseline communities (Week 0) are indicated in black, communities after the first antibiotic treatment are indicated in red, and the final communities are indicated in blue. The subsequent second and third antibiotic treatments are indicated in progressively lighter shades of red, and interim periods between antibiotic courses are indicated in progressively lighter shades of grey. This figure is used with permission from Ojima et al., (2020).

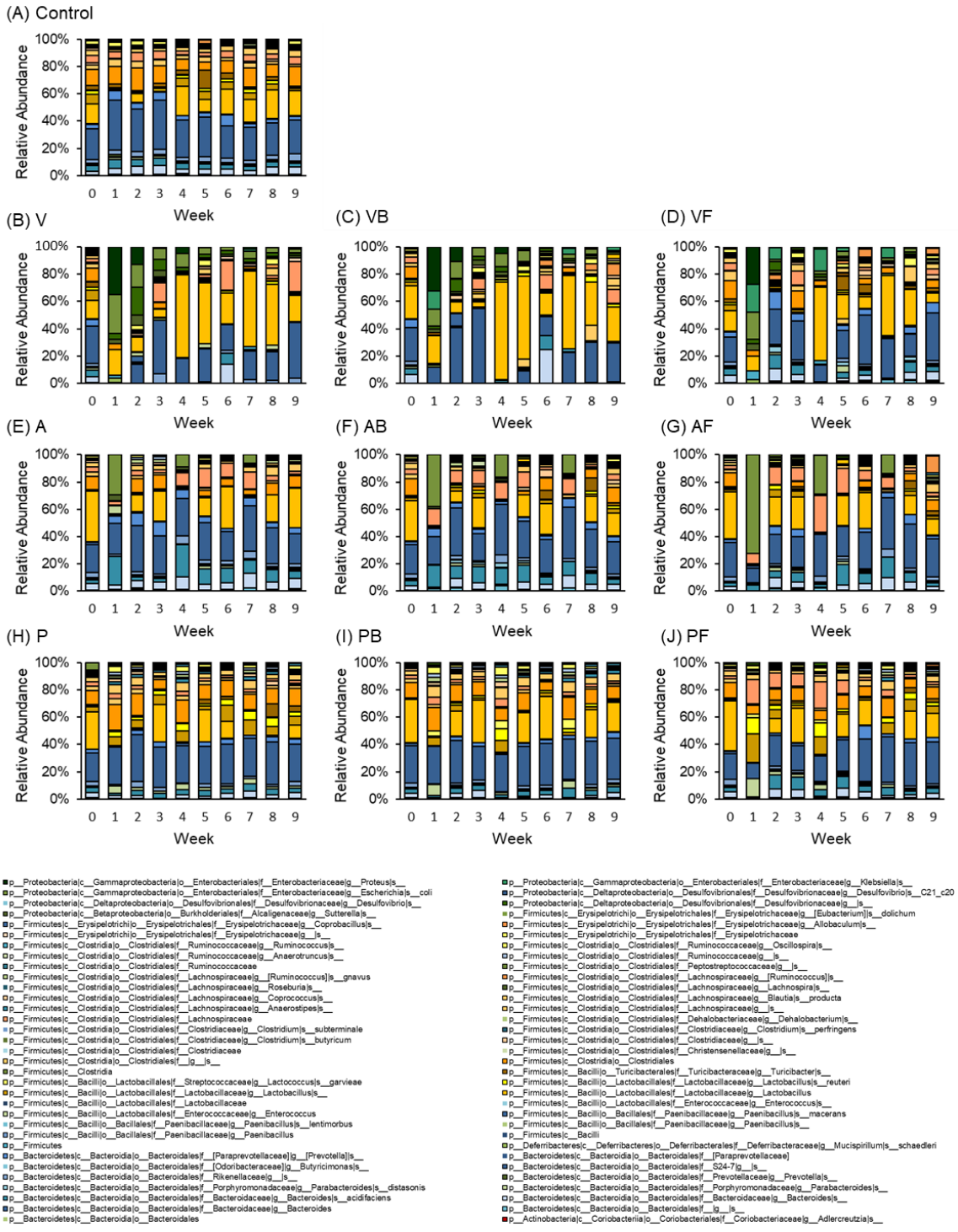

Supplementary Figure III-3 | Microbial community composition based on sequencing data of the V3-V4 regions of the 16S rRNA gene. The composition of the gut microbial community over time was determined based on sequencing data of the V3-V4 region of the 16S rRNA gene. For each treatment, relative abundance (%) of each taxon is shown (the lowest taxonomic rank for which information was available). A) C: control, B) V: vancomycin + natural recovery, C) VB: vancomycin + *B. bifidum*, D) VF: vancomycin + fecal transplant, E) A: amoxicillin + natural recovery, F) AB: amoxicillin + *B. bifidum*, G) AF: amoxicillin + fecal transplant, H) P: ciprofloxacin + natural recovery, I) PB: ciprofloxacin + *B. bifidum*, J) PF: ciprofloxacin + fecal transplant. This figure is used with permission from Ojima et al., (2020).

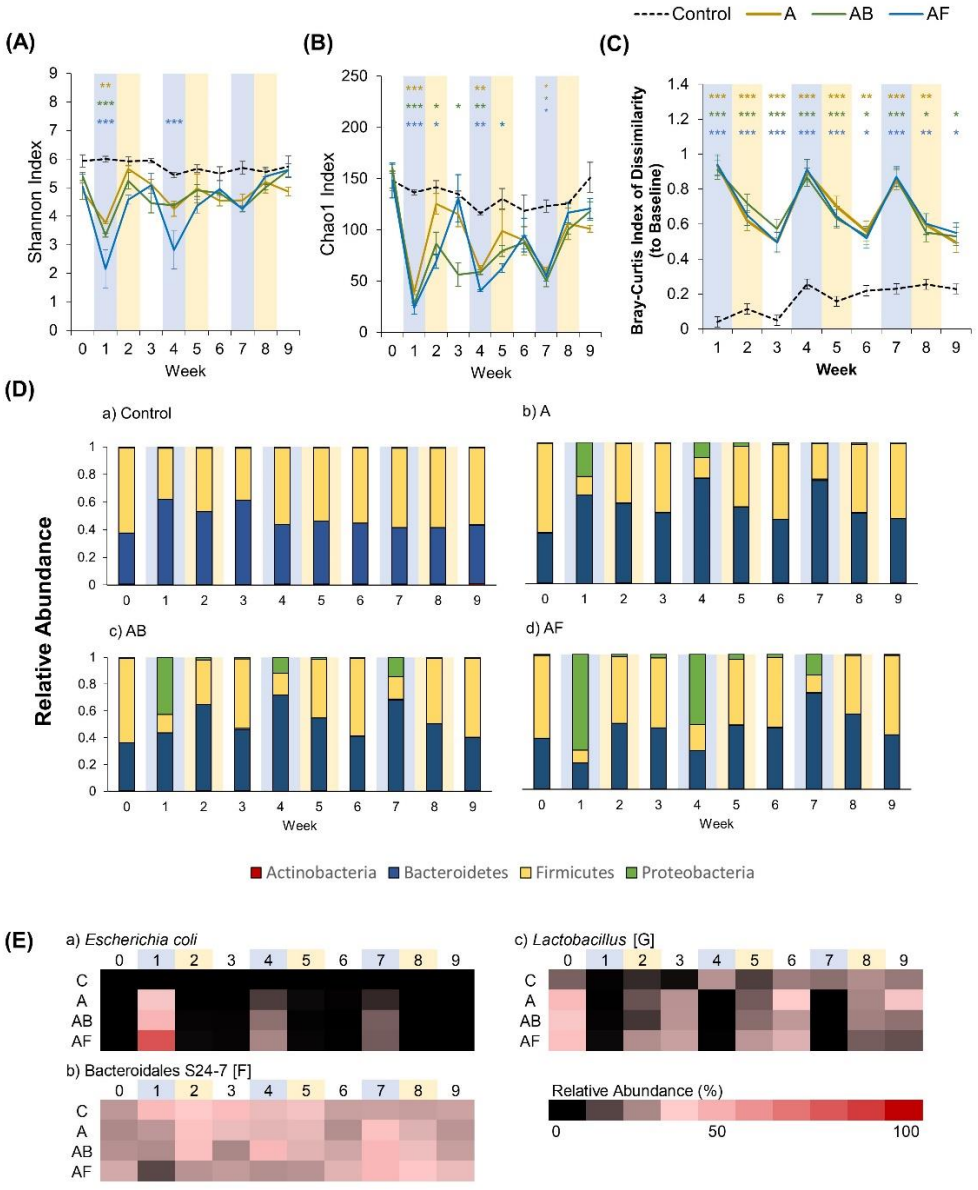

Supplementary Figure III-4 | The effect of recovery treatments on the gut microbiome after amoxicillin. Amoxicillin administration was followed by either natural recovery (NR), *Bifidobacterium bifidum* (PR), or fecal transplants (FT), and changes to the gut microbiome were observed over time.
Alpha diversity measured by A) Shannon Index and B) Chao1 Index for each treatment over time ± standard error. C) Bray-Curtis Index of Dissimilarity vs baseline for each treatment over time ± standard error. The Bray-Curtis Index was used to quantify the amount of microbial shift from the first day of the experiment (baseline) for each individual. Colored asterisks indicate significance vs control for NR, PR, and FT groups based on Two-Way rm-ANOVA and Tukey's HSD post hoc test (* $p < 0.05$, ** $p < 0.01$, *** $p < 0.001$). Data for the control samples are indicated as the black dotted line, with NR groups in red, PR groups in green, and FT groups in blue.
D) The microbial community at each time point at the phylum level for a) control, b) NR (A), c) PR (AB) and d) FT (AF). E) Heat map of taxa that significantly changed after antibiotic administration. Significant taxa were identified using factor analysis (factor loading > 0.2). The lowest taxonomic rank for which information was available is indicated in square brackets (F: family, G: genus). Weeks shaded in blue indicate weeks in which antibiotics were administered, and weeks shaded in yellow indicate weeks in which recovery treatments (natural recovery, probiotics, or fecal transplants) were administered. This figure is used with permission from Ojima et al., (2020).

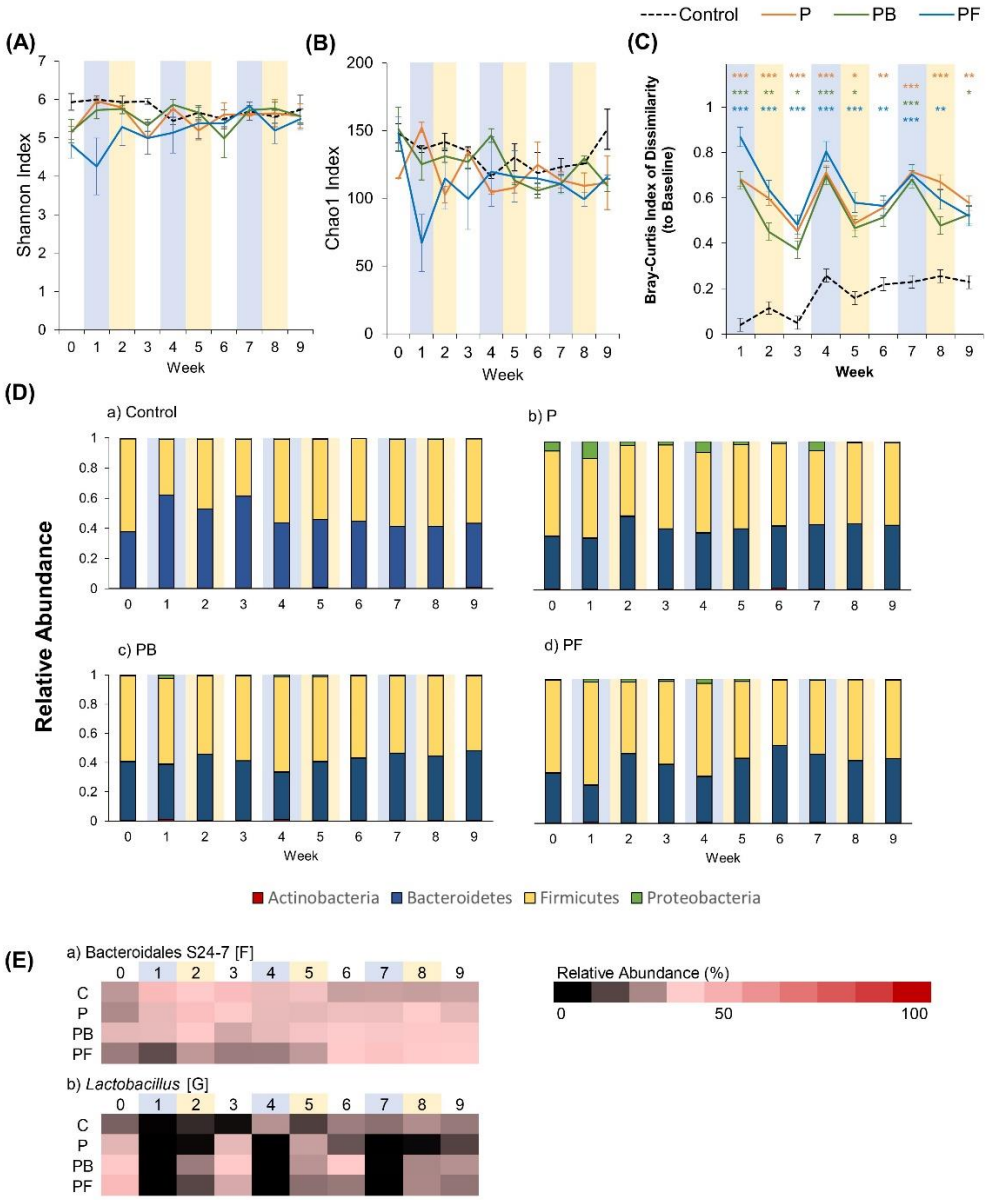

Supplementary Figure III-5 | The effect of recovery treatments on the gut microbiome after ciprofloxacin. Ciprofloxacin administration was followed by either natural recovery (NR), *Bifidobacterium bifidum* (PR), or fecal transplants (FT), and changes to the gut microbiome were observed over time.
Alpha diversity measured by A) Shannon Index and B) Chao1 Index for each treatment over time ± standard error. C) Bray-Curtis Index of Dissimilarity vs baseline for each treatment over time ± standard error. The Bray-Curtis Index was used to quantify the amount of microbial shift from the first day of the experiment (baseline) for each individual. Colored asterisks indicate significance vs control for NR, PR, and FT groups based on Two-Way rm-ANOVA and Tukey's HSD post hoc test (* $p < 0.05$, ** $p < 0.01$, *** $p < 0.001$). Data for the control samples are indicated as the black dotted line, with NR groups in red, PR groups in green, and FT groups in blue.
D) The microbial community at each time point at the phylum level for a) control, b) NR (P), c) PR (PB) and d) FT (PF). E) Heat map of taxa that significantly changed after antibiotic administration. Significant taxa were identified using factor analysis (factor loading > 0.2). The lowest taxonomic rank for which information was available is indicated in square brackets (F: family, G: genus). Weeks shaded in blue indicate weeks in which antibiotics were administered, and weeks shaded in yellow indicate weeks in which recovery treatments (natural recovery, probiotics, or fecal transplants) were administered. This figure is used with permission from Ojima et al., (2020).

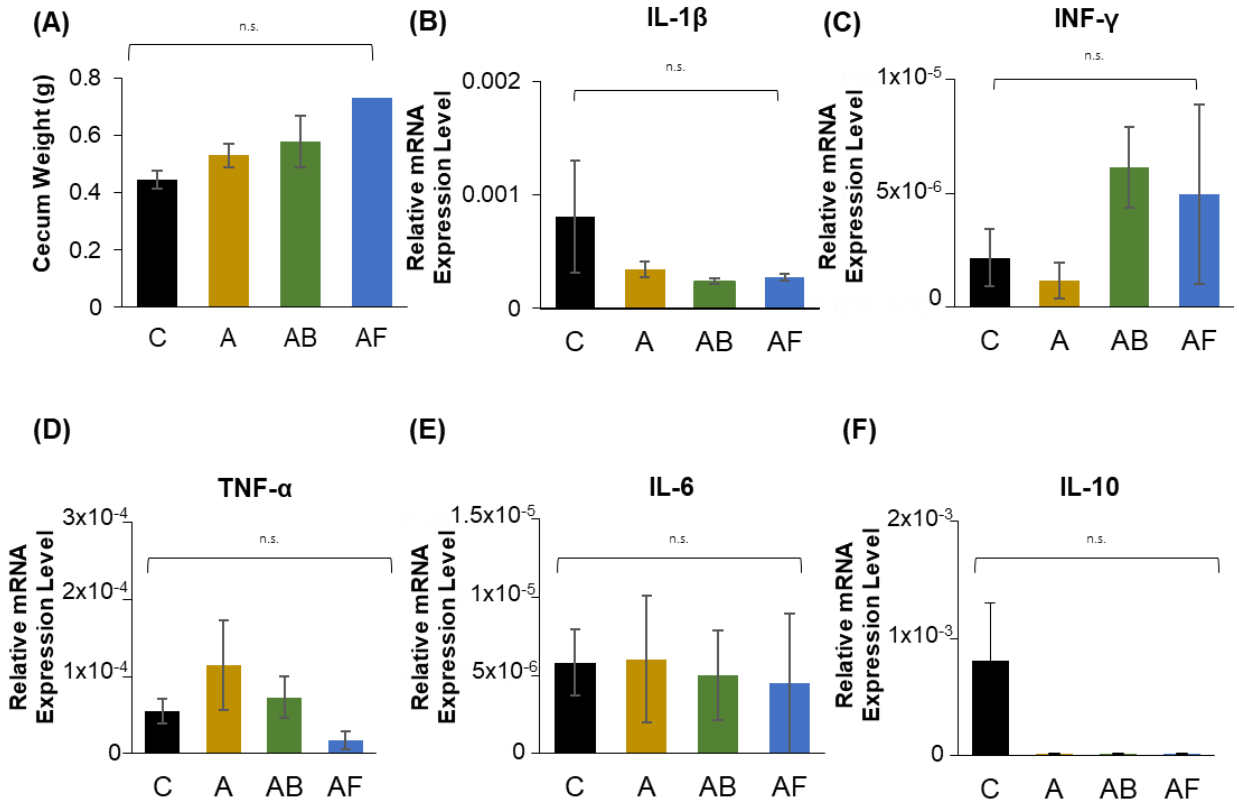

Supplementary Figure III-6 | Changes in cecum size and expression of inflammation-related genes in amoxicillin-treated mice. At the end of the experiment, cecum weight and the mRNA expression levels of inflammation-related genes in the large intestine for amoxicillin-treated mice (C: control, A: amoxicillin + natural recovery, AB: amoxicillin + *B. bifidum*, AF: amoxicillin + fecal transplant from control mice) were measured. A) Cecum weight, relative mRNA expression of genes encoding B) IL-β, C) TNF-α, D) INF-γ, E) IL-6, and F) IL-10 for amoxicillin-treated mice, using *Actb* as a reference gene. Error bars indicate standard error, and significance was determined by One-Way ANOVA and Dunnett's test. (* $p < 0.05$, ** $p < 0.01$, *** $p < 0.001$). This figure is used with permission from Ojima et al., (2020).

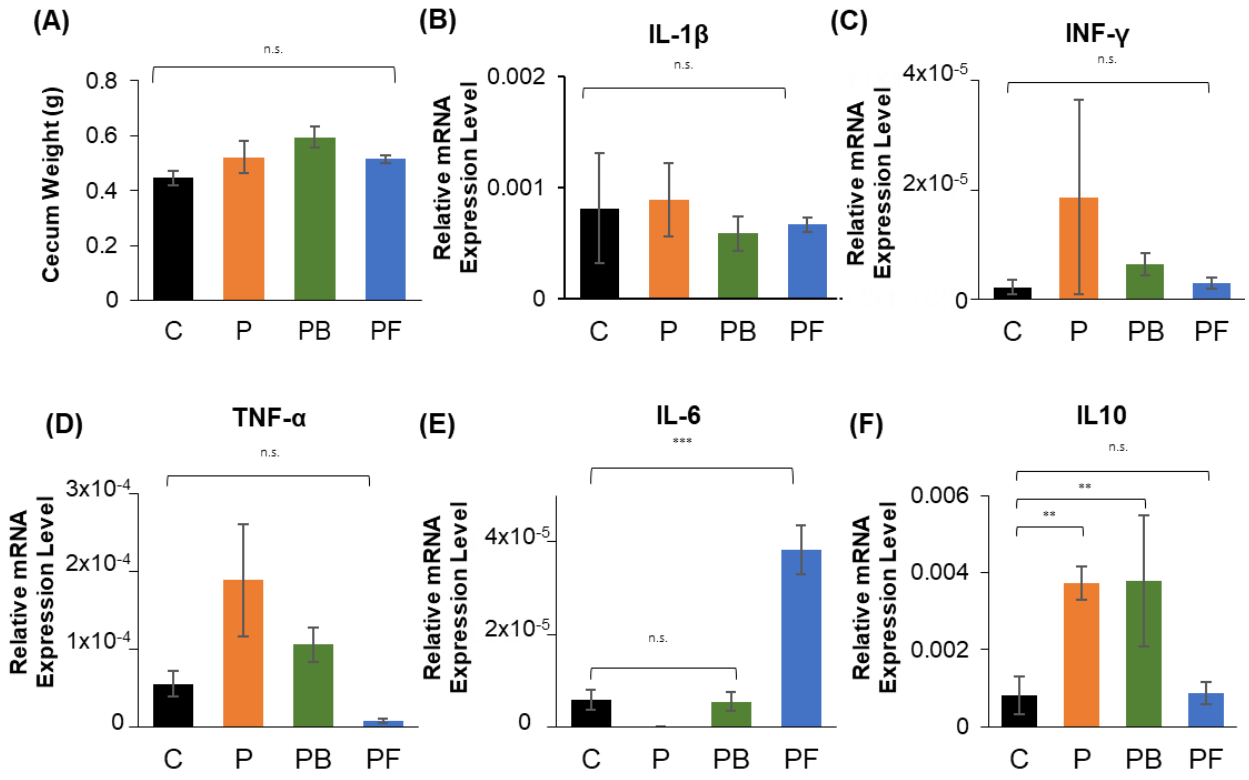

Supplementary Figure III-7 | Changes in cecum size and expression of inflammation-related genes in ciprofloxacin-treated mice. At the end of the experiment, cecum weight and the mRNA expression levels of inflammation-related genes in the large intestine for ciprofloxacin-treated mice (C: control, P: ciprofloxacin + natural recovery, PB: ciprofloxacin + *B. bifidum*, PF: ciprofloxacin + fecal transplant from control mice) were measured. A) Cecum weight, relative mRNA expression of genes encoding B) IL-β, C) TNF-α, D) INF-γ, E) IL-6, and F) IL-10 for ciprofloxacin-treated mice, using *Actb* as a reference gene. Error bars indicate standard error, and significance was determined by One-Way ANOVA and Dunnett's test. (* $p < 0.05$, ** $p < 0.01$, *** $p < 0.001$). This figure is used with permission from Ojima et al., (2020).

References

Akagawa, S., Tsuji, S., Onuma, C., Akagawa, Y., Yamaguchi, T., Yamagishi, M., et al. (2019). Effect of delivery mode and nutrition on gut microbiota in neonates. *Ann. Nutr. Metab.* 74, 132–139. doi:10.1159/000496427.

Alang, N., and Kelly, C. R. (2015). Weight Gain After Fecal Microbiota Transplantation. *Open Forum Infect. Dis.* 2, 1–2. doi:https://doi.org/10.1093/ofid/ofv004.

Anumula, K. R. (2006). Advances in fluorescence derivatization methods for high-performance liquid chromatographic analysis of glycoprotein carbohydrates. *Anal. Biochem.* 350, 1–23. doi:10.1016/j.ab.2005.09.037.

Arifin, W. N., and Zahiruddin, W. M. (2017). Sample size calculation in animal studies using resource equation approach. *Malaysian J. Med. Sci.* 24, 101–105. doi:10.21315/mjms2017.24.5.11.

Asakuma, S., Hatakeyama, E., Urashima, T., Yoshida, E., Katayama, T., Yamamoto, K., et al. (2011). Physiology of consumption of human milk oligosaccharides by infant gut-associated bifidobacteria. *J. Biol. Chem.* 286, 34583–34592. doi:10.1074/jbc.M111.248138.

Ashida, H., Miyake, A., Kiyohara, M., Wada, J., Yoshida, E., Kumagai, H., et al. (2009). Two distinct alpha-L-fucosidases from Bifidobacterium bifidum are essential for the utilization of fucosylated milk oligosaccharides and glycoconjugates. *Glycobiology* 19, 1010–7. doi:10.1093/glycob/cwp082.

Bäckhed, F., Manchester, J. K., Semenkovich, C. F., and Gordon, J. I. (2007). Mechanisms underlying the resistance to diet-induced obesity in germ-free mice. *Proc. Natl. Acad. Sci. U. S. A.* 104, 979–984. doi:10.1073/pnas.0605374104.

Bäckhed, F., Roswall, J., Peng, Y., Feng, Q., Jia, H., Kovatcheva-Datchary, P., et al. (2015). Dynamics and Stabilization of the Human Gut Microbiome during the First Year of Life. *Cell Host Microbe* 17, 690–703. doi:10.1016/j.chom.2015.04.004.

Baxter Healthcare (2007). Vancomycin Hydrochloride (vancomycin hydrochloride) Injection, Solution. 1–14. Available at: https://www.accessdata.fda.gov/drugsatfda_docs/label/2007/050671s010lbl.pdf.

Bayer HealthCare (2017). Cipro (ciprofloxacin) package insert. 1–53. Available at: https://www.accessdata.fda.gov/drugsatfda_docs/label/2016/019537s086lbl.pdf.

Bokulich, N. A., Chung, J., Battaglia, T., Henderson, N., Jay, M., Li, H., et al. (2016). Antibiotics, birth mode, and diet shape microbiome maturation during early life. *Sci. Transl. Med.* 8, 343ra82-343ra82. doi:10.1126/scitranslmed.aad7121.

Bray, J.R., and Curtis, J.T. (1957). An Ordination of the Upland Forest Communities of Southern Wisconsin. *Ecological Monographs* 27 (4), 325-349. doi.org/10.2307/1942268.

Brown, K. H., Black, R. E., Lopez de Romaña, G., and Creed de Kanashiro, H. (1989). Infant-feeding practices and their relationship with diarrheal and other diseases in Huascar (Lima), Peru. *Pediatrics* 83, 31–40.

Browne, H. P., Forster, S. C., Anonye, B. O., Kumar, N., Neville, B. A., Stares, M. D., et al. (2016). Culturing of "unculturable" human microbiota reveals novel taxa and extensive sporulation. *Nature* 533, 543–546. doi:10.1038/nature17645.

Burrello, C., Garavaglia, F., Cribiù, F. M., Ercoli, G., Lopez, G., Troisi, J., et al. (2018). Therapeutic faecal microbiota transplantation controls intestinal inflammation through IL10 secretion by immune cells. *Nat. Commun.* 9. doi:10.1038/s41467-018-07359-8.

Cabral, D. J., Penumutchu, S., Reinhart, E. M., Zhang, C., Korry, B. J., Wurster, J. I., et al. (2019).

Microbial Metabolism Modulates Antibiotic Susceptibility within the Murine Gut Microbiome. *Cell Metab.* 30, 800-823.e7. doi:10.1016/j.cmet.2019.08.020.

Callahan, B. J., Mcmurdie, P. J., Rosen, M. J., Han, A. W., and A, A. J. (2016). Dada2. *Nat Methods* 13, 581–583. doi:10.1038/nmeth.3869.DADA2.

Camacho, C., Coulouris, G., Avagyan, V., Ma, N., Papadopoulos, J., Bealer, K., et al. (2009). BLAST+: Architecture and applications. *BMC Bioinformatics* 10, 1–9. doi:10.1186/1471-2105-10-421.

Carlström, C. I., Field, C. M., Bortfeld-Miller, M., Müller, B., Sunagawa, S., and Vorholt, J. A. (2019). Synthetic microbiota reveal priority effects and keystone strains in the *Arabidopsis* phyllosphere. *Nat. Ecol. Evol.* 3, 1445–1454. doi:10.1038/s41559-019-0994-z.

Chao, A. (1984). Nonparametric Estimation of the Number of Classes in a Population. *Scandinavian Journal of Statistics.* 11 (4), 265–270.

Chase, J. M. (2003). Community assembly : when should history matter ? *Oecologia* 136, 489–498. doi:10.1007/s00442-003-1311-7.

Cheng, R. Y., Li, M., Li, S. S., He, M., Yu, X. H., Shi, L., et al. (2017). Vancomycin and ceftriaxone can damage intestinal microbiota and affect the development of the intestinal tract and immune system to different degrees in neonatal mice. *Pathog. Dis.* 75, 1–9. doi:10.1093/femspd/ftx104.

Cho, I., Yamanishi, S., Cox, L., Methé, B. A., Zavadil, J., Li, K., et al. (2012). Antibiotics in early life alter the murine colonic microbiome and adiposity. *Nature* 488, 621–626. doi:10.1038/nature11400.

Clarke, S. F., Murphy, E. F., Nilaweera, K., Ross, P. R., Shanahan, F., Cotter, P. W., et al. (2012). The gut microbiota and its relationship to diet and obesity:New insights. *Gut Microbes* 3, 1–17. doi:10.4161/gmic.20168.

Coates, A., Hu, Y., Bax, R., and Page, C. (2002). The future challenges facing the development of new antimicrobial drugs. *Nat. Rev. Drug Discov.* 1, 895–910. doi:10.1038/nrd940.

Cohenford, M. A., Abraham, A., Abraham, J., and Dain, J. A. (1989). Colorimetric assay for free and bound L-fucose. *Anal. Biochem.* 177, 172–177. doi:10.1016/0003-2697(89)90035-3.

Corcoran, B. M., Stanton, C., Fitzgerald, G. F., and Ross, R. P. (2005). Survival of Probiotic Lactobacilli in Acidic Environments Is Enhanced. *Appl. Environ. Microbiol.* 71, 3060–3067. doi:10.1128/AEM.71.6.3060.

Corr, S. C., Li, Y., Riedel, C. U., O'Toole, P. W., Hill, C., and Gahan, C. G. M. (2007). Bacteriocin production as a mechanism for the antiinfective activity of *Lactobacillus salivarius* UCC118. *Proc. Natl. Acad. Sci. U. S. A.* 104, 7617–7621. doi:10.1073/pnas.0700440104.

Costello, E. K., Stagaman, K., Dethlefsen, L., Bohannan, B. J. M., and Relman, D. a (2012). The Application of Ecological Theory. *Science (80-.).* 336, 1255–1262. doi:10.1126/science.1224203.

Costeloe, K., Hardy, P., Juszczak, E., Wilks, M., and Millar, M. R. (2016). *Bifidobacterium breve* BBG-001 in very preterm infants: A randomised controlled phase 3 trial. *Lancet* 387, 649–660. doi:10.1016/S0140-6736(15)01027-2.

Daïen, C. I., Pinget, G. V., Tan, J. K., and Macia, L. (2017). Detrimental impact of microbiota-accessible carbohydrate-deprived diet on gut and immune homeostasis: An overview. *Front. Immunol.* 8, 1–7. doi:10.3389/fimmu.2017.00548.

David, L. A., Maurice, C. F., Carmody, R. N., Gootenberg, D. B., Button, J. E., Wolfe, B. E., et al. (2014). Diet rapidly and reproducibly alters the human gut microbiome. *Nature* 505, 559–563.

doi:10.1038/nature12820.Diet.

De La Cochetière, M. F., Piloquet, H., Des Robert, C., Darmaun, D., Galmiche, J. P., and Rozé, J. C. (2004). Early intestinal bacterial colonization and necrotizing enterocolitis in premature infants: The putative role of *Clostridium*. *Pediatr. Res.* 56, 366–370. doi:10.1203/01.PDR.0000134251.45878.D5.

Dethlefsen, L., and Relman, D. A. (2011). Incomplete recovery and individualized responses of the human distal gut microbiota to repeated antibiotic perturbation. *Proc. Natl. Acad. Sci. U. S. A.*, 4554–61. doi:10.1073/pnas.1000087107.

Di Gioia, D., Aloisio, I., Mazzola, G., and Biavati, B. (2014). Bifidobacteria: their impact on gut microbiota composition and their applications as probiotics in infants. *Appl Microbiol Biotechnol.* 98. doi:10.1007/s00253-013-5405-9.

Dominguez-Bello, M. G., Costello, E. K., Contreras, M., Magris, M., Hidalgo, G., Fierer, N., et al. (2010). Delivery mode shapes the acquisition and structure of the initial microbiota across multiple body habitats in newborns. *Proc. Natl. Acad. Sci. U. S. A.* 107, 11971–11975. doi:10.1073/pnas.1002601107.

Duncan, S. H., Hold, G. L., Harmsen, H. J. M., Stewart, C. S., and Flint, H. J. (2002). Growth requirements and fermentation products of Fusobacterium prausnitzii, and a proposal to reclassify it as *Faecalibacterium prausnitzii* gen. nov., comb. nov. *Int. J. Syst. Evol. Microbiol.* 52, 2141–2146. doi:10.1099/ijs.0.02241-0.

Ekmekciu, I., von Klitzing, E., Fiebiger, U., Neumann, C., Bacher, P., Scheffold, A., et al. (2017). The probiotic compound VSL#3 modulates mucosal, peripheral, and systemic immunity following murine broad-spectrum antibiotic treatment. *Front. Cell. Infect. Microbiol.* 7, 1–19. doi:10.3389/fcimb.2017.00167.

Elseviers, M. M., Van Camp, Y., Nayaert, S., Duré, K., Annemans, L., Tanghe, A., et al. (2015). Prevalence and management of antibiotic associated diarrhea in general hospitals. *BMC Infect. Dis.* 15, 1–9. doi:10.1186/s12879-015-0869-0.

Engfer, M. B., Stahl, B., Finke, B., Sawatzki, G., and Daniel, H. (2000). Human milk oligosaccharides are resistant to enzymatic hydrolysis in the upper gastrointestinal tract. *Am. J. Clin. Nutr.* 71, 1589–1596.

Evans, C. C., LePard, K. J., Kwak, J. W., Stancukas, M. C., Laskowski, S., Dougherty, J., et al. (2014). Exercise prevents weight gain and alters the gut microbiota in a mouse model of high fat diet-induced obesity. *PLoS One* 9. doi:10.1371/journal.pone.0092193.

Faith, J. J., Guruge, J. L., Charbonneau, M., Subramanian, S., Seedorf, H., Goodman, A. L., et al. (2013). The long-term stability of the human gut microbiota. *Science (80-.).* 341. doi:10.1126/science.1237439.

Fallani, M., Young, D., Scott, J., Norin, E., Amarri, S., Adam, R., et al. (2010). Intestinal microbiota of 6-week-old infants across Europe: Geographic influence beyond delivery mode, breast-feeding, and antibiotics. *J. Pediatr. Gastroenterol. Nutr.* 51, 77–84. doi:10.1097/MPG.0b013e3181d1b11e.

Fei, N., and Zhao, L. (2013). An opportunistic pathogen isolated from the gut of an obese human causes obesity in germfree mice. *ISME J.* 7, 880–884. doi:10.1038/ismej.2012.153.

Ferrario, C., Duranti, S., Milani, C., Mancabelli, L., Lugli, G. A., Turroni, F., et al. (2015). Exploring Amino Acid Auxotrophy in *Bifidobacterium bifidum* PRL2010. *Front. Microbiol.* 6, 1–11. doi:10.3389/fmicb.2015.01331.

Ferretti, P., Pasolli, E., Tett, A., Huttenhower, C., Bork, P., Segata, N., et al. (2018). Mother-to-Infant Microbial Transmission from Different Body Sites Shapes the Developing Infant Gut Microbiome Article Mother-to-Infant Microbial Transmission from Different Body Sites Shapes the Developing Infant Gut Microbiome. *Cell Host Microbe* 24, 133–145. doi:10.1016/j.chom.2018.06.005.

Fodelianakis, S., Valenzuela-Cuevas, A., Barozzi, A., and Daffonchio, D. (2020). Direct quantification of ecological drift at the population level in synthetic bacterial communities. *ISME J.* doi:10.1038/s41396-020-00754-4.

Fukami, T. (2015). Historical Contingency in Community Assembly: Integrating Niches, Species Pools, and Priority Effects. *Annu. Rev. Ecol. Evol. Syst.* doi:10.1146/annurev-ecolsys-110411-160340.

Fukuda, S., Toh, H., Hase, K., Oshima, K., Nakanishi, Y., Yoshimura, K., et al. (2011). Bifidobacteria can protect from enteropathogenic infection through production of acetate. *Nature* 469, 543–549. doi:10.1038/nature09646.

Garrido, D., Kim, J. H., German, J. B., Raybould, H. E., and Mills, D. A. (2011). Oligosaccharide binding proteins from *Bifidobacterium longum* subsp. *infantis* reveal a preference for host glycans. *PLoS One* 6. doi:10.1371/journal.pone.0017315.

Garrido, D., Ruiz-Moyano, S., and Mills, D. A. (2012). Release and utilization of *N*-acetyl-D-glucosamine from human milk oligosaccharides by *Bifidobacterium longum* subsp. *infantis*. *Anaerobe* 18, 430–435. doi:10.1016/j.anaerobe.2012.04.012.

Gerber, J. S., Bryan, M., Ross, R. K., Daymont, C., Parks, E. P., Localio, A. R., et al. (2016). Antibiotic exposure during the first 6 months of life and weight gain during childhood. *JAMA - J. Am. Med. Assoc.* 315, 1258–1265. doi:10.1001/jama.2016.2395.

Ghalayini, M., Launay, A., Bridier-Nahmias, A., Clermont, O., Denamur, E., Lescat, M., et al. (2018). Evolution of a dominant natural isolate of *Escherichia coli* in the human gut over the course of a year suggests a neutral evolution with reduced effective population size. *Appl. Environ. Microbiol.* 84, 1–13. doi:10.1128/AEM.02377-17.

Gilbert, B., and Levine, J. M. (2017). Ecological drift and the distribution of species diversity. *Proc. R. Soc. B Biol. Sci.* 284. doi:10.1098/rspb.2017.0507.

GlaxoSmithKline (2006). Amoxil (amoxicillin capsules, tablets, chewable tablets, and powder for oral suspension). 4–21. Available at: https://www.accessdata.fda.gov/drugsatfda_docs/label/2008/050760s11,050761s11,050754s12,050542s25lbl.pdf.

Global Market Insights (2016). Probiotics Market Size to Exceed USD 64 Billion by 2023: Global Market Insights Inc. Available at: https://www.prnewswire.com/news-releases/probiotics-market-size-to-exceed-usd-64-billion-by-2023-global-market-insights-inc-578769201.html.

Goldenberg, S. D., Batra, R., Beales, I., Digby-Bell, J. L., Irving, P. M., Kellingray, L., et al. (2018). Comparison of Different Strategies for Providing Fecal Microbiota Transplantation to Treat Patients with Recurrent *Clostridium difficile* Infection in Two English Hospitals: A Review. *Infect. Dis. Ther.* 7, 71–86. doi:10.1007/s40121-018-0189-y.

Goldstein, E. J. C., and Citron, D. M. (1988). Comparative activities of cefuroxime, amoxicillin-clavulanic acid, ciprofloxacin, enoxacin, and ofloxacin against aerobic and anaerobic bacteria isolated from bite wounds. *Antimicrob. Agents Chemother.* 32, 1143–1148. doi:10.1128/AAC.32.8.1143.

Goossens, H., Ferech, M., Vander Stichele, R., and Elseviers, M. (2005). Outpatient antibiotic use in

Europe and association with resistance: A cross-national database study. *Lancet* 365, 579–587. doi:10.1016/S0140-6736(05)70799-6.

Gore, C., Munro, K., Lay, C., Bibiloni, R., Morris, J., Woodcock, A., et al. (2008). *Bifidobacterium pseudocatenulatum* is associated with atopic eczema: A nested case-control study investigating the fecal microbiota of infants. *J. Allergy Clin. Immunol.* 121, 135–140. doi:10.1016/j.jaci.2007.07.061.

Gotoh, A., Katoh, T., Sakanaka, M., Ling, Y., Yamada, C., Asakuma, S., et al. (2018). Sharing of human milk oligosaccharides degradants within bifidobacterial communities in faecal cultures supplemented with *Bifidobacterium bifidum*. *Sci. Rep.* 8, 1–14. doi:10.1038/s41598-018-32080-3.

Grazul, H., Kanda, L. L., and Gondek, D. (2016). Impact of probiotic supplements on microbiome diversity following antibiotic treatment of mice. *Gut Microbes* 7, 101–114. doi:10.1080/19490976.2016.1138197.

Gueimonde, M., Margolles, A., G. de los Reyes-Gavilán, C., and Salminen, S. (2007). Competitive exclusion of enteropathogens from human intestinal mucus by *Bifidobacterium* strains with acquired resistance to bile - A preliminary study. *Int. J. Food Microbiol.* 113, 228–232. doi:10.1016/j.ijfoodmicro.2006.05.017.

Gueimonde, M., Sánchez, B., de los Reyes-Gavilán, C. G., and Margolles, A. (2013). Antibiotic resistance in probiotic bacteria. *Front. Microbiol.* 4, 1–6. doi:10.3389/fmicb.2013.00202.

Guo, Q., Goldenberg, J. Z., Humphrey, C., El Dib, R., and Johnston, B. C. (2019). Probiotics for the prevention of pediatric antibiotic-associated diarrhea. *Cochrane Database Syst. Rev.* doi:10.1002/14651858.CD004827.pub5.

He, C., Cheng, D., Peng, C., Li, Y., Zhu, Y., and Lu, N. (2018). High-fat diet induces dysbiosis of gastric microbiota prior to gut microbiota in association with metabolic disorders in mice. *Front. Microbiol.* 9, 1–9. doi:10.3389/fmicb.2018.00639.

Ho, N. T., Li, F., Lee-Sarwar, K. A., Tun, H. M., Brown, B. P., Pannaraj, P. S., et al. (2018). Meta-analysis of effects of exclusive breastfeeding on infant gut microbiota across populations. *Nat. Commun.* 9. doi:10.1038/s41467-018-06473-x.

Hogenauer, C., Hammer, H. F., Krejs, G. J., and Reisinger, E. C. (1998). Mechanisms and Management of Antibiotic-Associated Diarrhea. *Clin. Infect. Dis.* 27, 702–710. doi:10.1086/514958.

Hotta, M., Sato, Y., Iwata, S., Yamashita, N., Sunakawa, K., Oikawa, T., et al. (1987). Clinical Effects of *Bifidobacterium* Preparations On Pediatric Intractable Diarrhea. *Keio J. Med.* 36, 298–314. doi:10.2302/kjm.36.298.

James, K., Motherway, M. O. C., Bottacini, F., and Van Sinderen, D. (2016). *Bifidobacterium breve* UCC2003 metabolises the human milk oligosaccharides lacto-*N*-tetraose and lacto-*N*-*neo*-tetraose through overlapping, yet distinct pathways. *Sci. Rep.* 6, 38560. doi:10.1038/srep38560.

Japan Ministry of Health Labour and Welfare (2016). 薬剤耐性（AMR）に関する背景、国際社会の動向及び我が国における現状について [Antimicrobial Resistance (AMR): Background, International Trends, and Current Conditions in Japan]. Available at: https://www.mhlw.go.jp/file/06-Seisakujouhou-10900000-Kenkoukyoku/0000121246_1.pdf.

Jernberg, C., Löfmark, S., Edlund, C., and Jansson, J. K. (2007). Long-term ecological impacts of antibiotic administration on the human intestinal microbiota. *ISME J.* 1, 56–66. doi:10.1038/ismej.2007.3.

Jiang, H. Q., Kushnir, N., Thurnheer, M. C., Bos, N. A., and Cebra, J. J. (2002). Monoassociation of

SCID mice with *Helicobacter muridarum*, but not four other enterics, provokes IBD upon receipt of T cells. *Gastroenterology* 122, 1346–1354. doi:10.1053/gast.2002.32959.

Kalliomäki, M., Kirjavainen, P., Eerola, E., Kero, P., Salminen, S., and Isolauri, E. (2001). Distinct patterns of neonatal gut microflora in infants in whom atopy was and was not developing. *J. Allergy Clin. Immunol.* 107, 129–34. doi:10.1067/mai.2001.111237.

Katayama, T. (2016). Host-derived glycans serve as selected nutrients for the gut microbe: Human milk oligosaccharides and bifidobacteria. *Biosci. Biotechnol. Biochem.* 80, 621–632. doi:10.1080/09168451.2015.1132153.

Katayama, T., Sakuma, A., Kimura, T., Makimura, Y., Hiratake, J., Sakata, K., et al. (2004). Molecular cloning and characterization of *Bifidobacterium bifidum* 1,2-alpha-L-fucosidase (AfcA), a novel inverting glycosidase (glycoside hydrolase family 95). *J. Bacteriol.* 186, 4885–93. doi:10.1128/JB.186.15.4885-4893.2004.

Kato, K., Odamaki, T., Mitsuyama, E., Sugahara, H., Xiao, J. Z., and Osawa, R. (2017). Age-Related Changes in the Composition of Gut Bifidobacterium Species. *Curr. Microbiol.* 74, 987–995. doi:10.1007/s00284-017-1272-4.

Katoh, T., Ojima, M. N., Sakanaka, M., Ashida, H., Gotoh, A., and Katayama, T. (2020). Enzymatic Adaptation of *Bifidobacterium bifidum* to Host Glycans , Viewed from Glycoside Hydrolyases and Carbohydrate-Binding Modules. *Microorganisms* 8, 1–18.

Kau, A. L., Ahern, P. P., Griffin, N. W., Goodman, A. L., and Gordon, J. I. (2011). Human nutrition, the gut microbiome and the immune system. *Nature* 474, 327–336. doi:10.1038/nature10213.

Kitajima, H., Sumida, Y., Tanaka, R., Yuki, N., Takayama, H., and Fujimura, M. (1997). Early administration of *Bifidobacterium breve* to preterm infants: Randomised controlled trial. *Arch. Dis. Child. Fetal Neonatal Ed.* 76, 101–107. doi:10.1136/fn.76.2.F101.

Kondo, S., Xiao, J. Z., Satoh, T., Odamaki, T., Takahashi, S., Sugahara, H., et al. (2010). Antiobesity effects of *Bifidobacterium breve* Strain B-3 supplementation in a mouse model with high-fat diet-Induced obesity. *Biosci. Biotechnol. Biochem.* 74, 1656–1661. doi:10.1271/bbb.100267.

Korpela, K., Salonen, A., Virta, L. J., Kumpu, M., Kekkonen, R. A., and De Vos, W. M. (2016). *Lactobacillus rhamnosus* GG Intake Modifies Preschool Children's Intestinal Microbiota, Alleviates Penicillin-Associated Changes, and Reduces Antibiotic Use. *PLoS One* 11, 1–16. doi:10.1371/journal.pone.0154012.

Koskella, B., Hall, L. J., and Metcalf, C. J. E. (2017). The microbiome beyond the horizon of ecological and evolutionary theory. *Nat. Ecol. Evol.* 1, 1606–1615. doi:10.1038/s41559-017-0340-2.

Kostic, A. D., Gevers, D., Siljander, H., Vatanen, T., Hyötyläinen, T., Hämäläinen, A. M., et al. (2015). The dynamics of the human infant gut microbiome in development and in progression toward type 1 diabetes. *Cell Host Microbe* 17, 260–273. doi:10.1016/j.chom.2015.01.001.

Kunz, C., Rudloff, S., Baier, W., Klein, N., and Strobel, S. (2000). Oligosaccharides in human milk: structural, functional, and metabolic aspects. *Annu. Rev. Nutr.* 20, 699–722. doi:10.1146/annurev.nutr.20.1.699.

Langmead, B., and Salzberg, S. L. (2012). Fast gapped-read alignment with Bowtie 2. *Nat. Methods* 9, 357–359. doi:10.1038/nmeth.1923.

Laursen, M. F., Sakanaka, M., von Burg, N., Andersen, D., Mörbe, U., Rivollier, A., et al. (2020). Breastmilk-promoted bifidobacteria produce aromatic lactic acids in the infant gut. *bioRxiv*.

doi:10.1101/2020.01.22.914994.

Le Leu, R. K., Hu, Y., Brown, I. L., Woodman, R. J., and Young, G. P. (2010). Synbiotic intervention of *Bifidobacterium lactis* and resistant starch protects against colorectal cancer development in rats. *Carcinogenesis* 31, 246–251. doi:10.1093/carcin/bgp197.

Lee, H. J., Lee, K. E., Kim, J. K., and Kim, D. H. (2019). Suppression of gut dysbiosis by *Bifidobacterium longum* alleviates cognitive decline in 5XFAD transgenic and aged mice. *Sci. Rep.* 9, 1–12. doi:10.1038/s41598-019-48342-7.

Lee, S. M., Donaldson, G. P., Mikulski, Z., Boyajian, S., Ley, K., and Mazmanian, S. K. (2013). Bacterial colonization factors control specificity and stability of the gut microbiota. *Nature*, 3–8. doi:10.1038/nature12447.

Lerner, A., Matthias, T., and Aminov, R. (2017). Potential effects of horizontal gene exchange in the human gut. *Front. Immunol.* 8, 1–14. doi:10.3389/fimmu.2017.01630.

Levy, S. B., and Marshall, B. (2004). Antibacterial resistance worldwide: Causes, challenges and responses. *Nat. Med.* 10, S122–S129. doi:10.1038/nm1145.

Lewis, Z. T., and Mills, D. A. (2017). Differential Establishment of Bifidobacteria in the Breastfed Infant Gut. *Nestle Nutr Inst Work. Ser.* 88, 149–159. doi:10.1159/000455399.Differential.

Ley, R. E., Bäckhed, F., Turnbaugh, P., Lozupone, C. A., Knight, R. D., and Gordon, J. I. (2005). Obesity alters gut microbial ecology. *Proc. Natl. Acad. Sci.* 102, 11070–11075. doi:10.1073/pnas.0504978102.

Liu, L., Chen, X., Skogerbø, G., Zhang, P., Chen, R., He, S., et al. (2012). The human microbiome: A hot spot of microbial horizontal gene transfer. *Genomics* 100, 265–270. doi:10.1016/j.ygeno.2012.07.012.

Lombard, V., Golaconda Ramulu, H., Drula, E., Coutinho, P. M., and Henrissat, B. (2014). The carbohydrate-active enzymes database (CAZy) in 2013. *Nucleic Acids Res.* 42, 490–495. doi:10.1093/nar/gkt1178.

López-Alarcón, M., Villalpando, S., and Fajardo, A. (1997). Breast-feeding lowers the frequency and duration of acute respiratory infection and diarrhea in infants under six months of age. *J. Nutr.* 127, 436–43.

MacPherson, C. W., Mathieu, O., Tremblay, J., Champagne, J., Nantel, A., Girard, S. A., et al. (2018). Gut Bacterial Microbiota and its Resistome Rapidly Recover to Basal State Levels after Short-term Amoxicillin-Clavulanic Acid Treatment in Healthy Adults. *Sci. Rep.* 8, 1–14. doi:10.1038/s41598-018-29229-5.

Macrobal, A., Barboza, M., Froehlich, J. W., Block, D. E., German, J. B., Lebrilla, C. B., et al. (2010). Consumption of Human Milk Oligosaccharides by Gut-related Microbes. *J. Agric. Food Chem.* 58, 5334–5340. doi:10.1021/jf9044205.

Macrobal, A., and Sonnenburg, J. L. (2012). Human milk oligosaccharide consumption by intestinal microbiota. *Clin Microbiol Infect* 18, 12–15. doi:10.1111/j.1469-0691.2012.03863.x.Human.

Margulis, L. (1991). “Symbiogenesis and Symbionticism,” in *Symbiosis as a Source of Evolutionary Innovation*, eds. L. Margulis and R. Fester (MIT Press), 1–14.

Martin, M. (2011). Cutadapt removes adapter sequences from high-throughput sequencing reads. *EMBnet* 17, 10–12.

Martínez, I., Maldonado-Gomez, M. X., Gomes-Neto, J. C., Kittana, H., Ding, H., Schmaltz, R., et al. (2018). Experimental evaluation of the importance of colonization history in early-life gut microbiota assembly. *Elife* 7, 1–26. doi:10.7554/eLife.36521.

Martínez, I., Wallace, G., Zhang, C., Legge, R., Benson, A. K., Carr, T. P., et al. (2009). Diet-induced metabolic improvements in a hamster model of hypercholesterolemia are strongly linked to alterations of the gut microbiota. *Appl. Environ. Microbiol.* 75, 4175–4184. doi:10.1128/AEM.00380-09.

Matsuki, T., Watanabe, K., Tanaka, R., and Oyaizu, H. (1998). Rapid identification of human intestinal bifidobacteria by 16S rRNA-targeted spcies- and group-specific primers. *FEMS Microbiology Letters.* 167, 113-121.

Matsuki, T., Yahagi, K., Mori, H., Matsumoto, H., Hara, T., Tajima, S., et al. (2016). A key genetic factor for fucosyllactose utilization affects infant gut microbiota development. *Nat. Commun.* 7, 11939. doi:10.1038/ncomms11939.

Medellin-Peña, M. J., Wang, H., Johnson, R., Anand, S., and Griffiths, M. W. (2007). Probiotics affect virulence-related gene expression in *Escherichia coli* O157:H7. *Appl. Environ. Microbiol.* 73, 4259–4267. doi:10.1128/AEM.00159-07.

Medina, M., De Palma, G., Ribes-Koninckx, C., Calabuig, M., and Sanz, Y. (2008). *Bifidobacterium* strains suppress in vitro the pro-inflammatory milieu triggered by the large intestinal microbiota of coeliac patients. *J. Inflamm.* 5, 1–13. doi:10.1186/1476-9255-5-19.

Meng, D., Sommella, E., Salviati, E., Campiglia, P., Ganguli, K., Djebali, K., et al. (2019). Indole-3-lactic acid, a metabolite of tryptophan, secreted by *Bifidobacterium longum* subspecies *infantis* is anti-inflammatory in the immature intestine. *Pediatr. Res.*, 0–1. doi:10.1038/s41390-019-0740-x.

Mohan, R., Koebnick, C., Schildt, J., Mueller, M., Radke, M., and Blaut, M. (2008). Effects of *Bifidobacterium lactis* Bb12 Supplementation on Body Weight, Fecal pH, Acetate, Lactate, Calprotectin, and IgA in Preterm Infants. *Pediatr. Res.* 64, 418–422. Available at: https://www.nature.com/articles/pr2008218.pdf.

Moossavi, S., Sepehri, S., Robertson, B., Bode, L., Goruk, S., Field, C. J., et al. (2019). Composition and Variation of the Human Milk Microbiota Are Influenced by Maternal and Early-Life Factors. *Cell Host Microbe* 25, 324-335.e4. doi:10.1016/j.chom.2019.01.011.

Mori, H., Maruyama, T., Yano, M., Yamada, T., and Kurokawa, K. (2018). VITCOMIC2: Visualization tool for the phylogenetic composition of microbial communities based on 16S rRNA gene amplicons and metagenomic shotgun sequencing. *BMC Syst. Biol.* 12. doi:10.1186/s12918-018-0545-2.

Moya-Pérez, A., Neef, A., and Sanz, Y. (2015). *Bifidobacterium pseudocatenulatum* CECT 7765 reduces obesity-associated inflammation by restoring the lymphocyte-macrophage balance and gut microbiota structure in high-fat diet-fed mice. *PLoS One* 10, 1–28. doi:10.1371/journal.pone.0126976.

Ninonuevo, M. R., and Lebrilla, C. B. (2009). Mass spectrometric methods for analysis of oligosaccharides in human milk. *Nutr. Rev.* 67. doi:10.1111/j.1753-4887.2009.00243.x.

Nishida, A., Inoue, R., Inatomi, O., Bamba, S., Naito, Y., and Andoh, A. (2018). Gut microbiota in the pathogenesis of inflammatory bowel disease. *Clin. J. Gastroenterol.* 11, 1–10. doi:10.1007/s12328-017-0813-5.

Nishimoto, M., and Kitaoka, M. (2007). Practical preparation of lacto-*N*-biose I, a candidate for the

bifidus factor in human milk. *Biosci. Biotechnol. Biochem.* 71, 2101–2104. doi:10.1271/bbb.70320.

O'Connell Motherway, M., Kinsella, M., Fitzgerald, G. F., and Van Sinderen, D. (2013). Transcriptional and functional characterization of genetic elements involved in galacto-oligosaccharide utilization by *Bifidobacterium breve* UCC2003. *Microb. Biotechnol.* 6, 67–79. doi:10.1111/1751-7915.12011.

O'May, G. A., Reynolds, N., Smith, A. R., Kennedy, A., and Macfarlane, G. T. (2005). Effect of pH and antibiotics on microbial overgrowth in the stomachs and duodena of patients undergoing percutaneous endoscopic gastrostomy feeding. *J. Clin. Microbiol.* 43, 3059–3065. doi:10.1128/JCM.43.7.3059-3065.2005.

Odamaki, T., Bottacini, F., Mitsuyama, E., Yoshida, K., Kato, K., Xiao, J. Z., et al. (2019). Impact of a bathing tradition on shared gut microbe among Japanese families. *Sci. Rep.* 9, 1–8. doi:10.1038/s41598-019-40938-3.

Ojima, M. N., Gotoh, A., Takada, H., Odamaki, T., Xiao, J., Katoh, T., et al. (2020). *Bifidobacterium bifidum* Suppresses Gut Inflammation Caused by Repeated Antibiotic Disturbance Without Recovering Gut Microbiome Diversity in Mice. *Front. Microbiol.* 11, 1–13. doi:10.3389/fmicb.2020.01349.

Oksanen, J., Blanchet, F. G., Friendly, M., Kindt, R., Legendre, P., McGlinn, D., et al. (2019). vegan: Community Ecology Package. Available at: https://cran.r-project.org/package=vegan%0A.

Ormerod, K. L., Wood, D. L. A., Lachner, N., Gellatly, S. L., Daly, J. N., Parsons, J. D., et al. (2016). Genomic characterization of the uncultured Bacteroidales family S24-7 inhabiting the guts of homeothermic animals. *Microbiome* 4, 1–17. doi:10.1186/s40168-016-0181-2.

Overbeek, R., Olson, R., Pusch, G. D., Olsen, G. J., Davis, J. J., Disz, T., et al. (2014). The SEED and the Rapid Annotation of microbial genomes using Subsystems Technology (RAST). *Nucleic Acids Res.* 42, 206–214. doi:10.1093/nar/gkt1226.

Palmer, C., Bik, E. M., DiGiulio, D. B., Relman, D. A., and Brown, P. O. (2007). Development of the human infant intestinal microbiota. *PLoS Biol.* 5, 1556–1573. doi:10.1371/journal.pbio.0050177.

Parche, S., Beleut, M., Rezzonico, E., Jacobs, D., Arigoni, F., Titgemeyer, F., et al. (2006). Lactose-over-glucose preference in *Bifidobacterium longum* NCC2705: glcP, encoding a glucose transporter, is subject to lactose repression. *J. Bacteriol.* 188, 1260–1265. doi:10.1128/JB.188.4.1260-1265.2006.

Petersen, C., and Round, J. L. (2014). Defining dysbiosis and its influence on host immunity and disease. *Cell. Microbiol.* 16, 1024–1033. doi:10.1111/cmi.12308.

Peterson, G., Allen, C. R., and Holling, C. S. (1998). Ecological Resilience, Biodiversity, and Scale. *Ecosystems* 1, 6–18. doi:10.1080/15210960.2017.1267517.

Plummer, E. L., Bulach, D. M., Murray, G. L., Jacobs, S. E., Tabrizi, S. N., and Garland, S. M. (2018). Gut microbiota of preterm infants supplemented with probiotics: sub-study of the ProPrems trial. *BMC Microbiol.* 18, 1–8. doi:10.1186/s12866-018-1326-1.

Price, M. N., and Arkin, A. P. (2017). PaperBLAST: Text-mining papers for information about homologs. *bioRxiv* 2, 1–10. doi:10.1101/133041.

Pu, Z., and Jiang, L. (2015). Dispersal among local communities does not reduce historical contingencies during metacommunity assembly. *Oikos* 124, 1327–1336. doi:10.1111/oik.02079.

Puhl, N. J., Uwiera, R. R. E., Jay Yanke, L., Brent Selinger, L., and Douglas Inglis, G. (2012). Antibiotics conspicuously affect community profiles and richness, but not the density of bacterial cells

associated with mucosa in the large and small intestines of mice. *Anaerobe* 18, 67–75. doi:10.1016/j.anaerobe.2011.12.007.

Qin, J., Li, Y., Cai, Z., Li, S., Zhu, J., Zhang, F., et al. (2012). A metagenome-wide association study of gut microbiota in type 2 diabetes. *Nature* 490, 55–60. doi:10.1038/nature11450.

Quin, C., Estaki, M., Vollman, D. M., Barnett, J. A., Gill, S. K., and Gibson, D. L. (2018). Probiotic supplementation and associated infant gut microbiome and health: A cautionary retrospective clinical comparison. *Sci. Rep.* 8, 1–16. doi:10.1038/s41598-018-26423-3.

Relman, D. A. (2012). The human microbiome: ecosystem resilience and health. *Nutr. Rev.* 70, 1–12. doi:10.1111/j.1753-4887.2012.00489.x.The.

Reyman, M., van Houten, M. A., van Baarle, D., Bosch, A. A. T. M., Man, W. H., Chu, M. L. J. N., et al. (2019). Impact of delivery mode-associated gut microbiota dynamics on health in the first year of life. *Nat. Commun.* 10, 1–12. doi:10.1038/s41467-019-13014-7.

Riedel, C. U., Foata, F., Philippe, D., Adolfsson, O., Eikmanns, B. J., and Blum, S. (2006). Anti-inflammatory effects of bifidobacteria by inhibition of LPS-induced NF-κB activation. *World J. Gastroenterol.* 12, 3729–3735. doi:10.3748/wjg.v12.i23.3729.

Roger, L. C., Costabile, A., Holland, D. T., Hoyles, L., and McCartney, A. L. (2010). Examination of faecal *Bifidobacterium* populations in breast- and formula-fed infants during the first 18 months of life. *Microbiology* 156, 3329–3341. doi:10.1099/mic.0.043224-0.

Rooks, M. G., Veiga, P., Wardwell-Scott, L. H., Tickle, T., Segata, N., Michaud, M., et al. (2014). Gut microbiome composition and function in experimental colitis during active disease and treatment-induced remission. *ISME J.* 8, 1403–1417. doi:10.1038/ismej.2014.3.

Rothschild, D., Weissbrod, O., Barkan, E., Kurilshikov, A., Korem, T., Zeevi, D., et al. (2018). Environment dominates over host genetics in shaping human gut microbiota. *Nature* 555. doi:10.1038/nature25973.

Round, J. L., and Mazmanian, S. K. (2009). The gut microbiota shapes intestinal immune responses during health and disease. *Nat. Rev. Immunol.* 9, 313–323. doi:10.1038/nri2515.

Rowland, I., Gibson, G., Heinken, A., Scott, K., Swann, J., Thiele, I., et al. (2018). Gut microbiota functions: metabolism of nutrients and other food components. *Eur. J. Nutr.* 57, 1–24. doi:10.1007/s00394-017-1445-8.

Ruiz-Moyano, S., Totten, S. M., Garrido, D. a., Smilowitz, J. T., Bruce German, J., Lebrilla, C. B., et al. (2013). Variation in consumption of human milk oligosaccharides by infant gut-associated strains of bifidobacterium breve. *Appl. Environ. Microbiol.* 79, 6040–6049. doi:10.1128/AEM.01843-13.

Saier, M. H., Reddy, V. S., Tsu, B. V., Ahmed, M. S., Li, C., and Moreno-Hagelsieb, G. (2016). The Transporter Classification Database (TCDB): Recent advances. *Nucleic Acids Res.* 44, D372–D379. doi:10.1093/nar/gkv1103.

Sakanaka, M., Gotoh, A., Yoshida, K., Odamaki, T., Koguchi, H., Xiao, J. Z., et al. (2020). Varied pathways of infant gut-associated *Bifidobacterium* to assimilate human milk oligosaccharides: Prevalence of the gene set and its correlation with bifidobacteria-rich microbiota formation. *Nutrients* 12, 1–21. doi:10.3390/nu12010071.

Sakanaka, M., Hansen, M. E., Gotoh, A., Katoh, T., Yoshida, K., Odamaki, T., et al. (2019). Evolutionary adaptation in fucosyllactose uptake systems supports bifidobacteria-infant symbiosis. *Sci. Adv.* 5, eaaw7696. doi:10.1126/sciadv.aaw7696.

Sakurai, T., Odamaki, T., and Xiao, J. Z. (2019). Production of indole-3-lactic acid by *Bifidobacterium* strains isolated fromhuman infants. *Microorganisms* 7. doi:10.3390/microorganisms7090340.

Sakurama, H., Kiyohara, M., Wada, J., Honda, Y., Yamaguchi, M., Fukiya, S., et al. (2013). Lacto-*N*-biosidase encoded by a novel gene of *Bifidobacterium longum* subspecies *longum* shows unique substrate specificity and requires a designated chaperone for its active expression. *J. Biol. Chem.* 288, 25194–206. doi:10.1074/jbc.M113.484733.

Schröder, A., Persson, L., and De Roos, A. M. (2005). Direct experimental evidence for alternative stable states: A review. *Oikos* 110, 3–19. doi:10.1111/j.0030-1299.2005.13962.x.

Schubert, A. M., Sinani, H., and Schloss, P. D. (2015). Antibiotic-induced alterations of the murine gut microbiota and subsequent effects on colonization resistance against *Clostridium difficile*. *mBio* 6, 1–10. doi:10.1128/mBio.00974-15.

Sekine, K., Hashimoto, Y., Saito, M., Kuboyama, M., and Kawashima, T. (1985). A New Morphologically Characterized Cell Wall Preparation (Whole Peptidoglycan) from *Bifidobacterium infantis* with a Higher Efficacy on the Regression of an Established Tumor in Mice. *Cancer Res.* 45, 1300–1307.

Sela, D. A., Chapman, J., Adeuya, A., Kim, J. H., Chen, F., Whitehead, T. R., et al. (2008). The genome sequence of *Bifidobacterium longum* subsp. *infantis* reveals adaptations for milk utilization within the infant microbiome. *Proc. Natl. Acad. Sci. U. S. A.* 105, 18964–9. doi:10.1073/pnas.0809584105.

Sela, D. A., Garrido, D., Lerno, L., Wu, S., Tan, K., Eom, H. J., et al. (2012). *Bifidobacterium longum* subsp. *infantis* ATCC 15697 α-fucosidases are active on fucosylated human milk oligosaccharides. *Appl. Environ. Microbiol.* 78, 795–803. doi:10.1128/AEM.06762-11.

Sender, R., Fuchs, S., and Milo, R. (2016). Revised Estimates for the Number of Human and Bacteria Cells in the Body. *PLoS Biol.* 14, 1–14. doi:10.1371/journal.pbio.1002533.

Shah, N. P. (2011). BACTERIA, BENEFICIAL | *Bifidobacterium* spp.: Morphology and Physiology. *Encycl. Dairy Sci.*, 381–387.

Shahinas, D., Silverman, M., Sittler, T., Chiu, C., Kim, P., Allen-Vercoe, E., et al. (2012). Toward an understanding of changes in diversity Associated with Fecal Microbiome Transplantation Based on 16S rRNA Gene Deep Sequencing Dea. *MBio* 3, 1–10. doi:10.1128/mBio.00338-12.Editor.

Shallcross, L., Beckley, N., Rait, G., Hayward, A., and Petersen, I. (2017). Antibiotic prescribing frequency amongst patients in primary care: A cohort study using electronic health records. *J. Antimicrob. Chemother.* 72, 1818–1824. doi:10.1093/jac/dkx048.

Shannon, C. E., and Weaver, W. (1949). The Mathematical Theory of Communication. *Math. theory Commun.* 27, 117. doi:10.2307/3611062.

Shin, N. R., Whon, T. W., and Bae, J. W. (2015). Proteobacteria: Microbial signature of dysbiosis in gut microbiota. *Trends Biotechnol.* 33, 496–503. doi:10.1016/j.tibtech.2015.06.011.

Sousa, W. P. (1984). The Role of Disturbance in Natural Communities. *Annu. Rev. Ecol. Syst.* 15, 353–391. Available at: https://www.jstor.org/stable/2096953.

Sprockett, D., Fukami, T., and Relman, D. A. (2018). Role of priority effects in the early-life assembly of the gut microbiota. *Nat. Rev. Gastroenterol. Hepatol.* 15, 197–205. doi:10.1038/nrgastro.2017.173.

Stenman, L. K., Waget, A., Garret, C., Klopp, P., Burcelin, R., and Lahtinen, S. (2014). Potential probiotic *Bifidobacterium animalis* ssp. lactis 420 prevents weight gain and glucose intolerance in

diet-induced obese mice. *Benef. Microbes* 5, 437–445. doi:10.3920/BM2014.0014.

Stokholm, J., Blaser, M. J., Thorsen, J., Rasmussen, M. A., Waage, J., Vinding, R. K., et al. (2018). Maturation of the gut microbiome and risk of asthma in childhood. *Nat. Commun.* 9, 1–10. doi:10.1038/s41467-017-02573-2.

Suez, J., Zmora, N., Segal, E., and Elinav, E. (2019). The pros, cons, and many unknowns of probiotics. *Nat. Med.* 25, 716–729. doi:10.1038/s41591-019-0439-x.

Suez, J., Zmora, N., Zilberman-Schapira, G., Mor, U., Dori-Bachash, M., Bashiardes, S., et al. (2018). Post-Antibiotic Gut Mucosal Microbiome Reconstitution Is Impaired by Probiotics and Improved by Autologous FMT. *Cell* 174, 1406–1423. doi:10.1016/j.cell.2018.08.047.

Suzuki, R., Wada, J., Katayama, T., Fushinobu, S., Wakagi, T., Shoun, H., et al. (2008). Structural and thermodynamic analyses of solute-binding protein from *Bifidobacterium longum* specific for core 1 disaccharide and lacto-*N*-biose. *J. Biol. Chem.* 283, 13165–13173. doi:10.1074/jbc.M709777200.

Tanizawa, Y., Fujisawa, T., Kaminuma, E., Nakamura, Y., and Arita, M. (2016). DFAST and DAGA: Web-based integrated genome annotation tools and resources. *Biosci. Microbiota, Food Heal.* 35, 173–184. doi:10.12938/bmfh.16-003.

Tannock, G. W., Lawley, B., Munro, K., Pathmanathan, S. G., Zhou, S. J., Makrides, M., et al. (2013). Comparison of the compositions of the stool microbiotas of infants fed goat milk formula, cow milk-based formula, or breast milk. *Appl. Environ. Microbiol.* 79, 3040–3048. doi:10.1128/AEM.03910-12.

Tannock, G. W., Lee, P. S., Wong, K. H., and Lawley, B. (2016). Why don’t all infants have bifidobacteria in their stool? *Front. Microbiol.* 7, 6–10. doi:10.3389/fmicb.2016.00834.

Thaiss, C. A., Zeevi, D., Levy, M., Zilberman-Schapira, G., Suez, J., Tengeler, A. C., et al. (2014). Transkingdom control of microbiota diurnal oscillations promotes metabolic homeostasis. *Cell* 159, 514–529. doi:10.1016/j.cell.2014.09.048.

Theriot, C. M., Koenigsknecht, M. J., Jr, P. E. C., Hatton, G. E., Nelson, A. M., Li, B., et al. (2014). Antibiotic-induced shifts in the mouse gut microbiome and metabolome increase susceptibility to Clostridium difficile infection. *Nat. Commun.* doi:10.1038/ncomms4114.Antibiotic-induced.

Tissier, H. (1900). Recherches sur la flore intestinale des nourrissons (etat normal et pathologique).

Toda, K., Hisata, K., Satoh, T., Katsumata, N., Odamaki, T., Mitsuyama, E., et al. (2019). Neonatal oral fluid as a transmission route for bifidobacteria to the infant gut immediately after birth. *Sci. Rep.* 9, 1–9. doi:10.1038/s41598-019-45198-9.

Turroni, F., Foroni, E., Pizzetti, P., Giubellini, V., Ribbera, A., Merusi, P., et al. (2009). Exploring the diversity of the bifidobacterial population in the human intestinal tract. *Appl. Environ. Microbiol.* 75, 1534–1545. doi:10.1128/AEM.02216-08.

Turroni, F., Milani, C., Duranti, S., Lugli, G. A., Bernasconi, S., Margolles, A., et al. (2020). The infant gut microbiome as a microbial organ influencing host well-being. *Ital. J. Pediatr.* 46, 1–13. doi:10.1186/s13052-020-0781-0.

U. S. Food and Drug Administration (2019). Important Safety Alert Regarding Use of Fecal Microbiota for Transplantation and Risk of Serious Adverse Reactions Due to Transmission of Multi-Drug Resistant Organisms. *2019 Saf. Availab. Commun.* Available at: https://www.fda.gov/vaccines-blood-biologics/safety-availability-biologics/important-safety-alert-regarding-use-fecal-microbiota-transplantation-and-risk-serious-adverse [Accessed July 1, 2019].

Underwood, M. A., Kalanetra, K. M., Bokulich, N. A., Lewis, Z. T., Mirmiran, M., Tancredi, D. J., et al. (2013). A comparison of two probiotic strains of bifidobacteria in preterm infants. *J. Pediatr.* 163, 1585–1591. doi:doi:10.1016/j.jpeds.2013.07.017.

Urashima, T., Asakuma, S., Leo, F., Fukuda, K., Messer, M., and Oftedal, O. T. (2012). The Glycobiology of Human Milk Oligosaccharides - The Predominance of Type I Oligosaccharides Is a Feature Specific to Human Breast Milk. *Adv. Nutr.* 3, 473S-482S. doi:10.3945/an.111.001412.473S.

Vellend, M. (2010). Conceptual synthesis in community ecology. *Q. Rev. Biol.* 85, 183–206. doi:10.1086/652373.

Verma, R., Lee, C., and Jeun, E. J. (2019). Cell Surface Polysaccharides of *Bifidobacterium bifidum* Induce the Generation of Foxp3 + Regulatory T Cells. *Sci. Immunol.* 103, 3–4. doi:10.1097/TP.0000000000002550A.

von Kries, R., Koletzko, B., Sauerwald, T., von Mutius, E., Barnert, D., Grunert, V., et al. (1999). Breast feeding and obesity: cross sectional study. *BMJ* 319, 147–50.

Vrieze, A., Out, C., Fuentes, S., Jonker, L., Reuling, I., Kootte, R. S., et al. (2014). Impact of oral vancomycin on gut microbiota, bile acid metabolism, and insulin sensitivity. *J. Hepatol.* 60, 824–831. doi:10.1016/j.jhep.2013.11.034.

Wada, J., Ando, T., Kiyohara, M., Ashida, H., Kitaoka, M., Yamaguchi, M., et al. (2008). *Bifidobacterium bifidum* lacto-*N*-biosidase, a critical enzyme for the degradation of human milk oligosaccharides with a type 1 structure. *Appl. Environ. Microbiol.* 74, 3996–4004. doi:10.1128/AEM.00149-08.

Walker, W. A. (2017). The importance of appropriate initial bacterial colonization of the intestine in newborn, child, and adult health. *Pediatr. Res.* 82, 387–395. doi:10.1038/pr.2017.111.

Walter, J., Armet, A. M., Finlay, B. B., and Shanahan, F. (2020). Establishing or Exaggerating Causality for the Gut Microbiome: Lessons from Human Microbiota-Associated Rodents. *Cell* 180, 221–232. doi:10.1016/j.cell.2019.12.025.

Whitaker, W. R., Shepherd, E. S., and Sonnenburg, J. L. (2017). Tunable Expression Tools Enable Single-Cell Strain Distinction in the Gut Microbiome. *Cell* 169, 538-546.e12. doi:10.1016/j.cell.2017.03.041.

Wiström, J., Norrby, S. R., Myhre, E. B., Eriksson, S., Granström, G., Lagergren, L., et al. (2001). Frequency of antibiotic-associated diarrhoea in 2462 antibiotic-treated hospitalized patients: a prospective study. *J. Antimicrob. Chemother.* 47, 43–50. Available at: http://www.ncbi.nlm.nih.gov/pubmed/11152430.

Yamada, C., Gotoh, A., Sakanaka, M., Hattie, M., Stubbs, K. A., Katayama-Ikegami, A., et al. (2017). Molecular Insight into Evolution of Symbiosis between Breast-Fed Infants and a Member of the Human Gut Microbiome *Bifidobacterium longum*. *Cell Chem. Biol.* 24, 515-524.e5. doi:10.1016/j.chembiol.2017.03.012.

Yarza, P., Ludwig, W., Euzéby, J., Amann, R., Schleifer, K. H., Glöckner, F. O., et al. (2010). Update of the all-species living tree project based on 16S and 23S rRNA sequence analyses. *Syst. Appl. Microbiol.* 33, 291–299. doi:10.1016/j.syapm.2010.08.001.

Yarza, P., Yilmaz, P., Pruesse, E., Glöckner, F. O., Ludwig, W., Schleifer, K. H., et al. (2014). Uniting the classification of cultured and uncultured bacteria and archaea using 16S rRNA gene sequences. *Nat. Rev. Microbiol.* 12, 635–645. doi:10.1038/nrmicro3330.

Yassour, M., Vatanen, T., Siljander, H., and Hämäläinen, A. (2016). Natural history of the infant gut microbiome and impact of antibiotic treatments on strain-level diversity and stability. *Sci. Transl. Med.* 8. doi:10.1126/scitranslmed.aad0917.Natural.

Yatsunenko, T., Rey, F. E., Manary, M. J., Trehan, I., Dominguez-Bello, M. G., Contreras, M., et al. (2012). Human gut microbiome viewed across age and geography. *Nature* 486, 222–7. doi:10.1038/nature11053.

Yoshida, E., Sakurama, H., Kiyohara, M., Nakajima, M., Kitaoka, M., Ashida, H., et al. (2012). *Bifidobacterium longum* subsp. infantis uses two different-galactosidases for selectively degrading type-1 and type-2 human milk oligosaccharides. *Glycobiology* 22, 361–368. doi:10.1093/glycob/cwr116.

Zhao, S., Lieberman, T. D., Poyet, M., Kauffman, K. M., Gibbons, S. M., Groussin, M., et al. (2019). Adaptive Evolution within Gut Microbiomes of Healthy People. *Cell Host Microbe* 25, 656-667.e8. doi:10.1016/j.chom.2019.03.007.

Acknowledgments

Chapter III of this dissertation is based on material contained in the following scholarly paper:

Miriam N. Ojima, Aina Gotoh, Hiromi Takada, Toshitaka Odamaki, Jin-Zhong Xiao, Toshihiko Katoh, and Takane Katayama (2020) *Bifidobacterium bifidum* suppresses gut inflammation caused by repeated antibiotic disturbance without recovering gut microbiome diversity in mice. *Frontiers in Microbiology*. 11:1349.

The contents of Chapter II are currently under preparation for publication elsewhere (as of January 5, 2021).

The completion of this dissertation would not have been possible without the kind support of the following individuals. I would first like to thank my advisor, Dr. Takane Katayama, for giving me the opportunity to research and pursue a doctorate in his lab. Although I came from a different field of study, I was able to learn new techniques and concepts in molecular biology under his guidance. I thank him for providing support and advice, while also giving me scientific freedom and autonomy to explore and synthesize new ideas. I also thank Dr. Mikiyasu Sakanaka, whose invaluable insight and support throughout the research, writing and preparation process substantially improved the quality of the studies in this dissertation. I would also like to thank Dr. Toshihiko Katoh and Dr. Aina Gotoh for imparting their skills and sharing their expertise, feedback, and advice as senior scientists. I thank each of them for the immeasurable support throughout the program. I would also like to mention Ms. Kumiko Shimizu and Ms. Chinatsu Wada, who always ensured that our lab was running smoothly. I would like to thank Dr. Seiji Masuda for his input and support. I also extend my thanks to my sub-advisors. I thank Dr. Masaya Nagao for the detailed feedback and guidance. I am also grateful to Dr. James Hejna for the support throughout the manuscript publication process and the objective advice regarding various aspects of research. I would like to thank my *douki*, Moonhak Choi, for help with proofreading, being a listening ear and constant source of support, and making the last three years in this program a memorable experience. I also thank each of the current and past members of Katayama Lab for their support and camaraderie as we navigated the unique set of challenges that come with graduate study.

I wish to especially thank Dr. Lin Jiang at the Georgia Institute of Technology for his continued guidance and encouragement. I credit my time with him as the scientific inspiration behind my projects, and his positive words have helped me manage the difficulties I faced in research.

I wish to recognize my collaborators and coauthors for their valuable support that drastically improved the quality of the studies presented in this dissertation. I would like to thank Dr. Jin-Zhong

Xiao, Dr. Toshitaka Odamaki, and Mr. Keisuke Yoshida at the Morinaga Milk Industry for the NGS analysis, without which I would not have been able to complete my studies. I also would like to thank Dr. Andrei Osterman, Dr. Dmitry Rodionov, and Mr. Aleksandr Arzamasov at the Sanford Burnham Prebys Institute for the bioinformatic analysis that has drastically improved the quality of our study. I am also grateful to Dr. Motomitsu Kitaoka at Niigata University for helping me purify human milk oligosaccharides from breastmilk samples. I would like to thank Glycom A/S for providing HMOs used for standards in this study, and Ms. Saeko Nagao of the Nagao Midwife Clinic for collecting breastmilk.

I would like to thank my friends and family, who have supported me outside of the laboratory. I thank my mother for being the constant listening ear and the loving and encouraging support, and my not-so-little-any-more brother, Joshua, who is wise beyond his years. I recognize my father for encouraging me to pursue higher education. I also thank my uncle Koei for being a role model, listening to my frustrations, and always cheering me on as a fellow biologist. I also could not have made it through this program without the support of my sisters-in-law in Nagoya, Mikiko Funahashi and Mihoko Nakamura, and my mother-in-law, Asako Nakamura, who is no longer with us. Thank you for welcoming me into the family and for station drop-offs and pickups at both early and late hours of the day. Finally, I thank my partner Tomohiro, for challenging me when I am wrong, giving me objective advice, cheering me up when I was discouraged, and being my unconditional, unwavering, and loving support.

Miriam Nozomi Ojima
March 2021